UNIVERSITY OF BIRMINGHAM

birmingham archaeology

Airborne Remote Sensing of Aggregate Landscapes

Keith Challis, HP Vista Centre, Birmingham Archaeology,
University of Birmingham, Edgbaston, Birmingham, B15 2TT
(0121 414 5563, k.challis@bham.ac.uk)

Mark Kincey, HP Vista Centre, Birmingham Archaeology,
University of Birmingham, Edgbaston, Birmingham, B15 2TT

Dr Andy J Howard, Institute of Archaeology and Antiquity,
University of Birmingham, Edgbaston, Birmingham B15 2TT
(0121 414 5497, a.j.howard@bham.ac.uk)

PNUM 5261

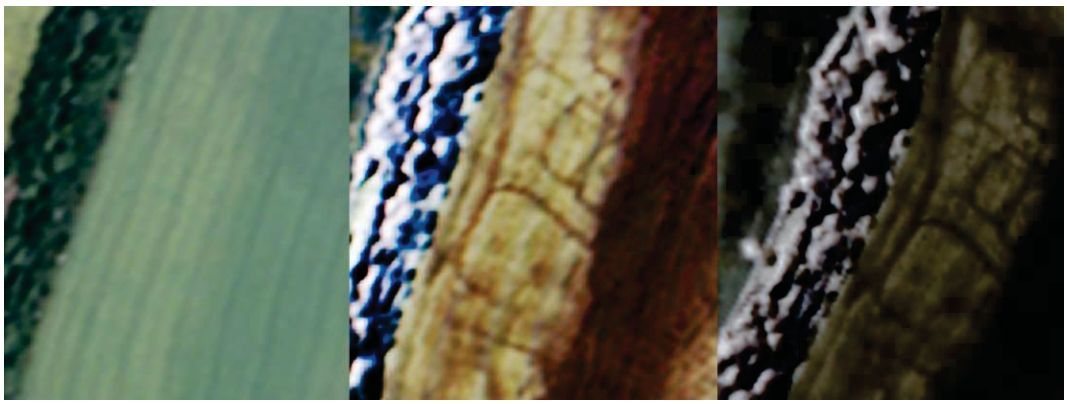

March 2008

Airborne Remote Sensing of Aggregate Landscapes

Keith Challis, HP Vista Centre, Birmingham Archaeology,
University of Birmingham, Edgbaston, Birmingham, B15 2TT
(0121 414 5563, k.challis@bham.ac.uk)

Mark Kincey, HP Vista Centre, Birmingham Archaeology,
University of Birmingham, Edgbaston, Birmingham, B15 2TT

Dr Andy J Howard, Institute of Archaeology and Antiquity,
University of Birmingham, Edgbaston, Birmingham B15 2TT
(0121 414 5497, a.j.howard@bham.ac.uk)

March 2008

PNUM 5261

LIST OF CONTENTS

LIST OF FIGURES

LIST OF TABLES

1 INTRODUCTION

1.1 BACKGROUND TO THE STUDY

This project investigated the potential of multispectral and hyperspectral methods of airborne remote sensing (RS) for the prospection of cultural, environmental and geoarchaeological remains in river valley floors. The project undertook systematic examination of Daedalus 1268 Airborne Thematic Mapper (ATM) and Compact Airborne Spectrographic Imager (CASI) multispectral data. AISA Eagle hyperspectral data for a small area were also examined. Work focused on the archaeologically rich, well-documented aggregate landscapes of the middle Trent Valley, Nottinghamshire.

1.2 REPORT STRUCTURE

The report is divided into eight sections. Section one provides general introductory material relating to the study area and instruments used; section two outlines the research methods employed; section three discusses the principles and practice of remote sensing of alluvial geoarchaeology; section four discusses results from the Daedalus ATM 1268 sensor; section five discusses results from the CASI sensor and section six those from the AISA Eagle sensor. The report concludes with some general observations on technique, results and future practice (section seven) a list of references cited (section eight) and additional illustrative material in appendix 1. Note that high resolution digital images are included on the DVD-ROM accompanying the report and bound into the back cover.

1.3 PREVIOUS WORK

To date, with the exception of Powlesland's work in the former peat filled lake basin of the Vale of Pickering (an environment radically different to the alluvial landscape of the Trent Valley, which is more characteristic of other river systems), airborne multispectral and hyperspectral remote sensing has received little attention for archaeological prospection in alluvial landscapes (Challis and Howard 2006). Such studies as have taken place have been dominated by use of the Daedalus Airborne Thematic Mapper 1268 and the Compact Airborne Spectrographic Imager.

The potential of such instruments for archaeological and geoarchaeological use has been mooted for some while (eg Allsop 1992) and work in the former lake basin of the Vale of Pickering and on Salisbury Plain (Powlesland 1997 and 2006; Barnes 2003) has demonstrated some success, although data were not subject to a comprehensive suite of analytical techniques such as the calculation of vegetation indices or multivariate analysis. Several studies have also considered uses of ATM and CASI data in other landscape types (eg Rowlands 2007 in the Mediterranean; Winterbotton 2006 in the Scottish Islands) and for non-archaeological purposes (eg Davidson and Watson 1995, Harris *et al*, 2006, Rainey *et al*, 2003). There are extensive published applications of the analysis of multispectral and hyperspectral airborne remote sensing that comprise studies of soil or vegetation properties that are directly analogous to those undertaken by archaeologists' (eg Ben-Dor et al 2002; Harris et al in press; Liu et al 2003; Rainey et al 2003).

Existing research documents use of a number of analytical techniques for use on ATM, CASI and similar remotely sensed data including false colour composites, thermal analysis, generation of vegetation indices and automatic image classification. **False colour composites** are produced by mapping different band combinations to the three colour channels of a computer graphics system. This will allow, for example, production of composite focused on reflectance in particular parts of the spectrum such as the near infrared where discrimination of variations in vegetation character or soils (enhancing visibility of crop and soil marks) may be greater (Winterbottom and Dawson, 2005). **Thermal images**, based on analysis of the emitted thermal band (11) of ATM imagery has proven particularly effective at identifying variations in the land surface representing underlying archaeological features (Rowlands and Sarris, 2007; Winterbottom and Dawson 2005; Ben-Dor, *et al*, 2001).

Vegetation Indices such as the Normalised Difference of Vegetation Index (NDVI), Enhanced NDVI and Soil Adjusted Difference of Vegetation Index (SDVI) use mathematical formula to express particular vegetation parameters as expressed by spectral reflectance, for example NDVI is an index of variations in green vegetation vigour. These techniques has proven effective at enhancing archaeological features such as cropmarks revealed by vegetation changes (Vining and Wiseman, 2007; Lasaponara and Masini, 2007; Winterbottom and Dawson, 2005). **Image classification** techniques rely upon the ability of computer analysis of the spectral data contained within multispectral images to identify homogenous clusters of pixels with distinctive spectral characteristics. Classification may be fully automatic (unsupervised), or based on a user intervention (supervised), for example to "train" a classification programme to locate areas with a particular spectral signature based on previous visual examination of the data, or on ground truth data. In general automatic classification techniques have performed poorly when applied to remotely sensed images for archaeological purposes, often because the spectral characteristics of archaeological objects are not sufficiently distinct from background data (Rowlands and Sarris, 2007; De Laet *et al*, 2007). Object-oriented approaches, where a two stage analysis first identifies spectrally homogenous areas within an image and then attempts a classification of these area, has proven somewhat more effective, but is still problematic (Rowlands and Sarris, 2007; Benz *et al,* 2004).

1.4 STUDY AREAS

This study undertook analysis of existing ATM and CASI data held by the NERC archive (and acquired in June 1996 for the NERC funded Land Ocean Interaction Study) for the Trent Valley roughly between the confluence with the Derwent and Devon – a length of some 50 km (Fig. 1) In addition AISA Eagle data acquired in October 2007 for an area of c 40km2 centred on Sturton-le-Steeple in north Nottinghamshire were also examined.

The Trent is well documented from earlier ALSF funded studies (eg Trent Valley GeoArchaeology 2002) and from extensive earlier fieldwork associated with gravel applications (including borrow pits) and major infrastructure schemes such as the Derby Southern Bypass (see Knight and Howard, 2004). Hence the geomorphological character of the floodplain and terraces and the distribution of

archaeological sites, particularly as revealed by cropmarks, are well known (e.g. Carey et al., 2006). This rich well-documented heritage provides an ideal backdrop against which to test the efficacy of new remote sensing techniques.

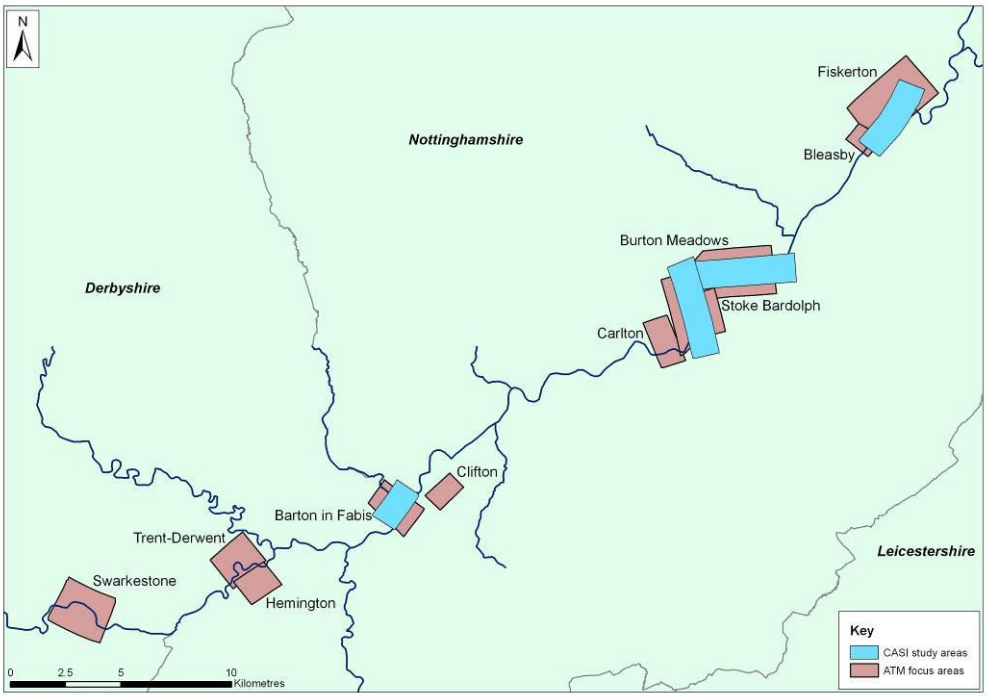

Figure 1. Locations of the 13 ATM and CASI study areas.

1.5 INSTRUMENT DETAILS

1.5.1 Daedalus 1268 ATM

The Daedalus 1268 ATM is a multispectral instrument recording spectral reflectance and infrared radiation in 11 discrete bands ranging in wavelength from visible blue to thermal infrared (0.42 – 13.0(m). Reflectance is recorded on an 8-bit digital scale (image pixel values from 0-255) at a typical spatial resolution of 2m.

Channel Bands	Wavelenght(nm)	Comment
1	0.42-0.45	
2	0.45-0.52	Vis Blue
3	0.52-0.60	Vis Green
4	0.60-0.62	
5	0.63-0.69	Vis Red
6	0.69-0.75	NIR
7	0.76-0.90	NIR
8	0.91-1.05	SWIR
9	1.55-1.75	SWIR
10	2.08-2.35	
11	8.5-13.0	Thermal IR

Table 1. ATM bandset

1.5.2 CASI-2

The CASI-2 instrument operated by NERC is a highly configurable hyperspectral scanner capable of recording spectral reflectance in up to 288 spectral channels at varying spatial resolution. In the archive data held by NERC the instrument has been operated in default mode (12 bands 430-875nm) with reflectance recorded on a 12-bit digital scale (image pixel values 0-4096) with a spatial resolution of 2m. In default mode CASI is particularly well suited to discrimination of vegetation character and can be expected to be particularly effective detecting variations in crop growth such as those responsible for cropmark formation.

Channel	Centre(nm)	Width(nm)	Start(nm)	End(nm)	Purpose
1	450	20	441.53	459.17	Blue Veg response
2	490	20	480.37	499.84	Veg.response
3	552	10	547.74	556.63	Green Veg max
4	670	10	665.57	674.74	Veg absorp max (1)
5	700	10	694.28	703.27	Red-edge (2)
6	710	10	705.07	711.06	Red-edge (3)
7	740	10	735.66	744.67	Red-edge (4)
8	750	7	746.47	753.68	Red-edge (5)
9	762	5	760.90	764.51	Oxygen absorp
10	780	10	775.34	784.37	Veg reflect.Max
11	820	10	815.13	824.18	Waterabsorp.
12	865	10	860.46	869.54	NIR plateau

Table 2. CASI Default Bandset

1.5.3 AISA Eagle

The AISA Eagle hyperspectral sensor is a complete pushbroom system with a 1000 pixel swath width, covering the visible and near infra-red spectrum 400 - 1003nm. The spectral resolution of the sensor is 2.9nm. Data for the present study were collected on 18th October 2007 over 34 spectral bands at a spatial resolution of 1m. Spectral details are provided in table 3.

1.5.4 Data Selection

Archive ATM and CASI data from the NERC Earth Observation Data Centre (NEODC) were downloaded via FTP using the HP Vista user account with NEODC. Other GIS, HER and remotely sensed data were extracted from archive and collated to form a coherent project GIS.

Overall, ATM and CASI data were available for approximately 50km of the Trent Valley (Figs.2 and 3). Much of these data covered areas of limited archaeological significance and in places some data were of poor quality. Analyses therefore focused on 13 study areas, selected because of the presence of known anthropogenic and geoarchaeological features and with high quality data coverage (Table 4).

Aisa Eagle data were available for an approximately 40km2 area of the Trent Valley focused on Sturton-le-Steeple, Nottinghamshire. These data were provided by Infoterra as geotiff files, projected to WGS84 datum and UTM co-ordinate system.

Channel	Centre(nm)	Width(nm)	Start(nm)	End(nm)	Comment
1	409.810006	16.360001	401.630005	417.990006	
2	426.180001	16.360001	418.000000	434.360001	
3	442.750013	16.660000	434.420013	451.080013	Blue Veg Response
4	459.930015	17.080000	451.390015	468.470015	
5	477.029990	17.080000	468.489990	485.569990	
6	494.129996	17.080000	485.589996	502.669996	Veg Response
7	511.230002	17.080000	502.690002	519.770002	
8	528.329978	17.080000	519.789978	536.869978	
9	545.775015	17.770000	536.890015	554.660015	Green Veg Max
10	563.209998	17.799999	554.309998	572.109997	
11	580.990027	17.799999	572.090027	589.890026	
12	598.769995	17.799999	589.869995	607.669994	
13	616.550024	17.799999	607.650024	625.450023	Vis Red
14	634.329993	17.799999	625.429993	643.229992	
15	652.119971	17.799999	643.219971	661.019970	
16	669.910010	17.799999	661.010010	678.810009	
17	687.709988	17.820000	678.799988	696.619988	
18	705.519976	17.840000	696.599976	714.439976	Red Edge
19	723.370012	17.840000	714.450012	732.290012	
20	741.329999	18.040001	732.309998	750.349999	
21	759.330022	18.240000	750.210022	768.450022	Oxigen Absorp
22	777.529973	18.240000	768.409973	786.649973	
23	795.779973	18.240000	786.659973	804.899973	Veg Reflect Max
24	814.039983	18.240000	804.919983	823.159983	Waterabsorp
25	832.289983	18.240000	823.169983	841.409983	
26	850.529973	18.240000	841.409973	859.649973	
27	868.760015	18.240000	859.640015	877.880015	NIR plateau
28	886.989995	18.240000	877.869995	896.109995	
29	905.229976	18.260000	896.099976	914.359976	
30	923.489977	18.280001	914.349976	932.629977	
31	941.770006	18.280001	932.630005	950.910006	
32	960.049974	18.280001	950.909973	969.189974	
33	978.340013	18.280001	969.200012	987.480013	
34	995.659981	16.360001	987.479980	1003.839981	

Table 3. AISA Eagle Bandset.

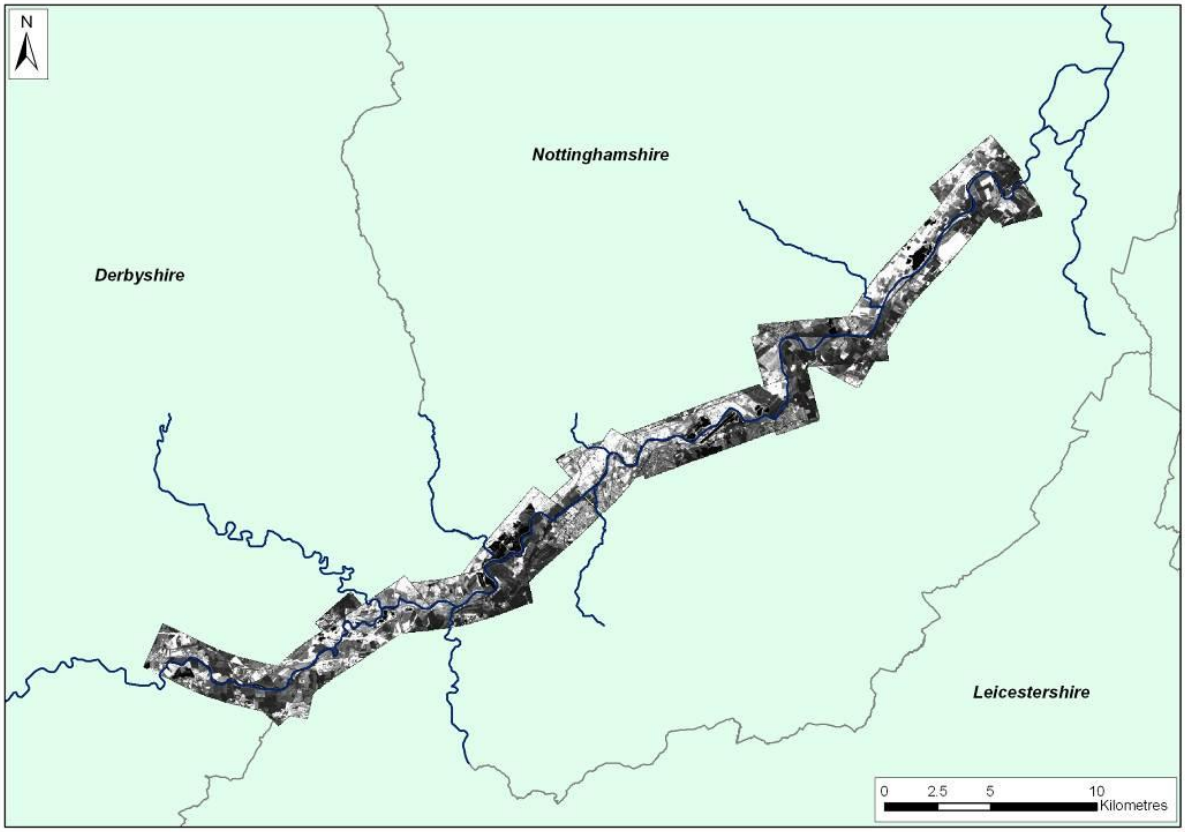

Figure 2. Extent of Daedalus 1268 ATM data for the study area.

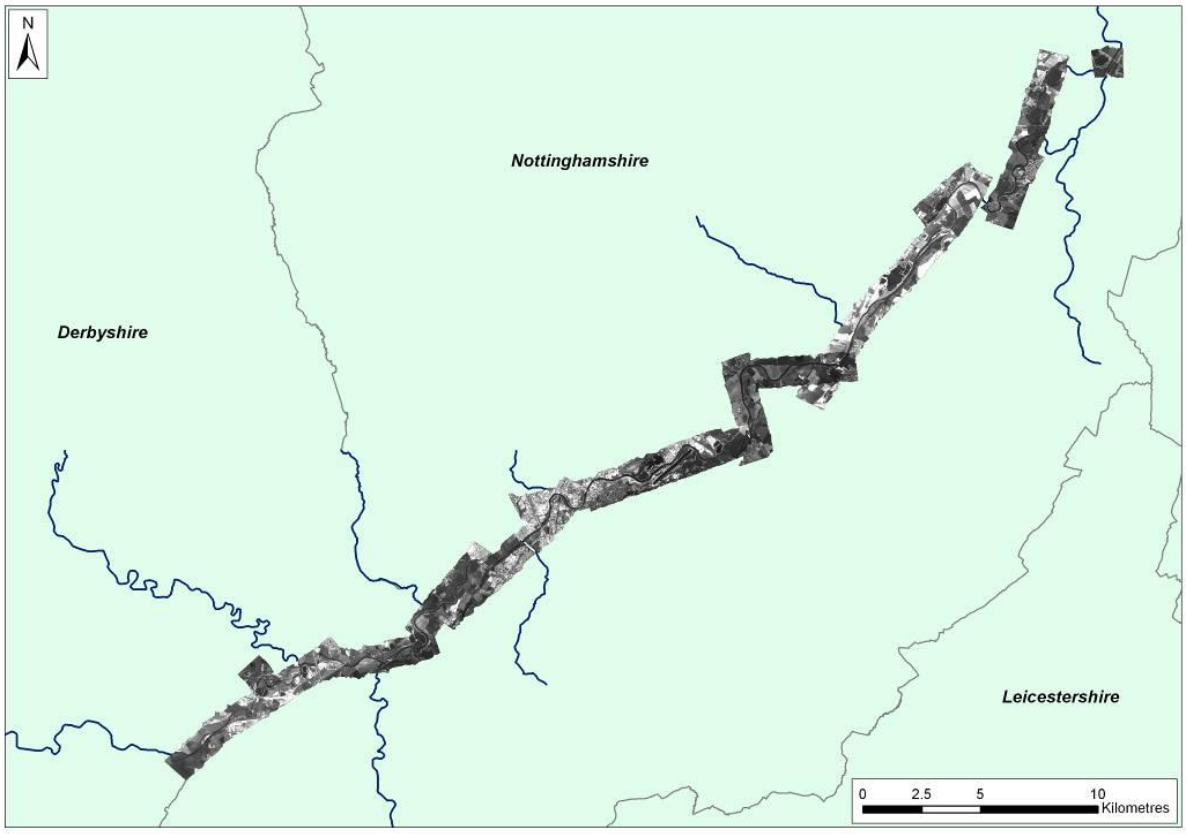

Figure 3. Extent of CASI data for the study area.

2 METHOD STATEMENTS

2.1 RADIOMETRIC AND ATMOSPHERIC CORRECTION

The digital imagery supplied by NERC comprise ATM and CASI data processed to level 1b, that is with radiometric correction but no other post processing, archived in HDF format comprising at sensor digital number (DN) pixel values and flight ephemera.

ATM Eagle and CASI data comprise a series of spectral bands, the pixels of which each have a digital number. The pixel DN is a linearly transformed representation of at-sensor radiance for a discrete resolved area of the Earth's surface. As pixel DN is a simple linear transformation of radiance the slope and offset of this linear transformation can be used to calculate radiance.

DN values are affected by both atmospheric and geometric distortion. Atmospheric correction requires conversion of at-sensor radiance to apparent at-sensor spectral reflectance by accounting for temporal changes in solar illumination due to Earth-Sun geometry. However, at-sensor reflectance still has atmospheric scattering effects present. In many cases it is essential to remove or alleviate atmospheric effects by suitable image processing, to produce true at surface radiance values. This is essential if quantitative comparisons are to be made from different sensors, with different sensor parameters, or from survey flights carried out at different times, where atmospheric conditions may vary between flights. The aim of atmospheric correction is to derive a good estimate of the true at-ground radiance (reflectance). Approaches commonly employed in remote sensing for atmospheric correction are:

- Complex physical modelling – this can be undertaken using specialised software packages.
- Semi-empirical modelling - this can be undertaken using specialised software packages.
- Empirical estimation approaches - based on image data relationships.

However, since in the present study only ratio analysis and classification of imagery was to be attempted, and no quantitative analysis was required, it was felt unnecessary to carry out atmospheric correction of the imagery used, particularly as in the absence of contemporary ground control and atmospheric data this would of necessity rely on less than accurate empirical estimation techniques.

2.2 GEOCORRECTION

2.2.1 ATM and CASI

Archive level 1b ATM and CASI data were pre-processed using Azimuth Systems Azgcorr 4.8 to combine flight ephemera and radiance data to produce automatically geocorrected level 3 images with real world co-ordinates (OSGB36 co-ordinate system). Where necessary further correction was undertaken using the geocorrection module of ArcGIS 9.2 using an Ordnance Survey 1:2500 base map as a source for ground control points (GCP).

In general it has proven possible to achieve high quality geocorrection of ATM and Eagle data. However, CASI data for the study area included significant image distortion (Fig. 4), which in some cases it has not proven possible to remove.

Figure 4. An example of geocorrected CASI data showing the distortion in the image data.

2.2.2 Geocorrection: AISA Eagle

Eagle data were supplied by Infoterra as level 3 processed flight lines (ie with some radiometric correction and geocorrected to the GPS co-ordinate system (WGS84)). Individual flight-lines were reprojected to the OSGB36 co-ordinate system using the reprojection module of Erdas Imagine. Flight-lines were then combined using the mosaic module of Imagine to produce a single multi-band image file. A rectangular area of interest (AOI) was extracted from the mosaic and imported into ArcGIS for image processing and analysis. Examination of the image showed that reprojection of the original data had produced imperfect results, probably largely due to errors introduced by the GPS and INS systems used at the time of data collection. The image was therefore subject to a second stage of geocorrection within ArcGIS, to fit GCP collected from OS 1:2500 mapping, before further analysis.

2.3 ANALYTICAL TECHNIQUES

A series of standard analytical techniques were employed on all imagery; these are discussed below and tabulated by focus area in table 4.

Focus Area	Imagery Available			Analytical techniques Used				
	ATM	CASI	Eagle	TCC/FCC	Thermal	NDVI	TC	PCA
Swarkestone, Derbyshire	A			A	A	A	A	A
Trent-Derwent Confluence, Derbyshire	A			A	A	A	A	A
Hemington, Leicestershire	A			A	A	A	A	A
Barton-in-Fabis, Nottinghamshire	A	C		A/C	A	A/C	A	A/C
Clifton, Nottinghamshire	A			A	A	A	A	A
Carlton, Nottinghamshire	A			A	A	A	A	A
Stoke Bardolph, Nottinghamshire	A	C		A/C	A	A/C	A	A/C
Burton Meadows, Nottinghamshire	A	C		A/C	A	A/C	A	A/C
Bleasby, Nottinghamshire	A			A	A	A	A	A
Fiskerton Nottinghamshire	A	C		A/C	A	A/C	A	A/C
Sturton-le-Steeple, Nottinghamshire			E	E		E		E

Table 4. Summary of analytical techniques and imagery available for each study area.

2.3.1 Colour Composites

True colour composite (TCC) and false colour composite (FCC) images were created by displaying combinations of geocorrected image bands within ArcGIS. TCC images for ATM data conventionally comprise bands 4-3-2, for CASI bands 4-3-2 are also utilised and for Eagle data bands 13-9-3.

FCC images focused on the NIR/R part of the spectrum tend to highlight variations in vegetation vigour reflected in the greenness of vegetation and hence its proportional absorption of red light and reflection of NIR. NIR/R reflectance is a good indicator of cropmark formation and may be expected to enhance cropmarks apparent within the visible spectrum and may expose “latent” variations in crop character apparent only beyond the visible spectrum.

FCC images using the middle and thermal infrared bands of ATM can be expected to be particularly effective at displaying variations in soil character and moisture content and may enhance visible and latent soilmarks. ATM FCC images will be prepared using bands 9-7-3 and 9-8-3. For CASI bands 13-10-3 were used, while for Eagle bands 33-21-13 proved effective.

2.3.2 Thermal Band Analysis

Band 11 of ATM imagery records energy emitted by the earth surface in the thermal infrared part of the spectrum (8.5-13.0nm; note that there is no equivalent band in CASI or Eagle imagery and so this component of the research was limited to ATM imagery only). The energy emitted at these wavelengths is generally related to variations in soil/ground moisture and microtopography, which together affect the temperature of ground. Analysis of the thermal band of ATM data has proven particularly effective at identifying archaeological features (*cf* Winterbottom and Dawson, 2005). The thermal band for ATM images was examined individually in order to identify archaeological and geomorphological features and assess the efficacy of thermal imagery for archaeological prospection in alluvial environments.

2.3.3 Vegetation Indices

Vegetation indices allow the differentiation of areas of differing vegetation and soil character based on the characteristic reflectance patterns of green vegetation, which

typically has low reflectance in the visible (especially red) portion of the spectrum with a sharp increase in reflectance in the near-infrared portion (cf Yang, 2007; Todd et al, 1998). The majority of indices are thus suitably adjusted ratios of red to NIR reflectance. The most common, the normalised difference vegetation index (NDVI) has been utilised with some success for the archaeological analysis of ATM imagery (Winterbottom and Dawson, 2005). In the present research analysis of ATM, CASI and Eagle data used the NDVI and TNDVI indices. Formulas for these indices are provided below (after Yang, 2007). Each was assessed to determine its effectiveness at revealing archaeological and geomorphological detail.

$$NDVI = \frac{(NIR - R)}{(NIR + R)} \qquad TNDVI = \sqrt{\frac{(NIR - R)}{(NIR + R)} + 0.5}$$

Band selection for generating these indices was based on selection of the maximum vegetation absorption (visible red) and maximum vegetation reflectance bands (NIR; table 5)

	Max veg absortion	Max Veg Reflectance
ATM	3	4
CASI	4	10
Eagle	13	26

Table 5. Band selection for NDVI generation.

Although such ratio indices are in common use for the derivation of properties about the surface conditions of scenes acquired by Earth observation., their use has been questioned, as are nearly always a surrogate variable of the physical property that is actually required by the application scientist. Therefore, it should be remembered that they may have little meaning in terms of the bio-physical properties of the acquired scene.

2.3.4 Tasselled Cap Transform

The tasselled cap transform was developed for Landsat MMS data and has been adapted for later generations of the Landsat sensor (Crist and Cicone, 1984). Tasselled Cap (TC) uses a matrix of factors (below) applied to six of Landsat's spectral bands to derive three new data layers highlighting greenness, wetness and brightness in the data. Although originally developed for estimations of biomass using satellite imagery TC should prove adaptable to the similar spectral bands of ATM imagery (Table 7; although not to CASI or Eagle which possess no equivalent of Landsat band 7). The application of TC to ATM data is however, use of the matrix values developed for Landsat TM on ATM produced promising results.

TCgreen = -0.2728(TM1)-0.2174(TM2)-0.5508(TM3)+0.722(TM4)+0.0733(TM5)-0.1648(TM7)

TCwet = 0.1446(TM1)+0.1761(TM2)+0.3322(TM3)+0.3396(TM4)-0.6210(TM5)+0.4186(TM7)

TCbright = 0.2909(TM1)+0.2493(TM2)+0.4806(TM3)+0.5568(TM4)+0.4438(TM5)+0.1706(TM7)

Table **6**. Landsat TM TC transform matrix values.

LandsatTM	ATM
TM1	2
TM2	3
TM3	5
TM4	7
TM5	9
TM7	10

Table 7. Landsat TM bands and equivalent ATM bands for the TC transform.

2.3.5 Principal Component Analysis

Principal component analysis (PCA) is a multivariate statistical technique used to reduce redundancy multispectral image due to the correlation of adjacent spectral bands. These principal components reflect the maximum change in the original data (Mather, 2004). The effect is to compress the changes in reflectance revealed across the 11 or 12 bands of ATM into a lesser number (usually three) principal components. Components may usually be related to particular earth surface properties. PCA has shown some potential in the analysis of Landsat imagery for archaeological purposes (Vining and Wiseman, 2007) while Kvamme (Kvamme 2006) has used PCA to analyse co-registered geophysical survey data from multiple sources. In the present research was used to visually assess multiband ATM, CASI and Eagle imagery. PCA implemented within ArcGIS was used on each ATM and CASI image.

- For ATM imagery, PCA was used to generate four principal components, based on analysis of the full 11 band image, enabling generation of a three band FCC image which contains the majority of the variability in the original 11 band data.

- For CASI imagery, PCA was used to generate five principal components, using bands 2-12 of the full 12 band image. Band was omitted as it appeared to suffer excessive atmospheric effects, which distorted the generation of principle components.

- For Eagle imagery, PCA was used to generate 5 principal components, using bands all bands of the full 34 band image.

In each instance, each image component was examined separately as a greyscale image, and each set of components in combination as a FCC image.

2.4 IMAGE CLASSIFICATION

Image processing techniques alter and enhance the spectral data contained within multispectral images in order to enhance their utility in identifying earth surface features. Image classification uses a variety of computer based and manual techniques to correlate recorded spectra with real world objects and phenomena such as vegetation and soil character, sediment mineralogy, etc.

Image classification techniques rely upon the ability of computer analysis of the spectral data contained within multispectral images to identify homogenous clusters of pixels with distinctive spectral characteristics. Classification may be fully automatic (unsupervised), or based on a user intervention (supervised), for example to "train" a classification programme to locate areas with a particular spectral signature based on previous visual examination of the data, or on ground truth data. In general automatic classification techniques have performed poorly when applied to remotely sensed images for archaeological purposes, often because the spectral characteristics of archaeological objects are not sufficiently distinct from background data (Rowlands and Sarris, 2007; De Laet *et al*, 2007). Object-oriented approaches, where a two stage analysis first identifies spectrally homogenous areas within an image and then attempts a classification of these area, has proven somewhat more effective, but is still problematic (Rowlands and Sarris, 2007; Benz *et al,* 2004).

The present study examined CASI and ATM imagery with a view to determining whether areas of crop and soil variation associated with archaeological and geomorphological features display distinctive spectral signatures using unsupervised classification techniques.

2.4.1 Unsupervised Classification

Unsupervised classification of CASI and ATM imagery and outputs from vegetation indices, TC transforms and PCA were examined for homogenous clusters of pixel values indicating cultural or geoarchaeological features. Unsupervised classification focused on several test areas of varying character where there is good apparent contrast between background soil and vegetation properties and archaeological features. Classification was undertaken within Erdas Imagine 9 software using the ISODATA clustering algorithm.

3 REMOTE SENSING OF ALLUVIAL GEOARCHAEOLOGY

3.1 INTRODUCTION: PRINCIPLES OF REMOTE SENSING

Both anthropogenic and natural features are evidenced buy one or more of the classic means of identification from the air: cropmarks, soilmarks and/or variations in illumination (shadow features). Effective processing of multi and hyperspectral imagery requires some understanding of the physical phenomena giving rise to these features.

3.1.1 Factors Affecting Cropmark Formation

The majority of archaeological features visible from the air in the present study areas are evidenced by cropmarks. Cropmarks are formed by sharply defined growth differences in crops, usually reflecting differences in leaf area index (LAI – the area of leaf surface in a crop stand covering a given unit of soil), plant colour and stem height (Jones and Evans 1975, 2). While many factors affect the growing season and crop growth, the micro scale variations that lead to the formation of archaeological cropmarks are usually caused by varying availability of soil moisture. Jones and Evans (1975) provided a detailed experimentally supported discussion of the factors leading to cropmark formation, which is summarised here.

Cropmarks usually form at times of soil moisture deficit (SMD) when the rate of water use by a plant (potential transpiration) exceeds the water in the soils supplied by rainfall. As soon as SMD develops plants begin to draw on water stored in the soil. When all the water in the soil is exhausted plants growth ceases and plants begin to wilt. However, different plants respond differently to SMD; there are also variations in vulnerability to SMD at different points in growth cycle; cereals for example are most vulnerable immediately before the head forms, usually late June to early July. Since the major concentrations of roots and nutrients are in the top 30-40cm of soils, exhaustion of available moisture supplies to a depth of *c* 40cm checks growth in most crops. Experimental evidence shows that a potential SMD of 50mm (corresponding to water in top 30-40cm of soils) limits the growth of most grasses and arable crops (ibid, 4 quoting Penman 1952). In experiments, sites producing cropmarks annually began to display marks when SMD was between 50 and 65mm. 32% of observed sites showed cropmarks with SMD in the in range 50-100mm, 41% in the range 100-150mm and 20% in the range 150-200mm. Significantly, cropmarks may be faint in very high SMD as the whole crop becomes wilted. Furthermore, once the crop is ripe transpiration is negligible and SMD of little importance. The period of desiccation, when potential SMD affects growth in non senescent crops may extend from late June to mid-late August depending on soil depth.

The expression of buried archaeological features as cropmarks occurs because buried negative features provide greater reserves of water and nutrients, delaying the onset and severity of SMD. Conversely, buried positive features that restrict the availability of nutrients and moisture, accelerate the onset and impact of SMD causing crops to grow with less vigour and ripen more rapidly. During soil moisture deficit the growth of first leaves, then stems and finally roots of plants is affected. In wheat and barley, soil moisture deficit affecting leaves (ie LAI) cause most cropmarks. Variations in availability of nutrients may also cause cropmark formation. Absence of nitrogen and calcium is particularly significant and cropmarks due to

variations in greenness, LAI and stem height are usually the result of differential nitrogen uptake. For example crops growing in deep soil over a ditch have access to greater reserves of nitrogen and so grow greener and have a larger LAI (ibid, 9). Physical phenomena such as crop lodging may also occur due to excess nitrogen uptake causing over vigorous growth. Variations in availability of phosphorous (purple stems) and magnesium (yellow colour) may also produce cropmarks expressed as changes in crop colour.

In general, all of these phenomena are most evident in freely draining soils and substrates, which are commonly subject to summer moisture stress. Soils that tend to retain water are less prone to cropmark formation. Furthermore, some crops, such as certain cereals, are particularly prone to cropmark formation, while others, such as potatoes rarely develop cropmarks.

3.1.2 Factors Affecting Soilmark Formation

Archaeological soilmarks are largely the results of plough disturbance truncating archaeological features and deposits and by so doing introducing discrete areas of sediment of different character into the plough zone. They are most readily seen in areas of shallow soil, with a subsoil of contrasting colour. Differences in sediment character might relate to a number of characteristic, including organic content, mineralogy and particle size. Soilmarks of palaeochannels are perhaps more likely to be betrayed by variations in soil moisture, sediment character (silt/clay channel fills) and organic content of soil if peat or other organic sediments are disturbed. Jones and Evans report that the tonal colours of soils vary considerably with soil moisture content. The greatest colour contrasts are achieved at moisture content of 5-6% (1975, 1)

3.1.3 Prevailing Weather Conditions

Weather conditions play a significant role in determining appropriate conditions for airborne remote sensing, both in terms of the availability of cloud free days for flying and in the creation of appropriate ground conditions for the formation of archaeological crop and soil marks and for their detection. The potential impact of weather conditions prevailing at the time of the survey flights examined here is discussed below, summarized from the CEH annual hydrological report for 1996 (CEH 1996) and the monthly summary for October 2007 (CEH 2007).

The 1996 rainfall total for the UK was 940 mm - 86% of the 1961-90 average and ranking tenth driest this century (Fig. 5). England and Wales registered its driest year since 1973, and the fifth lowest rainfall total in the last 110 years. The spatial distribution of the rainfall was notable - wide regional and local variations characterising most of the country - with less than 65% of average recorded in several parts of the English lowlands. Rainfall through the spring (March-May) was less than 55% of average and it was the driest spring in some catchments for 20 years.

Annual potential evaporation totals were above average in much of eastern, central and southern England. In the English lowlands soil moisture deficits remained above 100 mm for a protracted period - from late May to late October (Fig. 6). Soil moisture

deficits began to build in the spring and increased rapidly from late May. By the end of July they were above average throughout much of the English lowlands. Conditions in the Trent Valley in June 1996 were therefore favorable for cropmark formation in early heading crops.

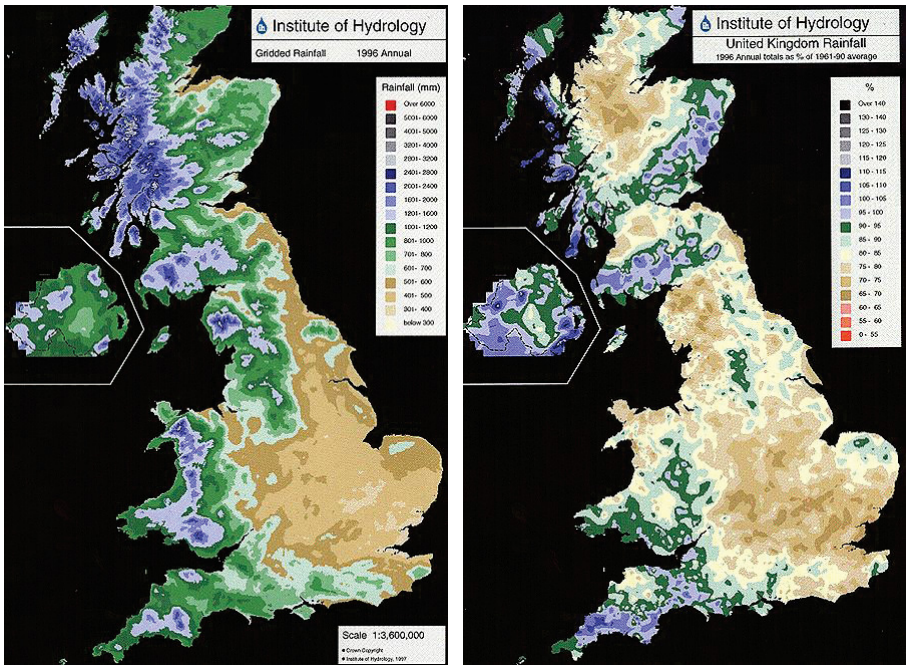

Figure 5. Total rainfall and rainfall as a percentage of 1961-1990 totals for 1996.

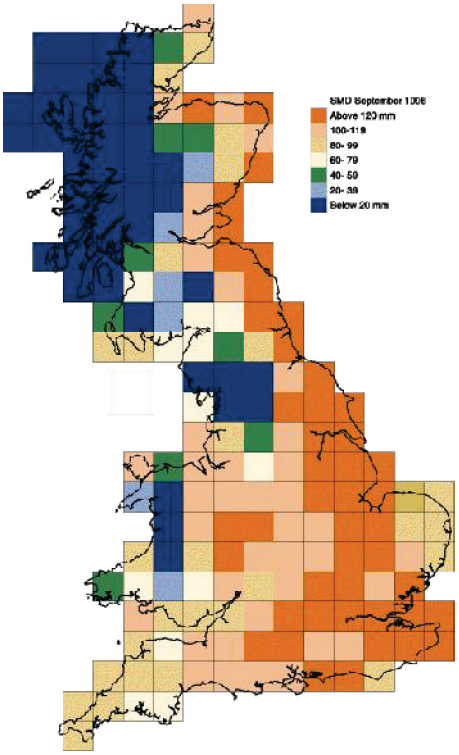

Figure 6. Soil Moisture Deficits for end September 1996.

October 2007 was a mild and relatively dry month across most of the country; vying with 2003 as the second driest October since 1977 for the UK as a whole. October rainfall totals in most catchment were well below average. Relatively dry conditions

prevailed from late July across much of the country; the August-October rainfall total for England and Wales was the second lowest since 1978 with the Severn-Trent region recorded its second lowest rainfall (after 2003) in over 40 years (Fig. 7). Soil moisture conditions showed substantial regional and local variations in October. In the Trent Valley the average October SMD of 80mm was amongst the highest in the UK. While the absence of arable crops, with harvest long completed by October, precludes the formation of arable cropmarks, ground conditions were suited for the formation of parchmarks in pasture and for the enhancement of soilmarks.

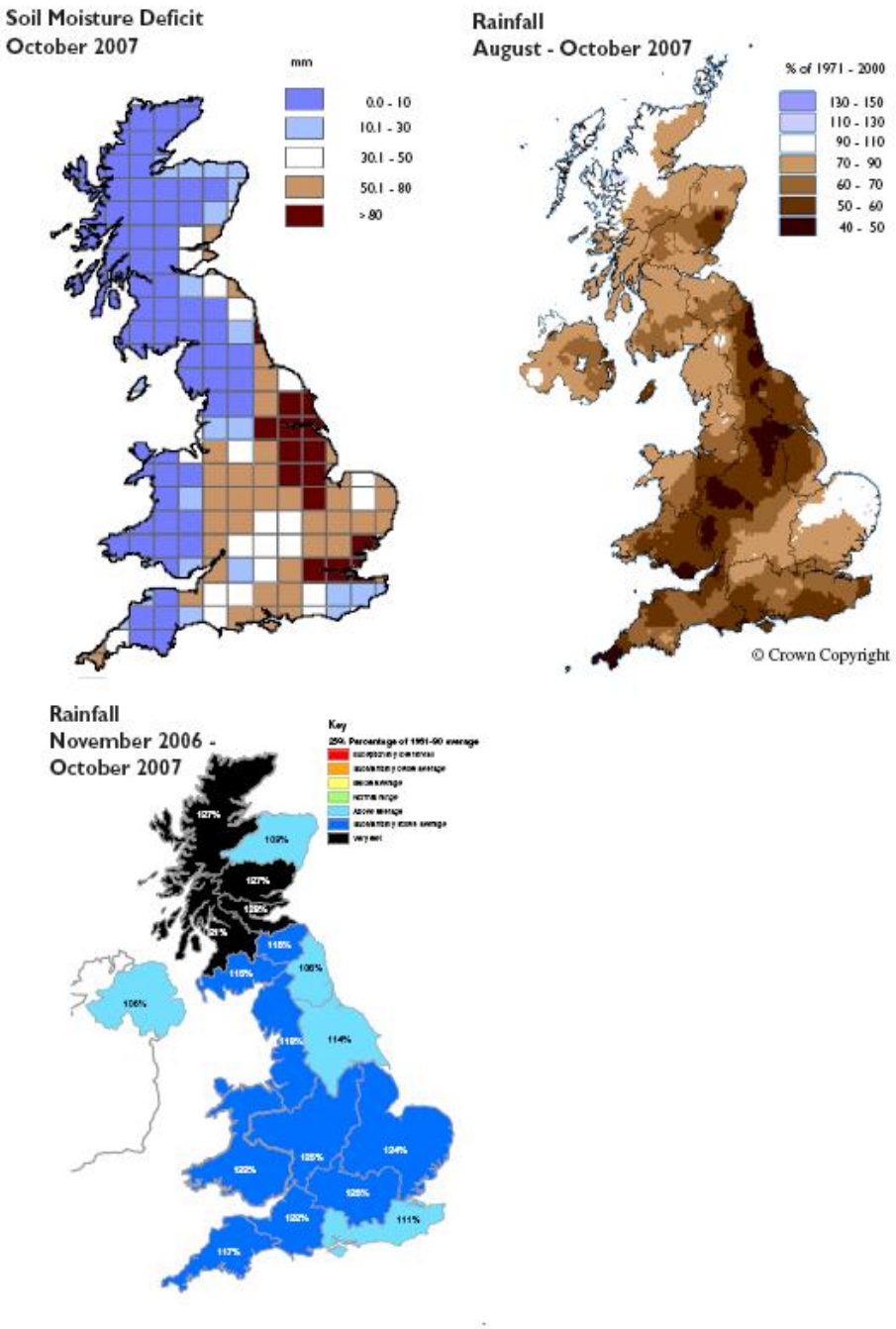

Figure 7. Soil Moisture Deficit and rainfall October 2007.

3.2 MULTI SPECTRAL REMOTE SENSING OF CROP AND SOIL MARKS

Multispectral and hyperspectral remote sensing platforms such as those used in the present study are passive sensing instrument in that they record the amount of the sun's energy reflected by the earth's surface using devices that convert the amount of reflected energy received by the sensor first into an electrical signal and subsequently into a digital number for recording. Remotely sensed images are thus built up from a sequence of numbers, digitally recording spatial variations in the energy reflected by the earth's surface. Beam splitting prisms, or filters may be used to divide the energy detected by the sensors into discrete spectral regions, allowing a simultaneous record to be made of the amount of the sun's energy reflected by the earth surface in different parts of the spectrum.

Different earth surface materials reflect or absorb the sun's energy to a varying degree across the spectrum. For example green vegetation strongly absorbs light in the red and blue parts of the spectrum, but strongly reflects light in the green and near infrared (NIR) part of the spectrum (Fig. 8). These variations in the absorption and reflectance characteristics of different materials make it possible to distinguish objects based on their distinctive reflectance. Examination of the spectral reflectance of typical materials of interest to archaeologists, such as vegetation, make it evident that remote sensing beyond the visible part of the spectrum, ie beyond c.700nm greatly enhances our ability to distinguish some materials from each other, eg the difference between green and dry vegetation, one of the principal features of an archaeological crop mark, is most marked in the NIR.

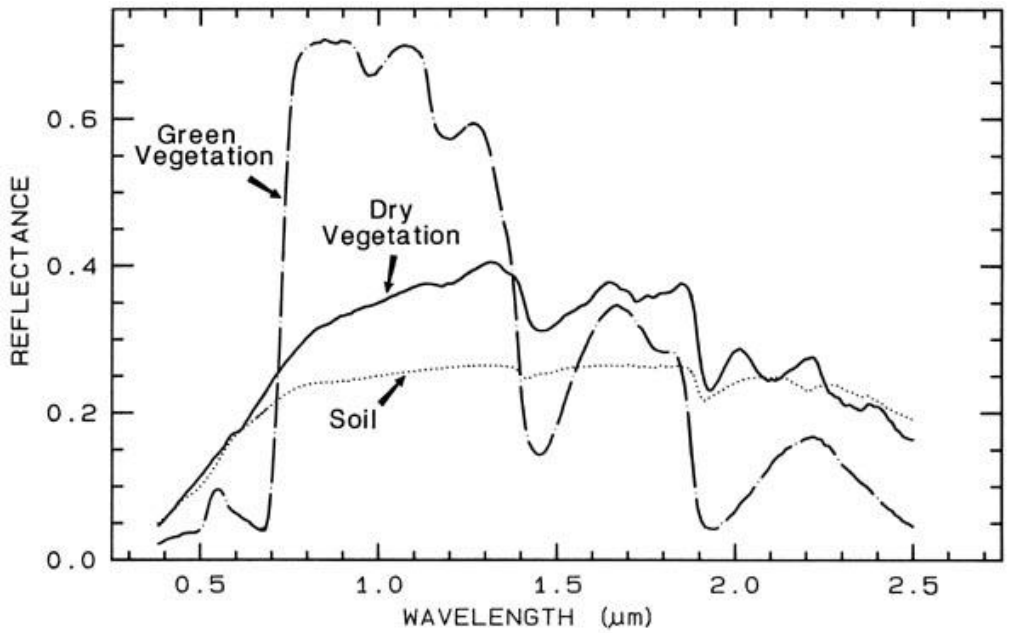

Figure 8. Ideal reflectance curves for green vegetation, dry vegetation and soil, illustrating the degree to which the ability to distinguish these three varies across the spectrum.

In general the amount of sunlight (solar radiation) reflected by different earth surface materials varies greatly in both intensity and wavelength across different materials. Such differences may be a result of their different:

1. bio-physical properties,
2. chemical composition
3. surface geometry (roughness).

3.2.1 Cropmarks

As has been discussed, archaeological cropmarks are produced when buried archaeology affects the growth of overlying crops. The essential element of the cropmark is the variation in crop colour and vigour (both height and leaf area). Spectral response in the visible and NIR parts of spectrum reflects changes in vegetation type, leaf moisture content and the presence of key nutrients. In the v**isible** part of the spectrum (400 – 700nm) the amount of solar radiation reflected is determined by composition and concentration of chlorophylls a and b, caretenoids and xanthophylls which vary due to vegetation type and nutrients status. In the **Near Infrared (NIR)** part of the spectrum (700-1300nm) the principal variations in spectral reflectance are caused by the number and configuration of internal air spaces within leaf and moisture content of plant. In the **Short Wave Infrared (SWIR)** part of the spectrum, between 1350 and 2500nm, reflection is most affected by water concentration in plant tissue.

The visibility of a typical anthropogenic cropmark across the spectrum is illustrated in Fig. 10.2-10.11. The cropmark, in this instance of a rectilinear enclosure and other features at Fiskerton, Notts, is apparent in the Daedalus ATM true colour composite image Fig. 9 showing solar reflectance in the visible spectrum, as a series of well-marked darker green features, of unripe, probably cereal crop, against a background of pale and therefore ripe and somewhat parched crop. By examining the same scene in each of 10 bands of ATM imagery (bands 1 and 12 are omitted; 1 is badly affected by atmospheric haze and 12 is a duplicate of 11) it is possible to identify the varying degree to which cropmarks are apparent across the spectrum.

In the visible blue part of the spectrum (Figure 10.2; 450-520nm ATM band 2) the cropmark is fairly well evident and comparison with the idealised spectral response shows that there is a small difference between the reflectance of dry vegetation (high and therefore pale grey tones on the image) and green vegetation (low reflectance and therefore dark gray tines). In the visible green (Figure 10.3; 520-600nm ATM band 3) there is marginally greater contrast between the cropmark and the background.

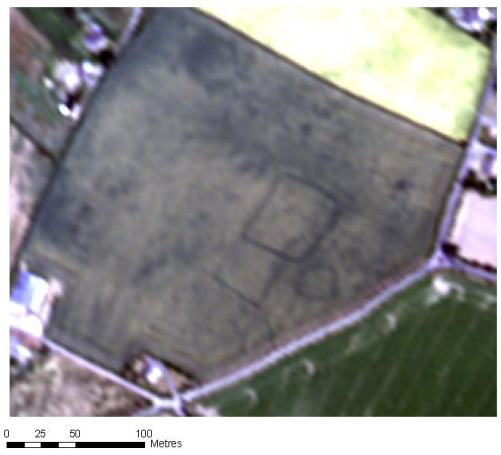

Figure 9. Daedalus 1268 ATM TCC (4-3-2) showing cropmarks of a rectilinear enclosure and other features at Fiskerton, Notts.

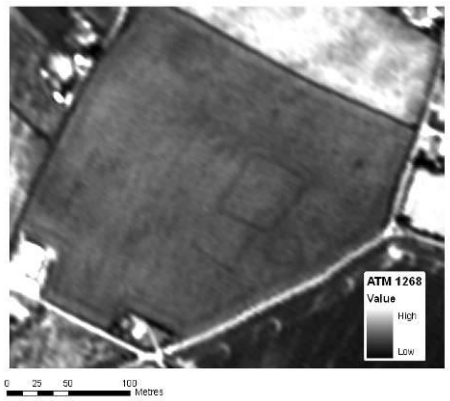

2

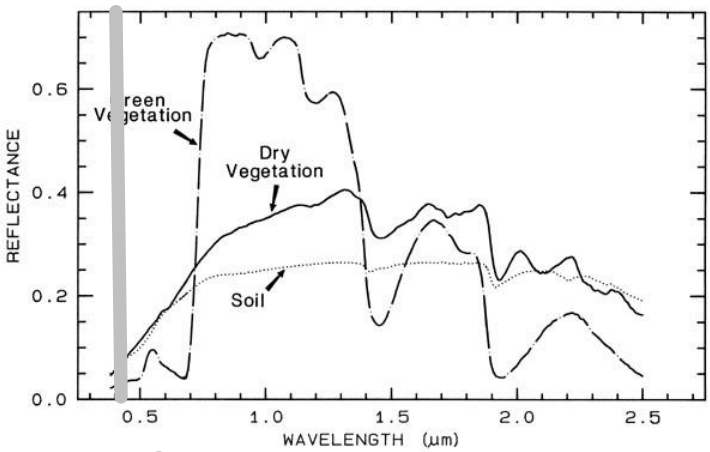

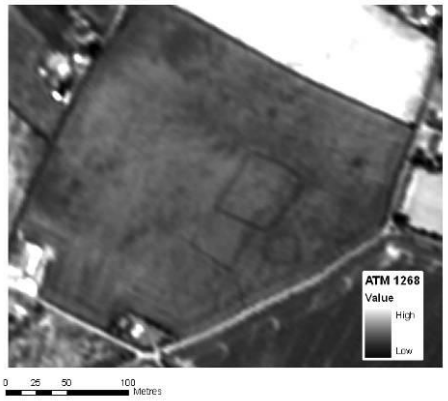

3

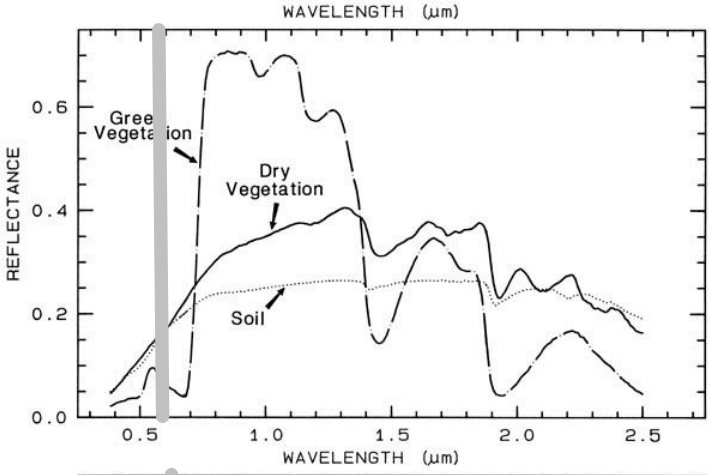

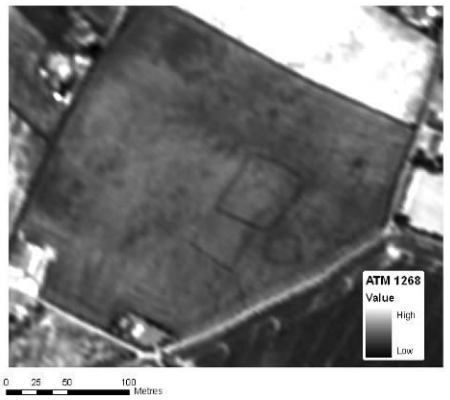

4

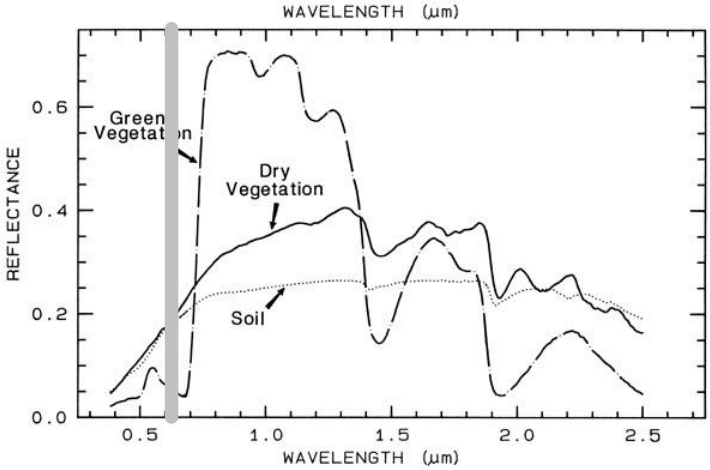

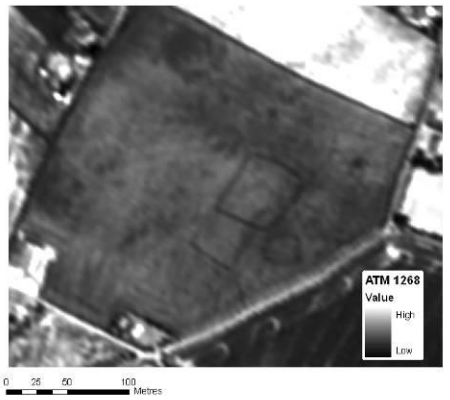

5

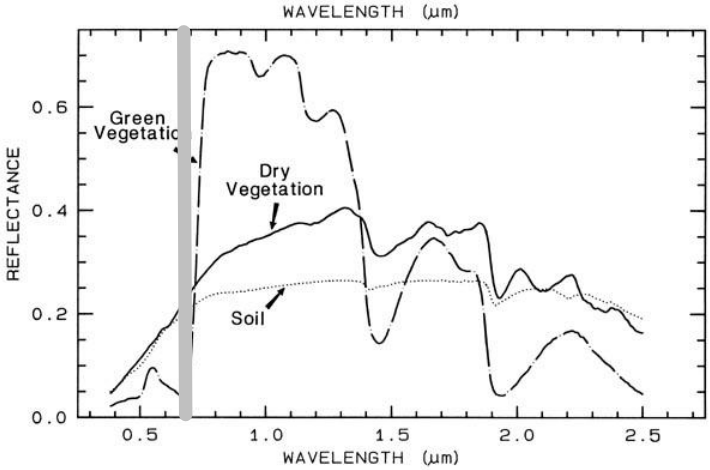

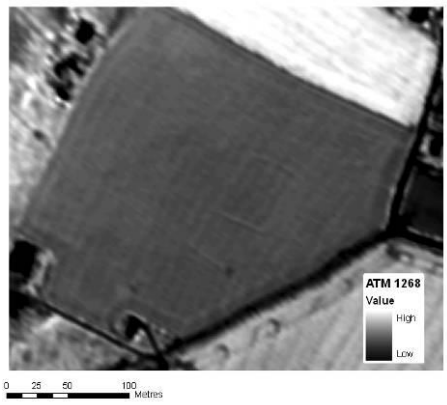

6

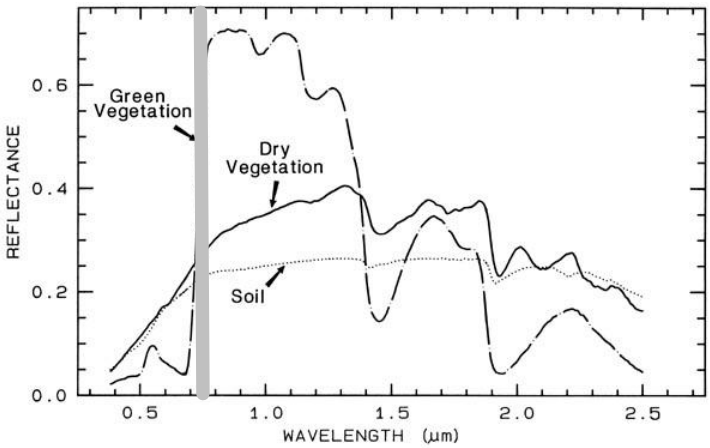

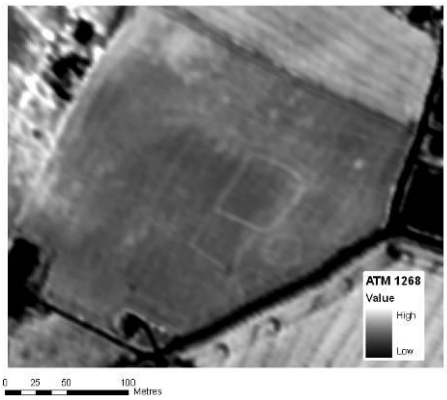

7

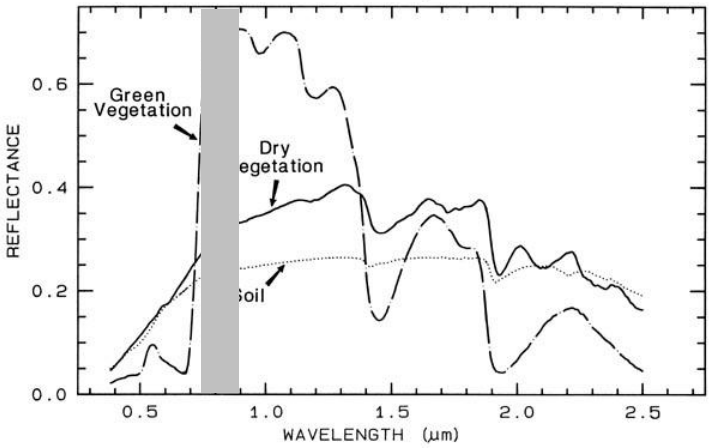

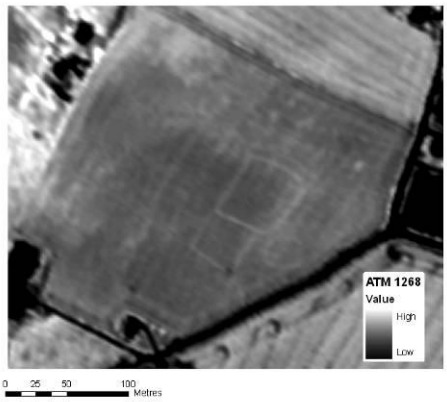

8

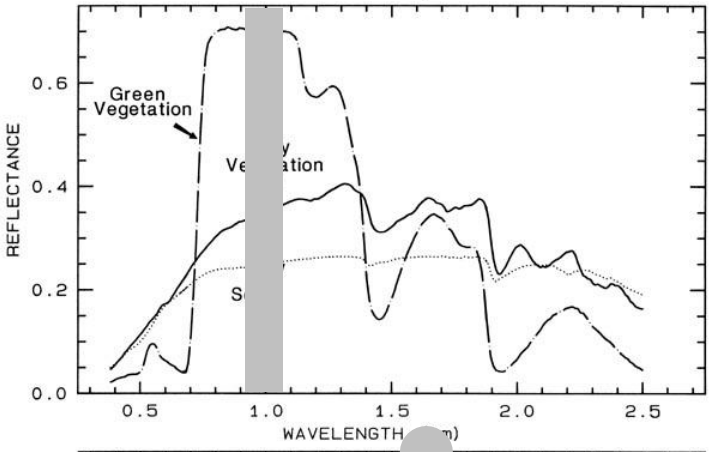

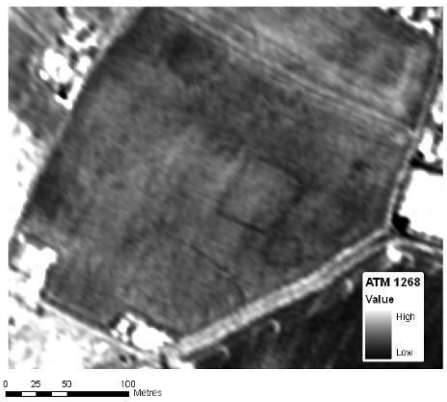

9

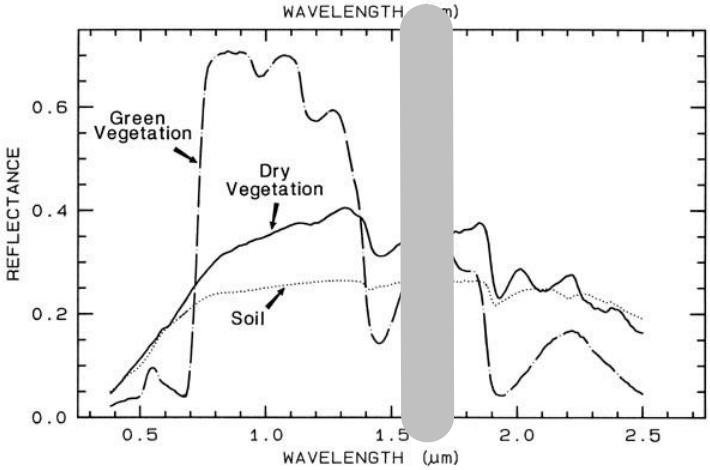

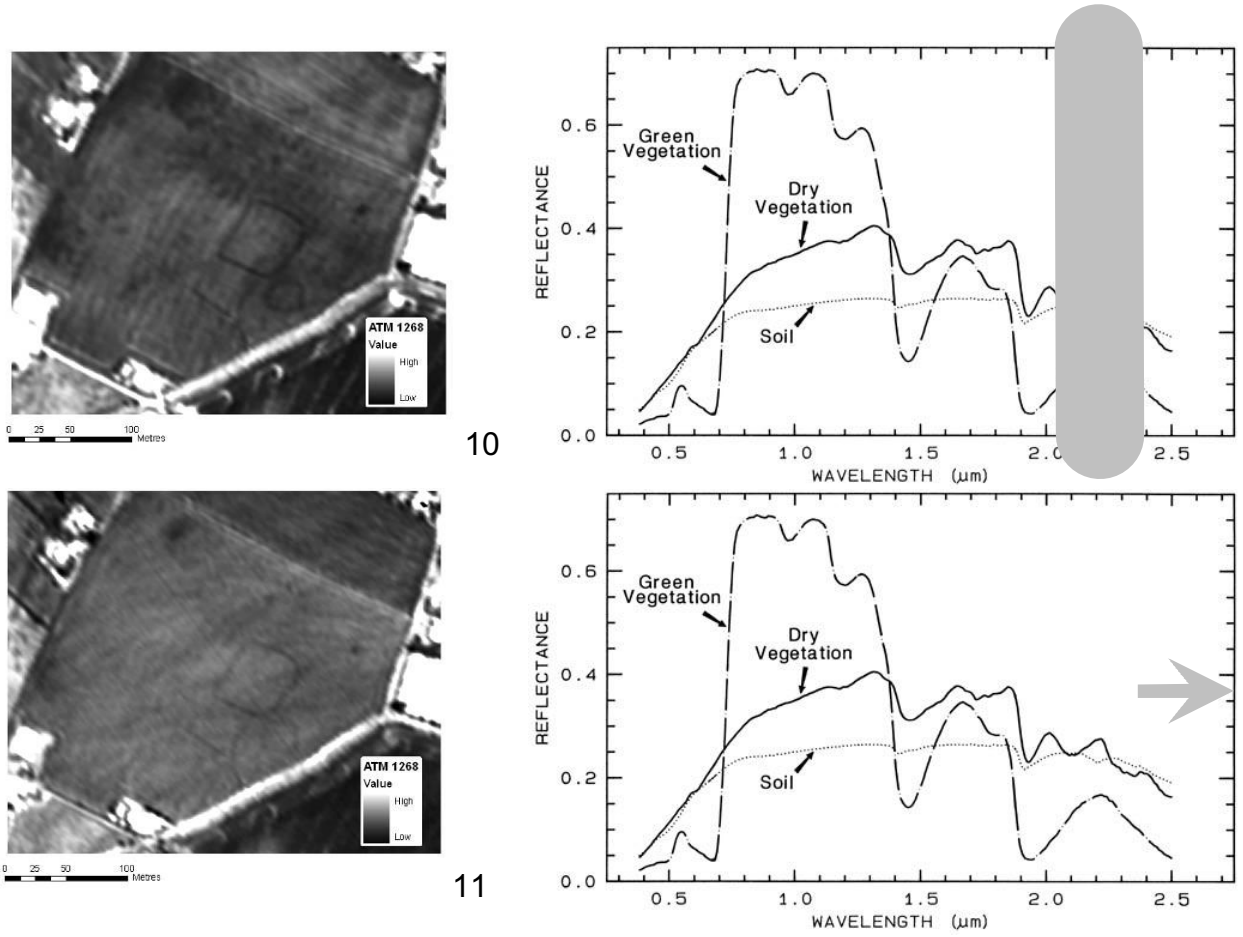

Figure 10. Greyscale images showing single spectral bands for ATM bands 2-11 idealised spectral response graphs showing the bandwidth and reflectance curves for dry vegetation, green vegetation and soil.

In the visible red part of the spectrum (Figure 10.4; 600-620nm ATM band 4) there is even greater clarify between cropmark and background as the green vegetation of the cropmark reflects significantly less red light than the parched crop that surrounds it. At the extreme red end of the visible spectrum (Figure 10.5; 630-690nm ATM band 5) the contrast between cropmark and background is further enhanced. Band 6 of ATM imagery coincides with the so-called red-edge, the boundary between low reflectance of red light by green vegetation in the visible spectrum and high reflectance in the near infrared. The precise location of the red edge varies in relation to the character of plant materials. In this instance band 6 coincides almost exactly with the point of equal reflectance between green and dry vegetation; the cropmark almost vanishes (Figure 10.6; 690-750nm ATM band 6). Beyond this point the visual character of the cropmark in the imagery is reversed as in the NIR green vegetation is far more reflective than dry (Figure 10.7 and 10.8: ATM band 7 and 8).

In the SWIR, from c 1500nm, the situation is again reversed, with dry vegetation more reflective than green. The cropmarks again appear as dark features against a pale background, contrast is better in ATM band 10 (Figure 10.10) than in band 9 (Figure 10.9) where reflectance of green and dry vegetation tends to merge.

ATM band 11 (Figure 10.11) represents the thermal infrared; that is emitted heat rather than reflected solar radiation. The cropmark as poorly represented as darker, and therefore cooler features.

Given the above, it should be readily apparent which ATM band combinations and hence which parts of the spectrum, are most effectively examined for archaeological cropmarks. These variations in reflectance and absorption at different wavelength form the underlying basis of the ratio techniques used for much of the image analysis herein, which serve to accentuate differences in reflectance properties of materials across the spectrum. The physical character and spectral properties of a selection of anthropogenic and geoarchaeological cropmarks is further examined in section 3.3-3.4.

3.2.2 Soilmarks

In general soils of varying type exhibit a fairly uniform reflectance of solar radiation across the spectrum. However, particular soil constituents, such as iron oxides, organic matter and some minerals, may produce characteristic reflectance peaks. Since many soilmark forming features are likely to introduce sediment of different physical and chemical composition into the ploughsoil the detection of soilmarks might be enhanced by looking for these variations.

Many gross soils and sediment variations are particularly likely to be evident in the **thermal infrared (TIR)** part of the spectrum where variations in soil and sediment moisture and microtopography may affect ground temperature. Similarly, shadow features caused by variations in illumination of the ground surface due to upstanding earthwork features may differentially affect the amount of solar radiation reaching the ground surface. This shadow effect may also lead to local variations in the thermal properties of the ground evident in the TIR.

3.3 IDENTIFYING ANTHROPGENIC CROPMARKS

The following section examines the spectral characteristics and appropriate image enhancement techniques for anthropogenic cropmarks using as examples cropmarks at two locations; Fiskerton and Stoke Bardolph, and ATM multispectral data.

3.3.1 Spectral characteristics of anthropogenic cropmarks

The spectral characteristics of cropmark and non-cropmark areas were examined by directly querying image data using Imagine Spectral Workstation software to generate spectral profiles at specific sample locations (Figs. 11 and 16).

The cropmarks at Fiskerton (discussed previously in section 3.2.1) appear as darker, green features, against a generally pale, parched background, suggesting positive cropmarks formed over buried ditches which have locally provided the crop with access to additional moisture and nutrients, thus reducing the affect of SMD and delaying ripening. In terms of their spectral signature the cropmarks reflect strongly in the visible red part and NIR parts of the spectrum and less so in the middle infrared (Fig. 11) a classic pattern for green vegetation. The non cropmark area (of parched crop) shows lower reflection in the red and NIR, but significantly enhanced reflection in the middle infrared, with the greatest contrast between cropmark and non-cropmark between 1500 and 1600nm.

At Stoke Bardolph, cropmarks of a series of rectilinear enclosures are not at all apparent in the visible spectrum (Fig. 11) where the spectral profile reveals that there is little difference in reflectance between cropmark areas and the still green background crop. It seems likely that at this site cropmark formation was still in progress at the time of the survey flight and that local SMD was either insufficient, or was still in the process, of affecting crop growth to the extent that clearly developed visible cropmarks might form. However, examination of the spectral profile shows that once again in the middle infrared, between 1500 and 1600nm, there is a clear contrast between the cropmark areas (lower reflectance) and the background, marginally more stressed crop (higher reflectance). Clearly examination of image data beyond the visible spectrum, in particular in the middle infrared, where the difference between dry and green vegetation is enhanced, greatly improves the definition of both conventionally visible and nascent anthropogenic cropmarks.

3.3.2 Image enhancement of anthropogenic cropmarks

The impact of a number of standard image enhancement techniques on the visibility of anthropogenic cropmarks is explored in Figs. 12 – 20. At both Fiskerton and Stoke Bardolph examination of the ATM thermal band cropmarks are evident as darker (therefore cooler) features (Figs.12 and 17). Here the differences may largely be due to the thermal properties of soils, with the marginally damper soils giving rise to cropmarks remaining cooler compared to the surrounding areas. The cropmarks at Stoke Bardolph are only just evident in the thermal data, suggesting that soil moisture differences are very slight here.

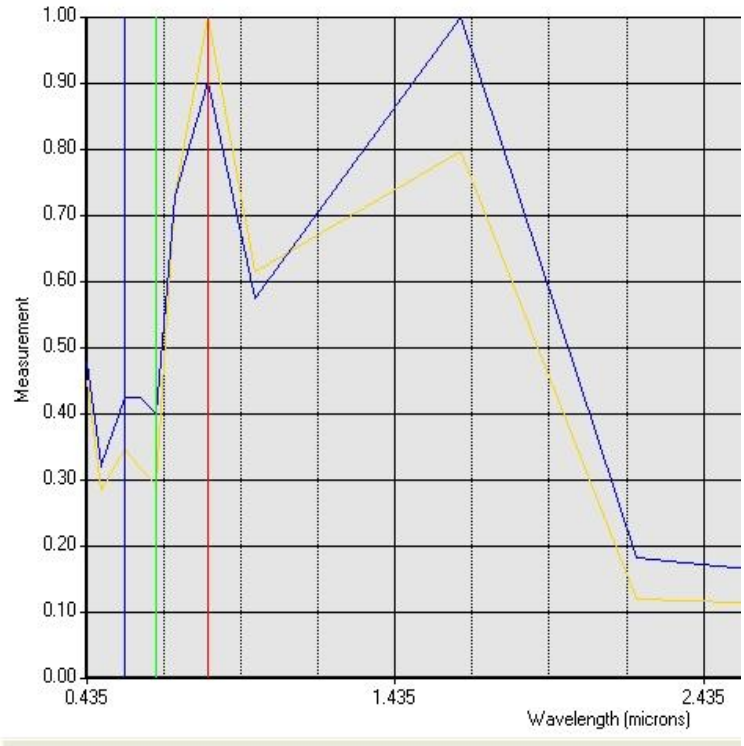

Figure 11. Top: cropmarks at Fiskerton (ATM TCC) showing sample locations. Bottom: spectral profiles at sample locations.

Figure 12. Fiskerton ATM band 11.

Figure 13. Fiskerton ATM TNDVI.

Figure 14. Fiskerton ATM Tasselled Cap Green.

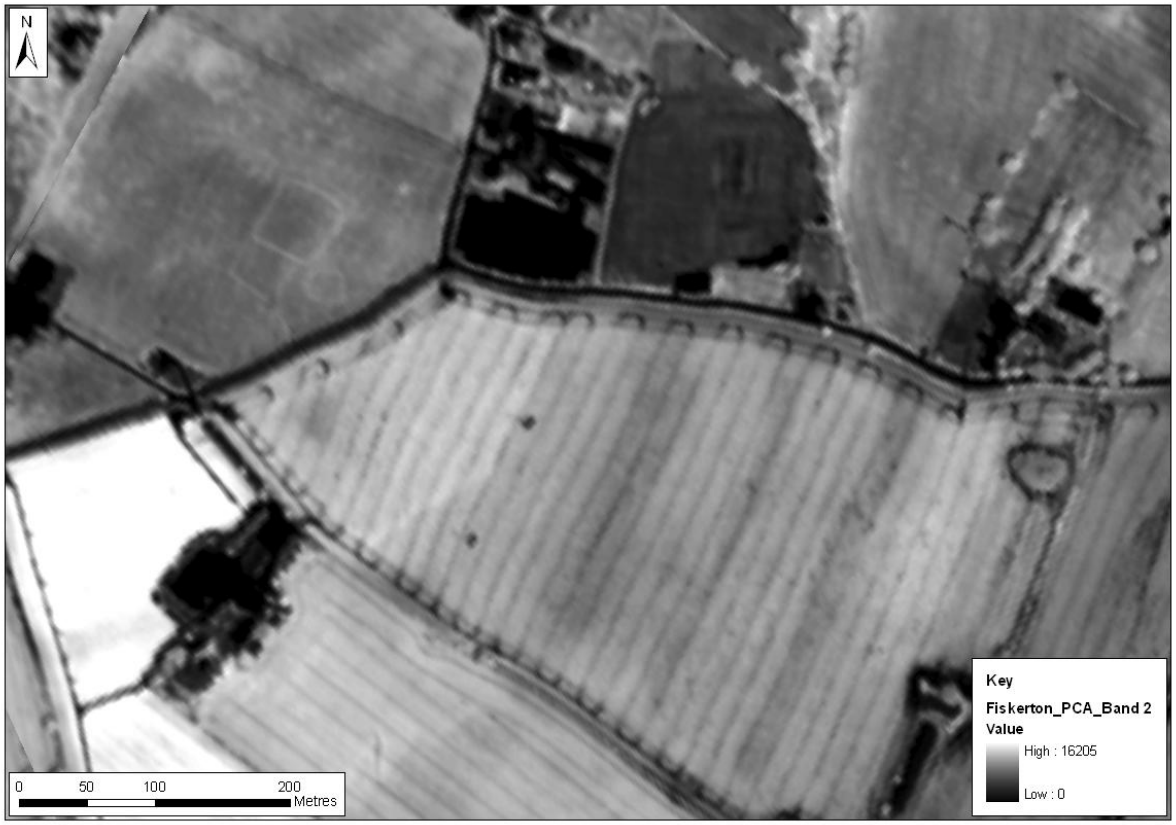

Figure 15. Fiskerton ATM Second Principal Component.

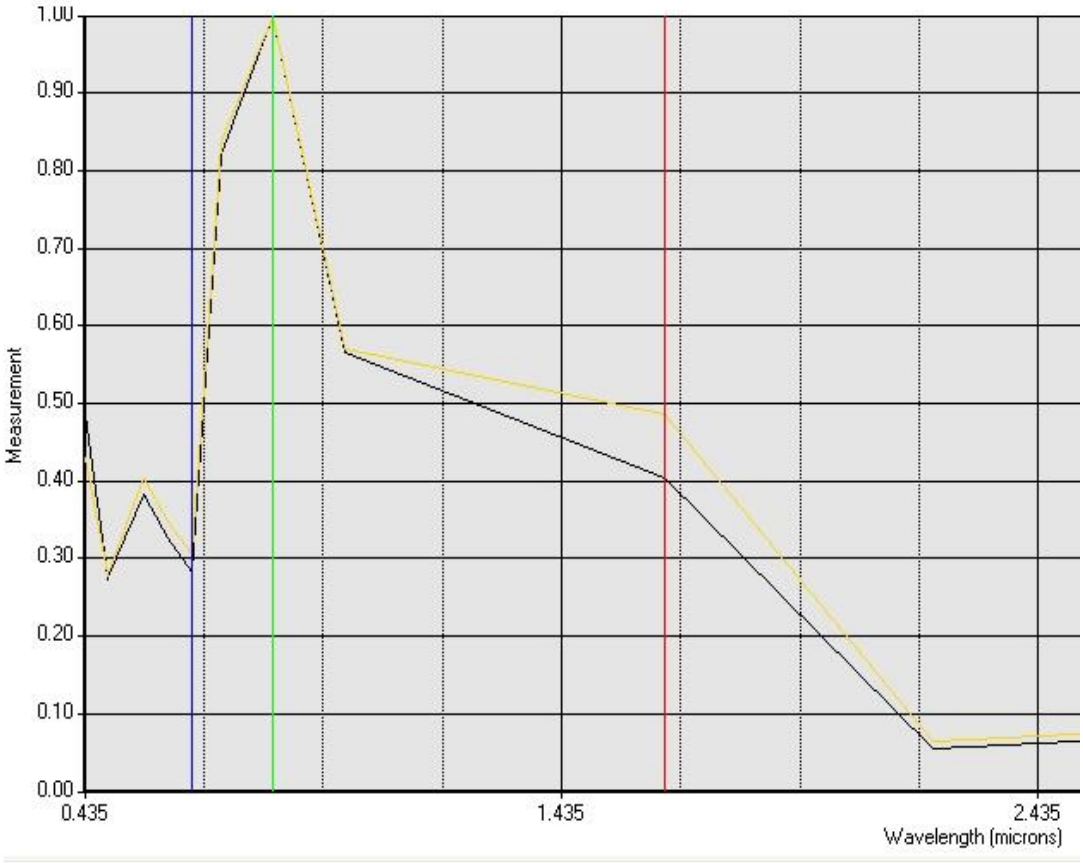

Figure 16. Top: cropmarks at Stoke Bardolph (ATM TCC) showing sample locations. Bottom: spectral profiles at sample locations.

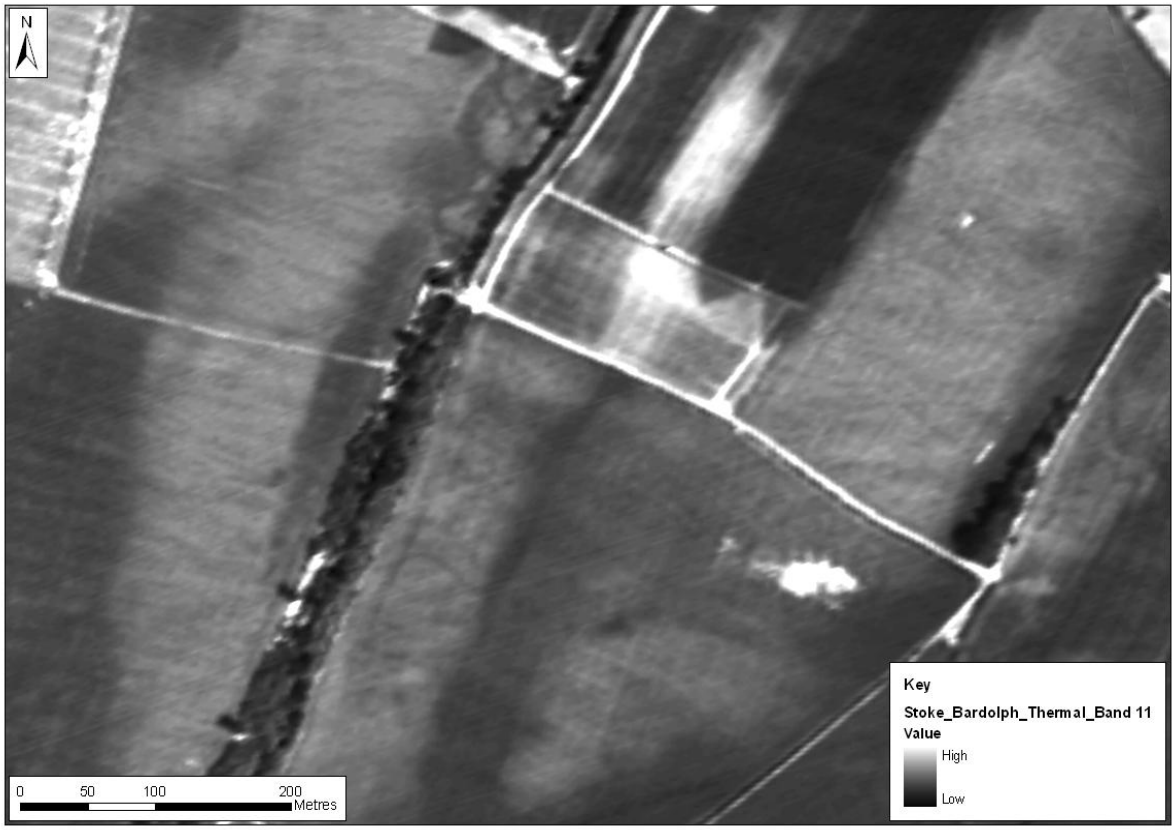

Figure 17. Stoke Bardolph, ATM band 11.

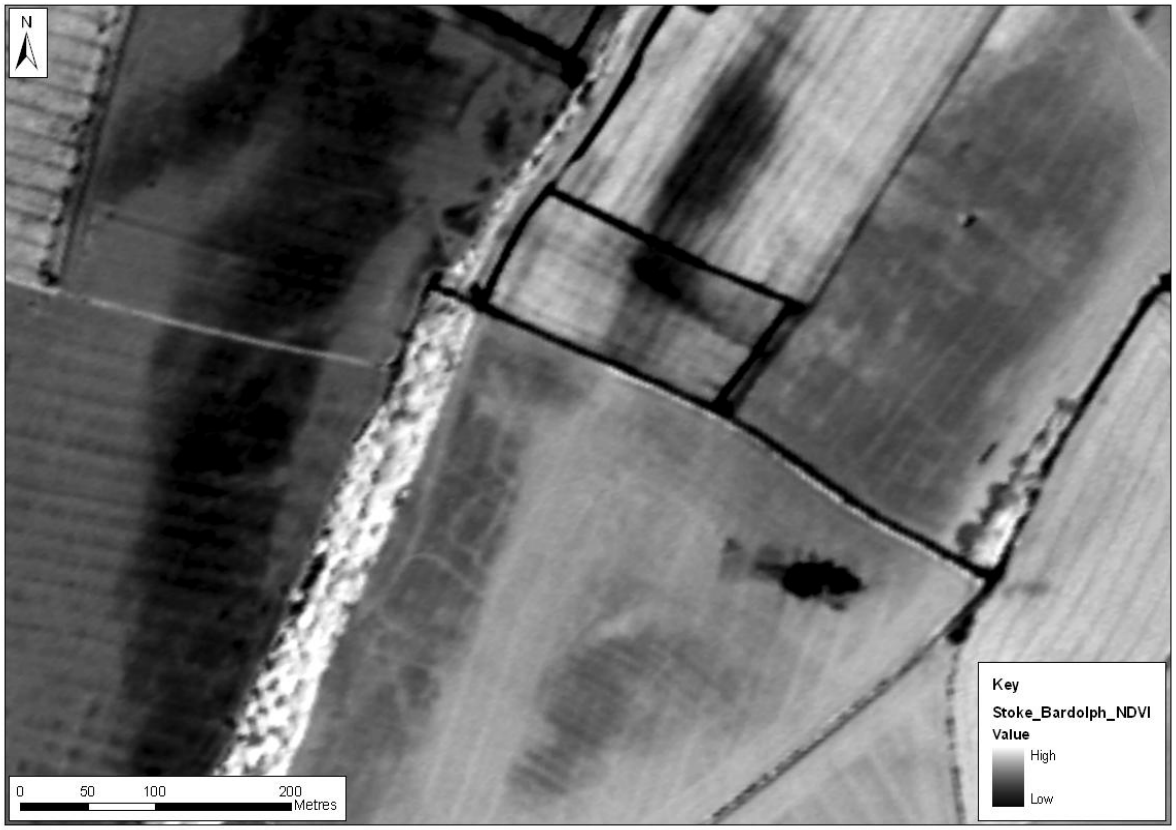

Figure 18 Stoke Bardolph, ATM NDVI.

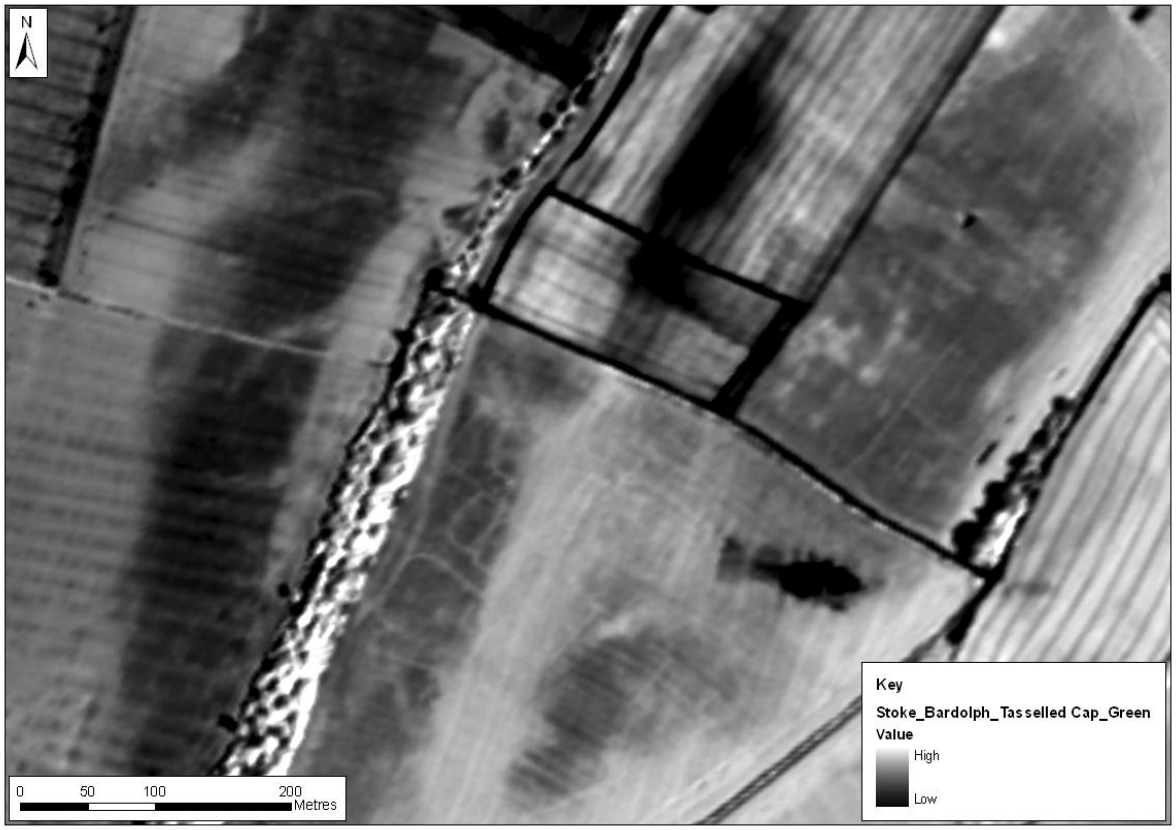

Figure 19. Stoke Bardolph, ATM Tasselled Cap Green.

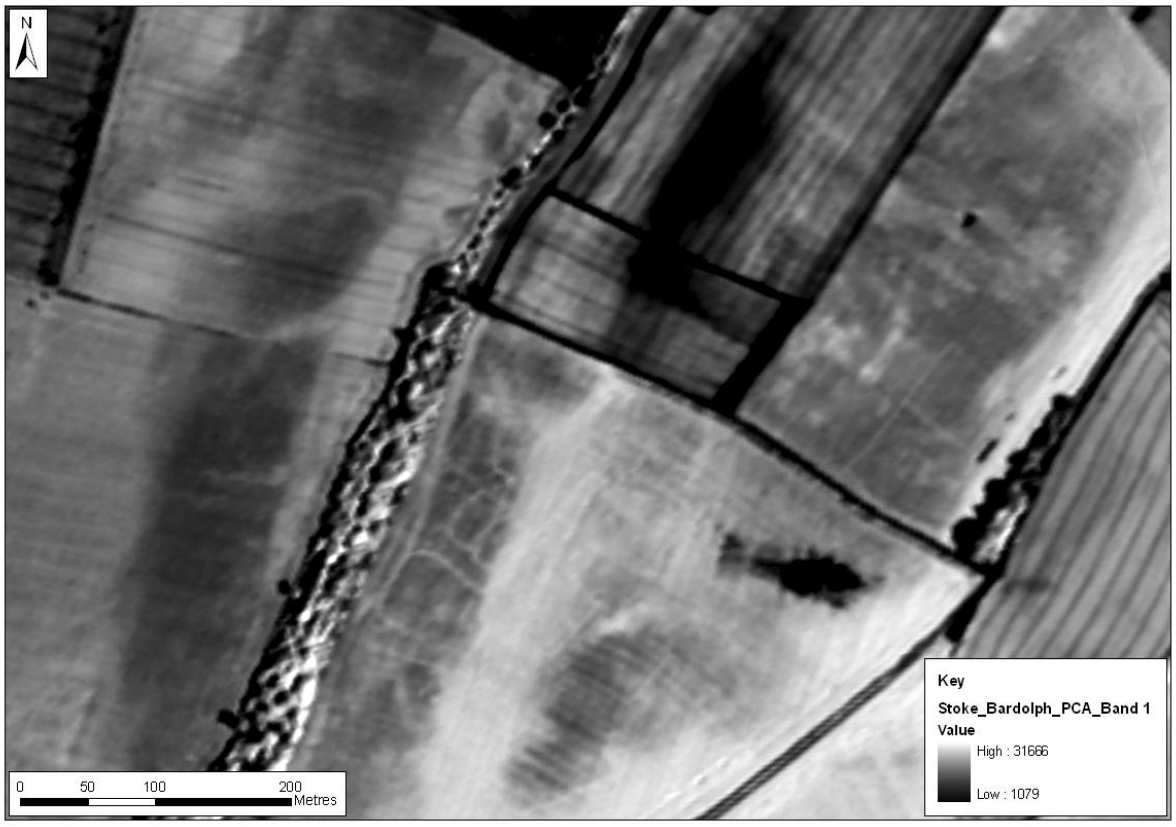

Figure 20. Stoke Bardolph, ATM first Principal Component.

Given that it has already been established that the cropmarks at both sites reflect differently to the background vegetation in the red and infrared parts of the spectrum, it is no surprise that vegetation indices that examine differential reflectance in these regions (NDVI Figs 13 and 18 and Tasselled Cap, Figs 14 and 19) succeed in significantly enhancing cropmark visibility. At both Fiskerton and Stoke Bardolph cropmarks are apparent as areas of more vigorous vegetation (lighter, higher index value NDVI) and greener vegetation. At Stoke Bardolph the degree to which these indices, tasselled cap in particular, enhance cropmark visibility is quite startling; an area apparently devoid of cropmarks in the visible spectrum is shown to be replete with features when visible and infrared data are examined together.

Finally, at both sites principal component analysis was used to compress change apparent across all 11 bands of the ATM imagery into three useful summary components. At Fiskerton component two (Fig. 15) reveals the cropmarks most clearly, and appears to summarise change in the infrared components of the image, while at Stoke Bardolph component one (Fig. 20) produces very clear definition of all cropmark features again by summarising change in the infrared parts of the image data.

3.4 CROPMARKS AND GEOARCHAEOLOGY

Geoarchaeological cropmarks, although exhibiting the same basic formation processes as anthropogenic cropmarks, represent larger scale phenomena. In this section both the spectral characteristics and image enhancement techniques for geoarchaeological cropmark are considered by examining ATM data and spectral profiles for two sites, at Barton in Fabis and Burton Meadows.

3.4.1 Spectral characteristics of geoarchaeological cropmarks

The spectral characteristics of different areas of cropmark, corresponding to terrace, palaeochannels and other relict fluvial features were examined by directly querying image data using Imagine Spectral Workstation software to generate spectral profiles at specific sample locations (Figs. 21 and 26).

In general the distinction between areas of terrace and palaeochannels is quite clearly evident in the TCC images at both test sites (Figs. 21 and 26) with terrace showing as pale green vegetation and palaeochannels as substantially darker green. Examination of the spectral response at sample locations shows a reasonable degree of difference between the reflectance characteristics of terrace and palaeochannels in the visible spectrum, particularly in the green and red bands. In the near infrared there is very little difference in reflectance between terrace and palaeochannels and it is only in the middle infrared, particularly between 1400 and 1600nm (ATM band 9) that there is a very clear difference in reflectance between terrace and palaeochannel. This difference is undoubtedly caused by spatial variations in SMD leading to corresponding variations in crop colour and vigour. Crops growing over palaeochannel features have access to a greater supply of moisture and nutrients and so grow with greater vigour and mature later than those on adjacent terrace areas.

3.4.2 Image enhancement and geoarchaeological cropmarks

The impact of a number of standard image enhancement techniques on the visibility of geoarchaeological cropmarks is explored in Figs. 22 – 30. Perhaps the most dramatic improvement in the visibility of geoarchaeological cropmarks is experienced by examining only the ATM thermal band (Figs. 22 and 27; band 11). The cropmarks are revealed with great contrast ands clarity and in many areas, particularly at the Barton test site, the masking affect of crop differences in adjacent fields is removed. It seems likely that this increase in clarity is due to the fact that the substantial geoarchaeological features under examination engender large thermal differences in soils and sediments; certainly to a much greater degree than is the case for anthropogenic cropmarks, and probably as a result of substantial differences in soil and sediment moisture content between terrace and channel.

Indices examining ratio differences between red and infrared reflectance are also highly effective at enhancing geoarchaeological cropmark definition. At both test sites the NDVI highlights the variations in vegetation vigour between terrace and channel (Figs. 23 and 28). The tasselled cap green image transform (Figs. 24 and 29) provides a rather more effective view of green vegetation vigour than NDVI, and at both Barton and Burton the effects of vegetation change between adjacent fields is substantially reduced.

Finally, the tasselled cap wet transform (Figs 25 and 30) which gives an indication of the wetness of soils and sediment provides useful additional information. At Burton in particular this transform highlights channel details in two bare earth fields in the mid-right quadrant of the image that, because of the absence of green vegetation, were not susceptible to vegetation based indices such as NDVI and TC green.

3.4.3 Image Classification

Image classification techniques rely upon the ability of computer analysis of the spectral data contained within multispectral images to identify homogenous clusters of pixels with distinctive spectral characteristics. In the present study unsupervised classification using an ISODATA algorithm was employed to examine a number of ATM and CASI scenes including both geoarchaeological and anthropogenic cropmarks. Typical results are shown in Fig. 31, which shows a 26 class unsupervised classification of anthropogenic cropmarks at Fiskerton. Here and elsewhere results were uniformly poor, and in spite of numerous adjustments to the parameter controlling the classification algorithm, the technique failed to completely isolate pixel values relating to cropmark features from background values. This is not unexpected, as other archaeological users have reported similar problems (*cf* Rowlands and Sarris, 2007). The principal reason that classification fails is due to the similarity of multi-dimensional pixel vales in adjacent classes, in effect a lack of contrast. This is amply illustrated by examining the spectral profiles of the 26 classes of the test classification (Fig. 32). It will be seen that adjacent classes have very similar pixel values. While classification may be effective at distinguishing spectral properties of large bodies with aggregate class values, for example the contrast between a field of barley and one of grass, it does not function at the level of an individual cropmark, in effect spectral variation within one vegetation body.

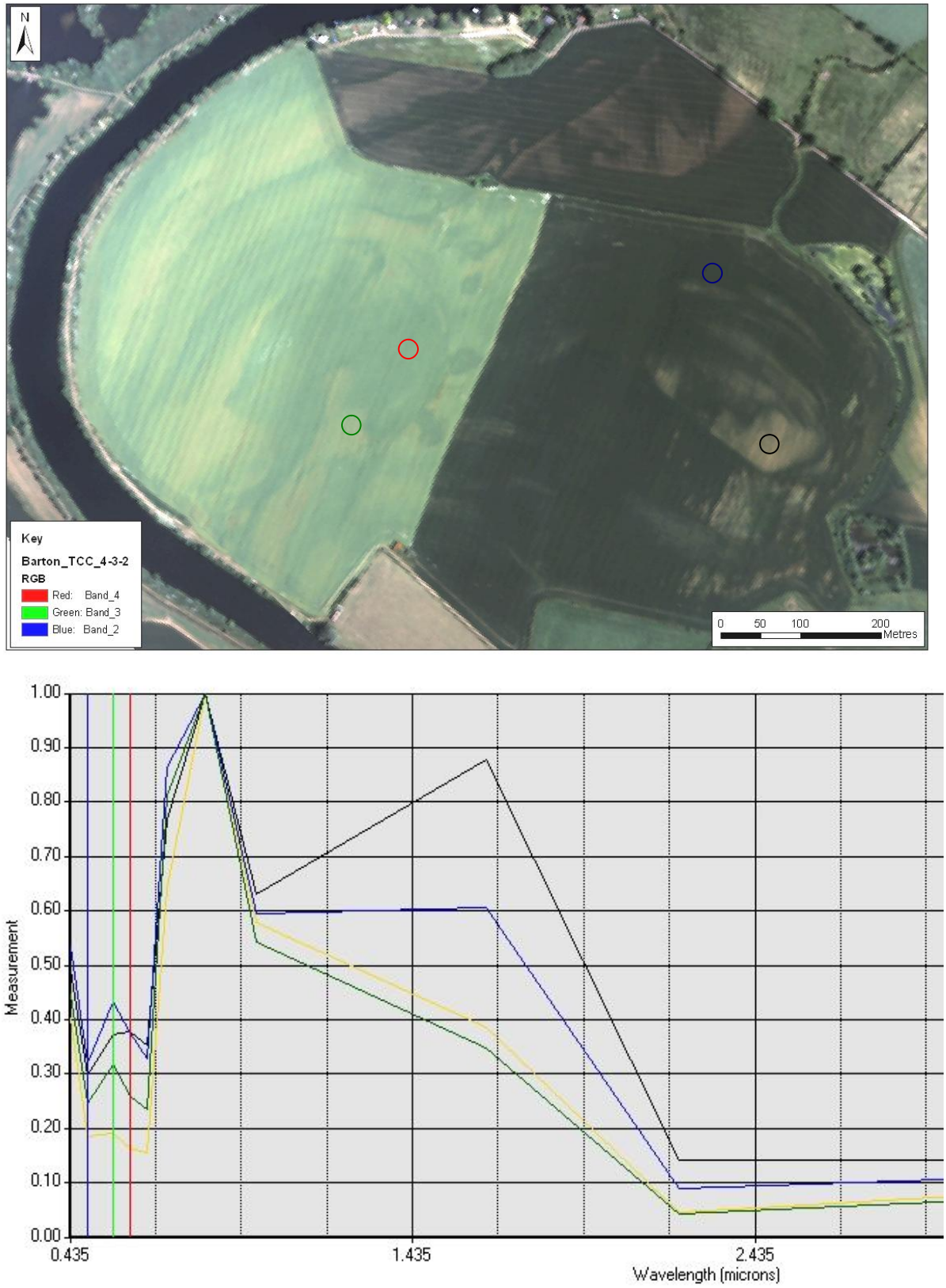

Figure 21. Top: cropmarks at Barton in Fabis (ATM TCC) showing sample locations. Bottom: spectral profiles at sample locations.

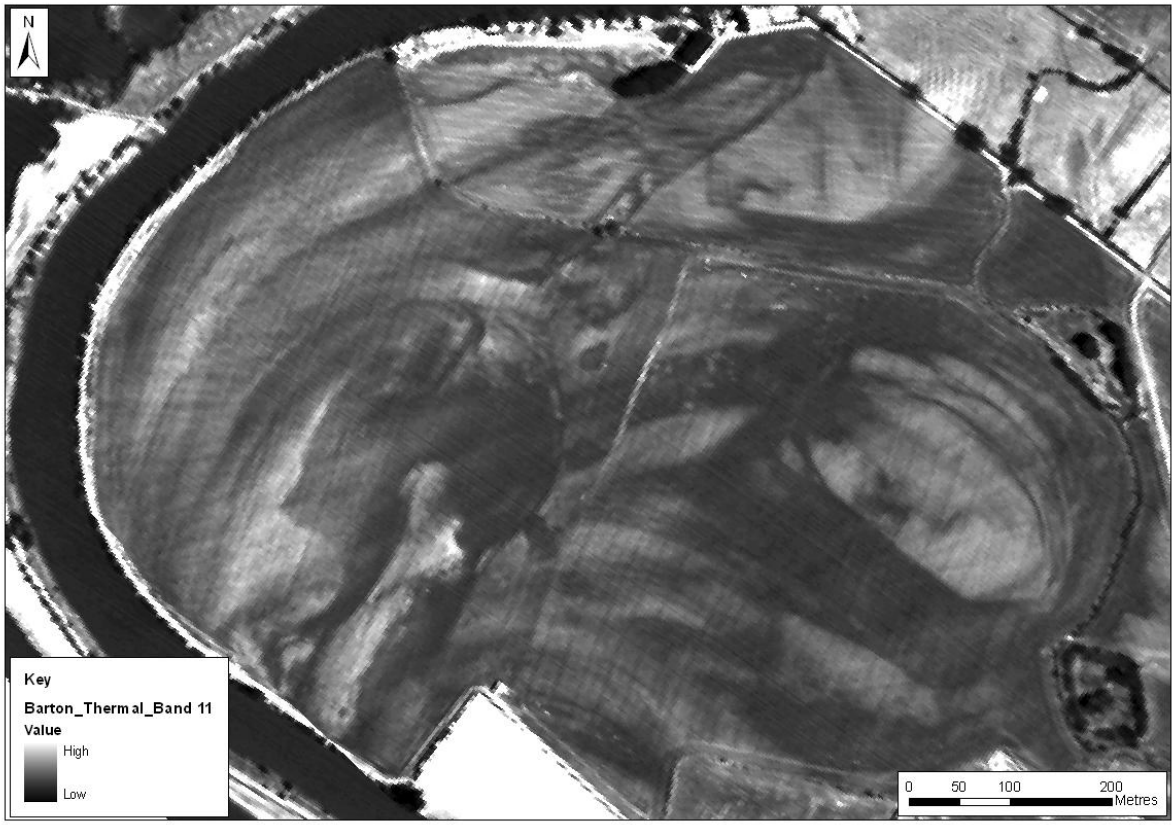

Figure 22. Barton in Fabis, ATM band 11.

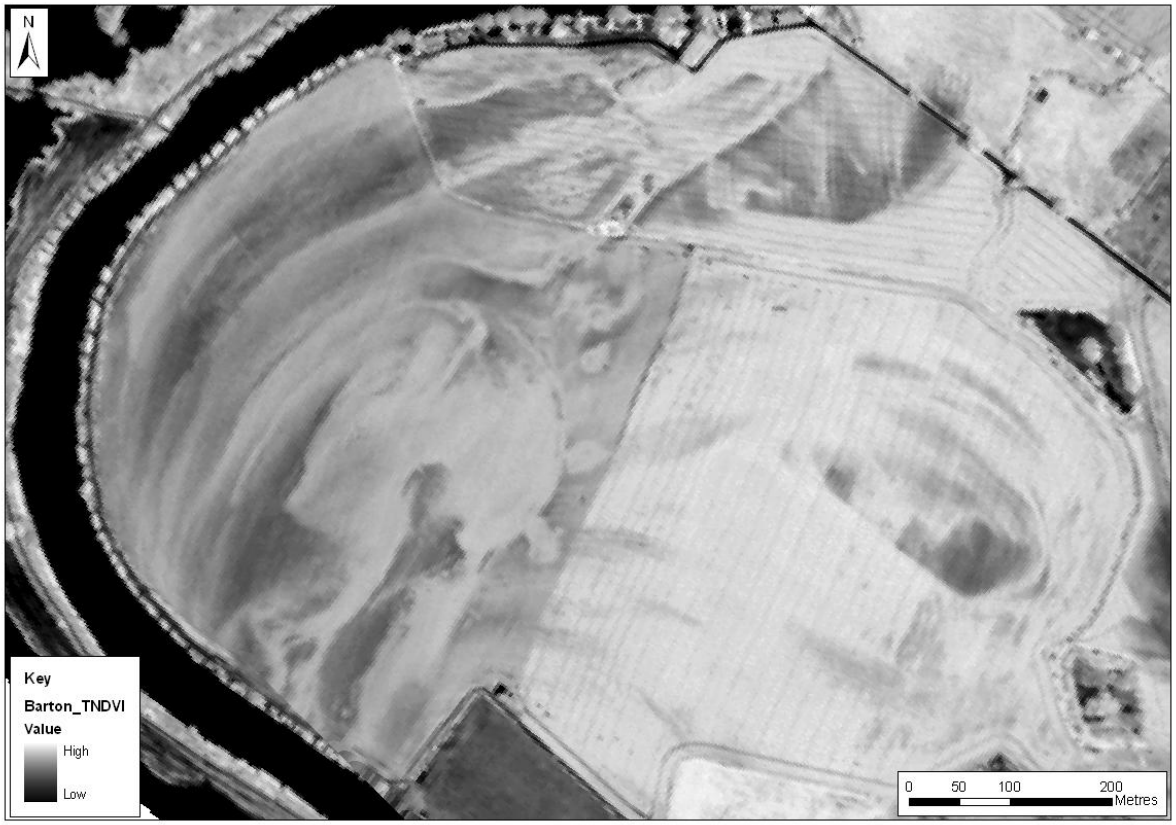

Figure 23. Barton in Fabis, ATM TNDVI.

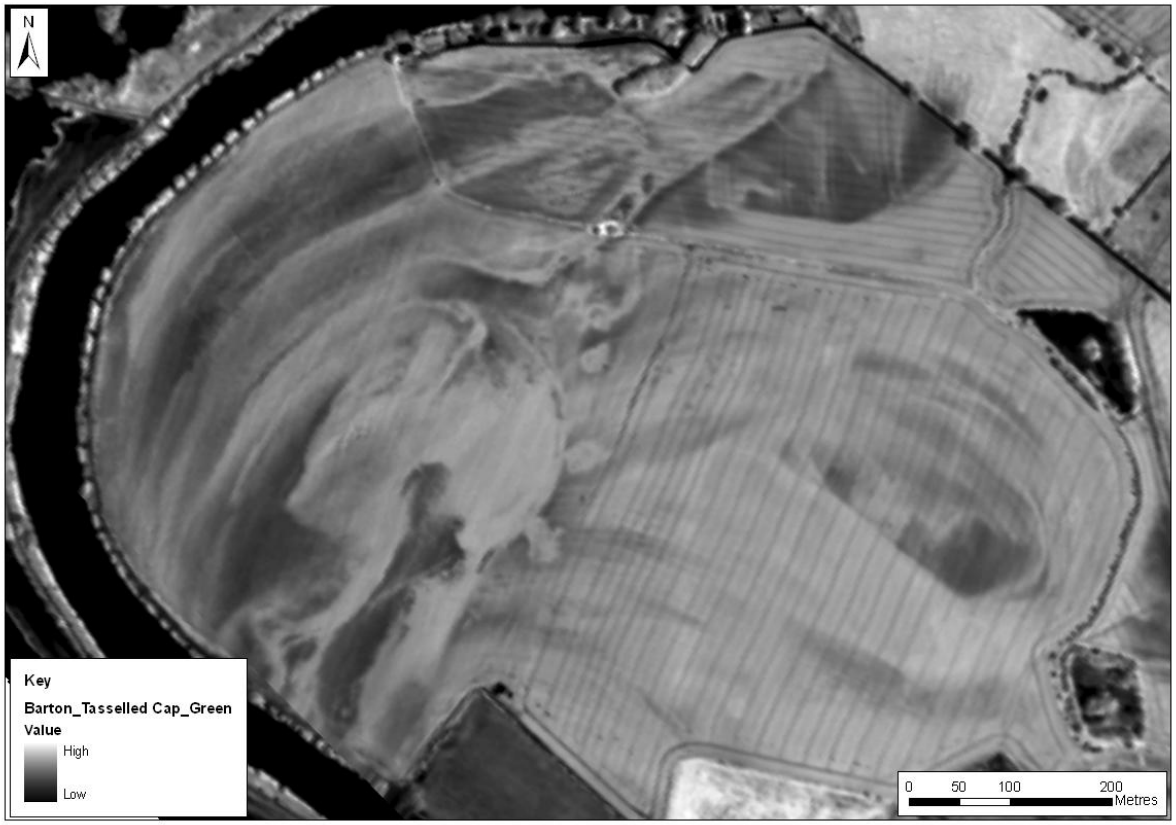

Figure 24. Barton in Fabis, ATM Tasselled Cap, Green.

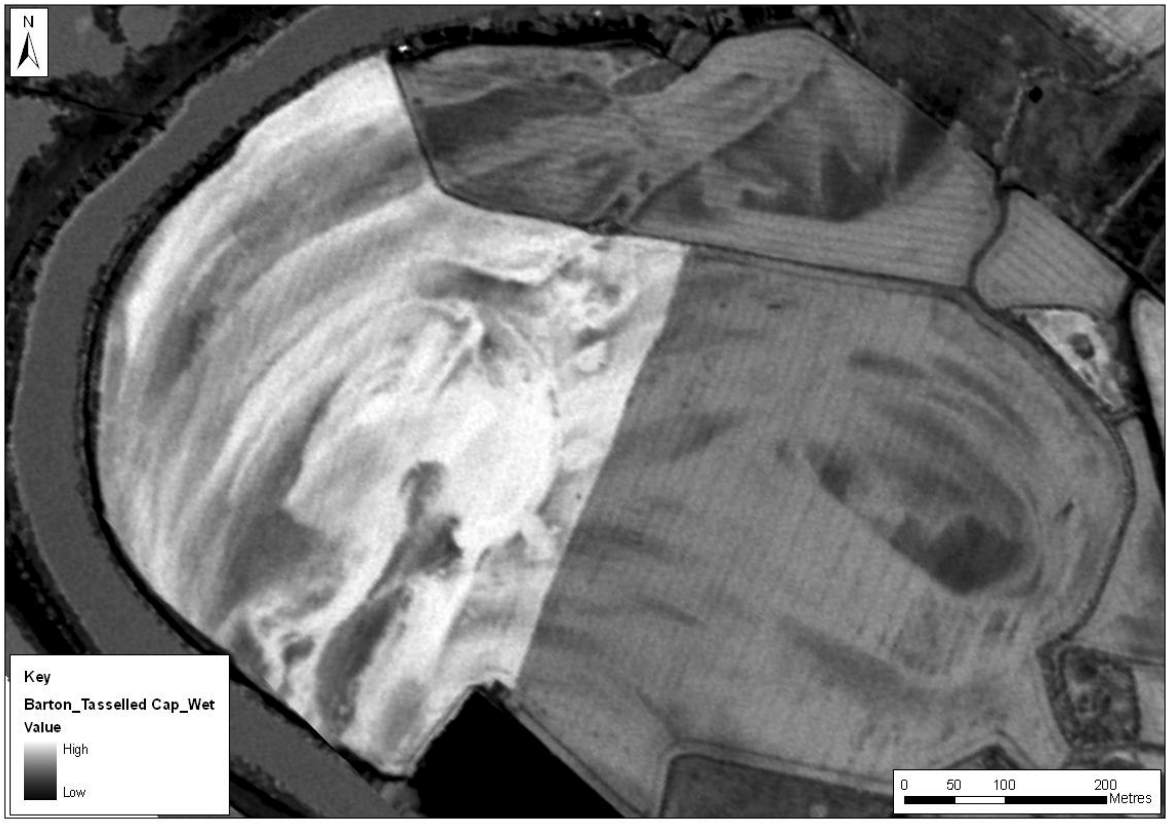

Figure 25. Barton in Fabis, ATM Tasselled Cap, Wet.

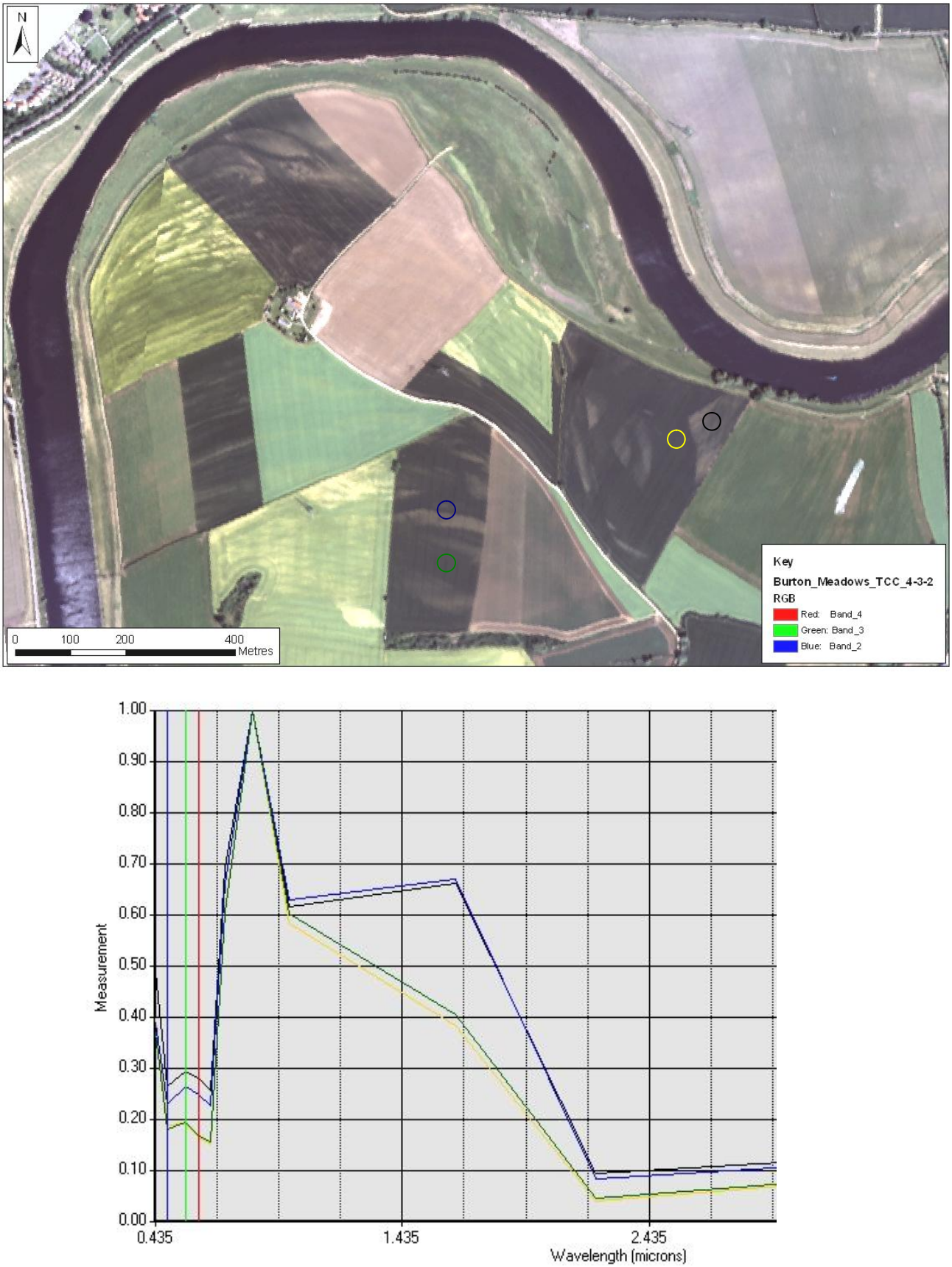

Figure 26. Top: cropmarks at Burton Meadows (ATM TCC) showing sample locations. Bottom: spectral profiles at sample locations.

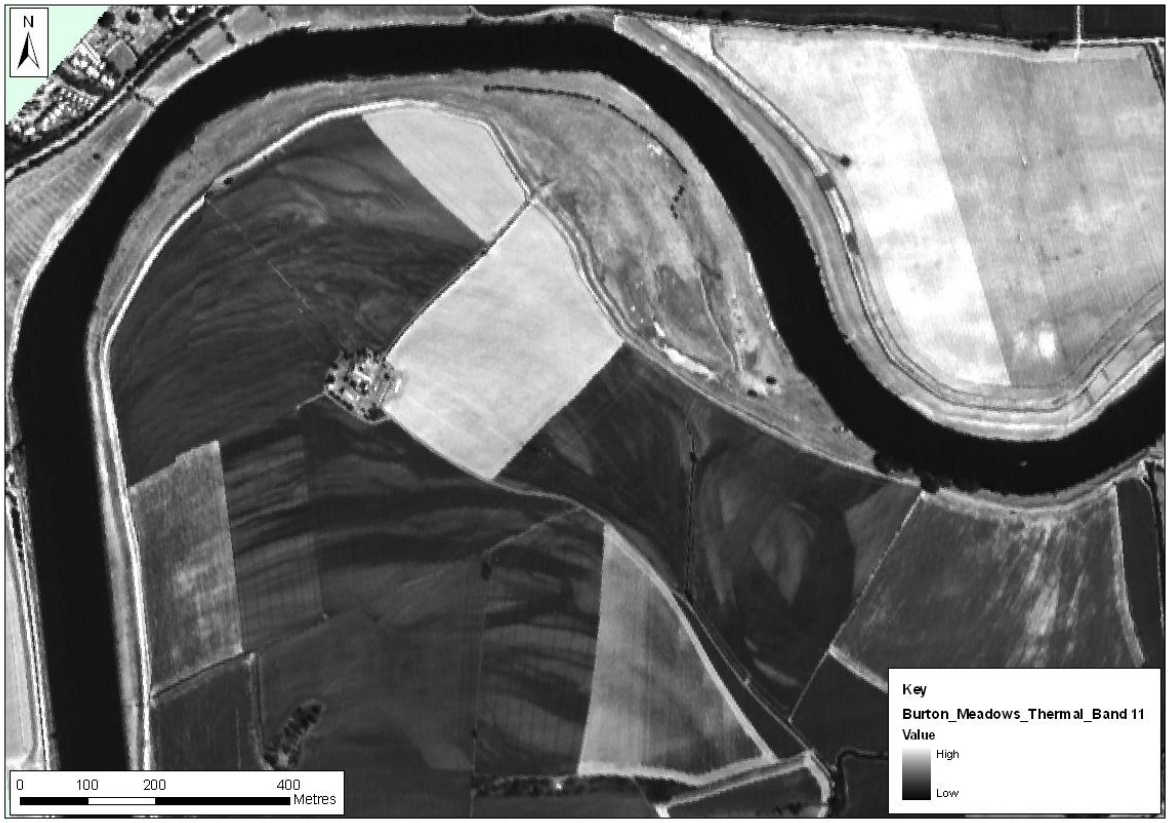

Figure 27. Burton Meadows, ATM Band 11.

Figure 28. Burton Meadows, ATM NDVI.

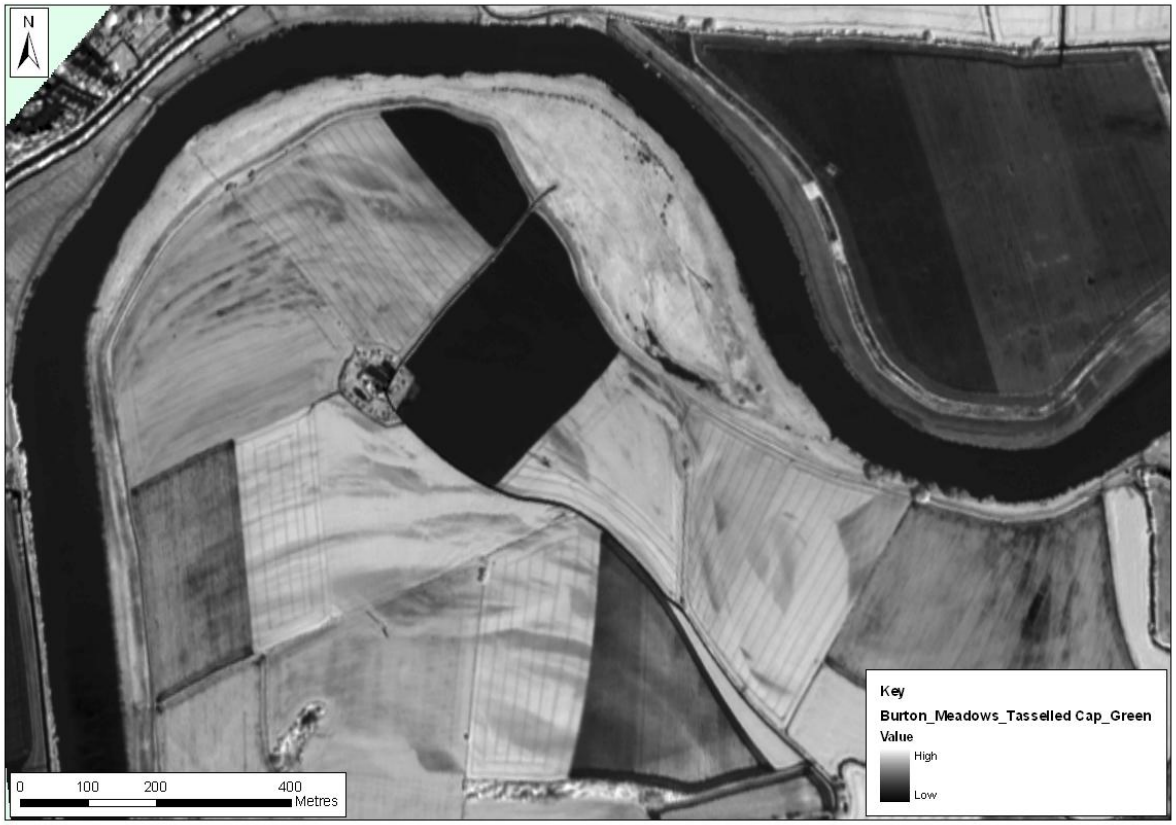

Figure 29. Burton Meadows, ATM Tasselled Cap, Green

Figure 30.Burton Meadows, ATM Tasselled Cap, Wet.

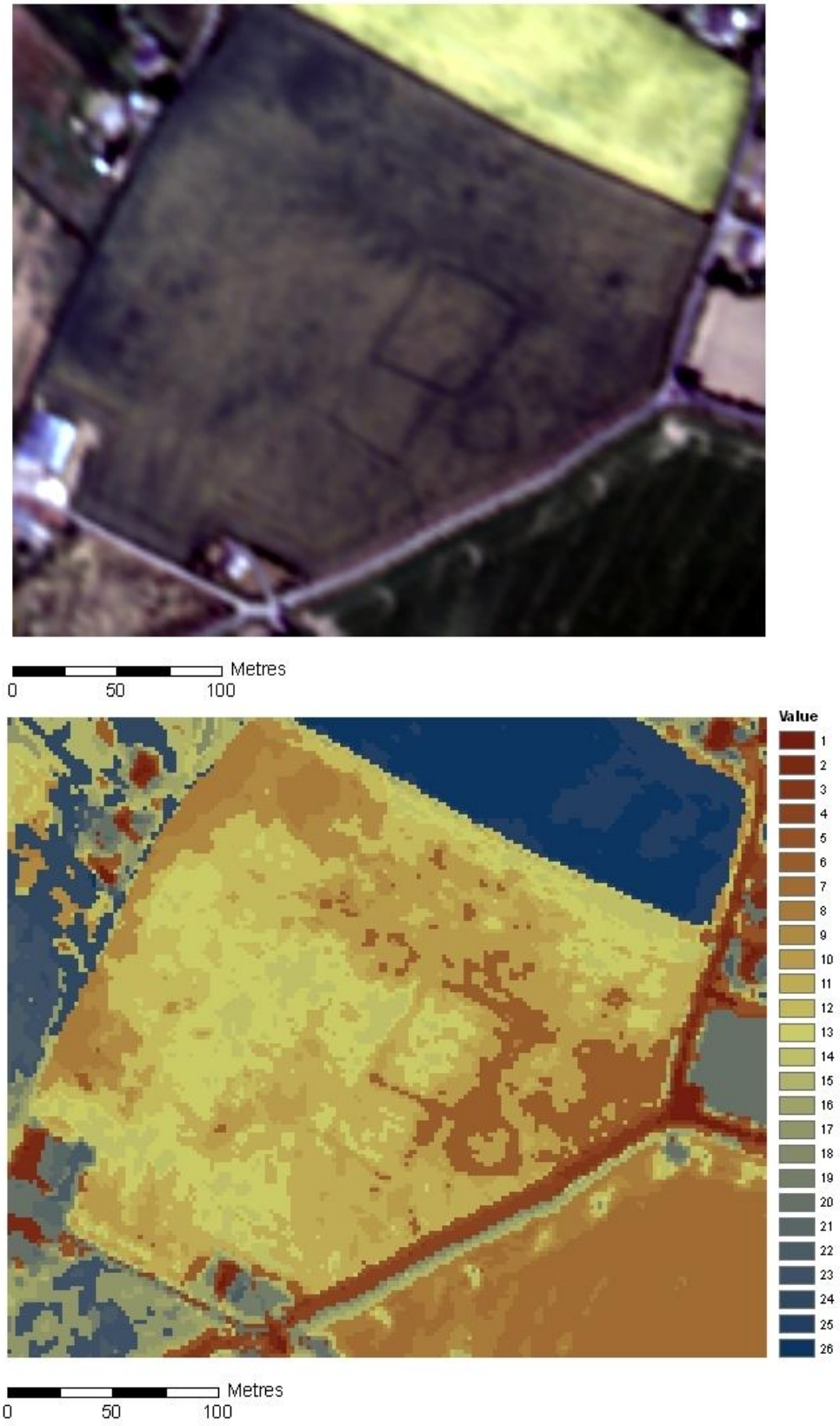

Figure 31. Fiskerton. Top ATM TCC showing cropmarks. Bottom unsupervised classification (ISODATA Clustering; 26 classes) of the image data.

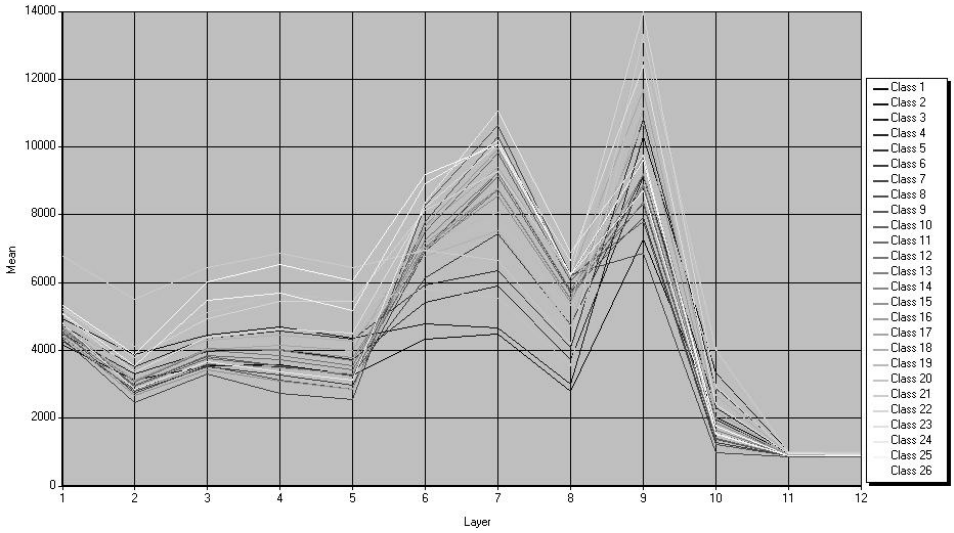

Figure 32. Spectral profiles of the 26 classes developed by the ISODATA algorithm and shown in figure 31.

In general it must be concluded that as an aid to interpretation of ATM and CASI images for archaeological purposes image in most cases classification has little to offer.

3.5 CONCLUSIONS

Examination of spectral profiles and image enhancements methods for anthropogenic and geoarchaeological cropmarks has demonstrated that a number of techniques are particularly effective:

- Both anthropogenic and geoarchaeological cropmark are most clearly distinguished in the middle infrared parts of the spectrum, between 1400 and 1600nm.

- Cropmarks may be revealed by examining the infrared parts of the spectrum in areas apparently devoid of cropmarks when viewed in the visible spectrum

- Cropmarks are effectively enhanced by indices examining ratios of red and infrared reflectance such as NDVI and TC green

- Thermal data (ATM band 11) is highly effective for defining fluvial geoarchaeological features due to the substantial soil moisture differences between terrace and channel.

- The TC wet index is able to reveal geoarchaeological detail in unvegetated areas.

- Automatic classification of imagery does not significantly assist in identification of features of archaeological interest or interpretation as there is generally insufficient difference in spectral characteristics between archaeological features and background values.

4 RESULTS: DAEDALUS 1268 AIRBORNE THEMATIC MAPPER

4.1 INTRODUCTION

The following section considers the results obtained from analysis of Daedalus 1268 Airborne Thematic Mapper data for ten test areas in the Middle Trent Valley (Fig. 1). In each instance an identical suite on analytical techniques was employed and is discussed in summary. Techniques comprised production of:

- True Colour Composite (Bands 4-3-2)
- False Colour Composite (Bands 9-7-3)
- Thermal Band (11)
- NDVI
- Principal Component Analysis
- Tasselled Cap Green
- Tasselled Cap Wet

Test sites and the efficacy of the imagery and the analytical techniques employed are discussed in turn below. Figures showing the results of all analytical techniques are shown in appendix 1; high resolution digital versions of the illustrative figures are provided on the DVD-ROM that accompanies this report.

4.2 SWARKESTONE, DERBYSHIRE

The Swarkestone test area covers a roughly 5km2 area of the Trent Valley between Swarkestone in the north and Stanton-by-Bridge in the south and centres on Swarkestone Bridge (Fig. 33).

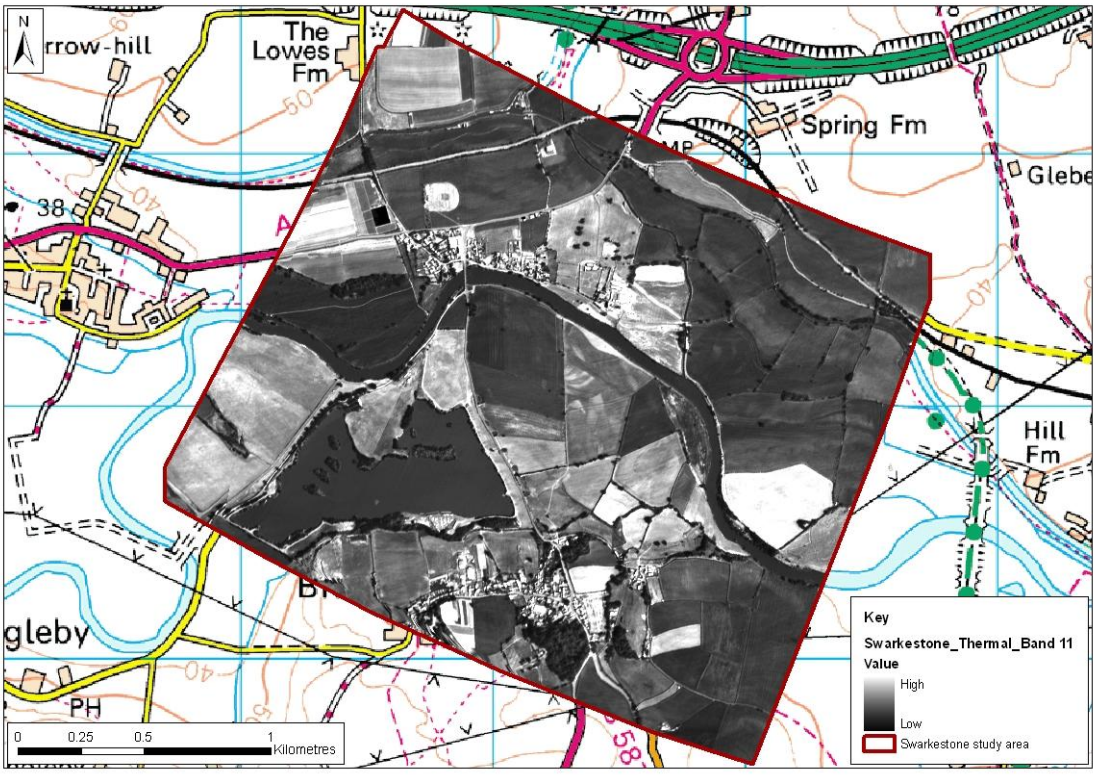

Figure 33. Swakestone, Derbyshire. ATM thermal data (band 11).

A meander of the Trent crosses the centre of the study area, which comprises both terrace and floodplain. The extreme north of the study area includes part of the Bronze Age barrow cemetery of Swarkestone Lowes, although no evidence of the barrows is apparent in the ATM data, which chiefly reveals aspects of the floodplain and terrace geomorphology. Thermal data (band 11; Fig. 33) are particularly effective in this study area and reveal palaeochannels locations and terrace fragments to the south and east of the present course of the Trent. Further channel features are also evident to the north of the present channel between Swarkestone village and the Trent & Mersey canal, which follows the floodplain edge at this point. Vegetation indices, in particular TC Green and NDVI (Fig. 59, appendix 1) are also effective at enhancing geomorphological detail in this largely arable landscape.

4.3 TRENT-DERWENT CONFLUENCE, DERBYSHIRE

This study area comprises an approximately 3km2 at the confluence of the River Trent with its tributary the River Derwent (Fig. 34) Aspects of the complex geomorphology of this confluence zone are apparent in the TCC (Fig. 60; appendix 1) but are most clearly revealed in the thermal data (band 11, Fig. 34) and TC green transform (Fig. 60; appendix 1). Together these reveal a sequence of sinuous palaeochannels, most probably of the Derwent, to the west of the present confluence suggesting either evulsive movement of the Derwent or that the confluence has migrated eastwards over time. Significant ridge and swale topography are apparent within the meander of the Trent. Thermal data and vegetation indices also effectively highlight vegetation differences associated with earthwork ridge and furrow to the north east of the Trent.

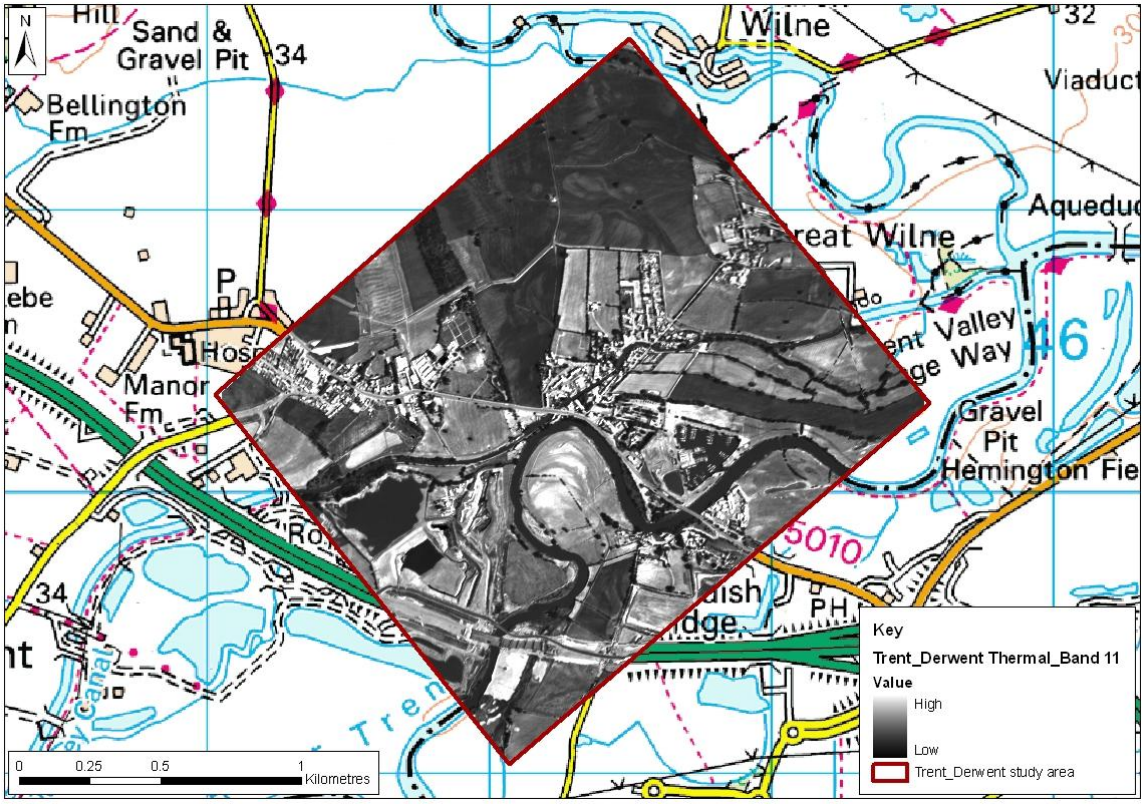

Figure 34. Trent-Derwent Confluence, Derbyshire. ATM thermal data (band 11).

4.4 HEMINGTON, LEICESTERSHIRE

This approximately 3km2 study area is immediately to the west of the Trent-Derwent confluence and includes largely the reworked sands and gravels of the Holocene Hemington Terrace of the Trent. A sequence of timber bridges crossing the Trent was recovered from gravel workings at Hemington Fields Gravel Pit, indicating the reworking of the terrace deposits continued well into the last millennia. Once again TCC data reveal little of the geomorphology of this study area (Fig. 61; appendix 1). In this study area once again thermal data (band 11; Fig. 35) and vegetation indices, in particular NDVI (Fig. 61; appendix 1) are most effective at revealing otherwise obscured aspects of floodplain and terrace geomorphology, including internal details of the relict meander of the Trent indicated by a curving hedge line to the south of the line of the A50 (under construction t the time of the survey flight). Some internal detail of the Hemington Terrace adjacent to Hemington Fields Gravel Pit is also apparent in these data, indicating the presence of relict channels followed by surviving stream lines.

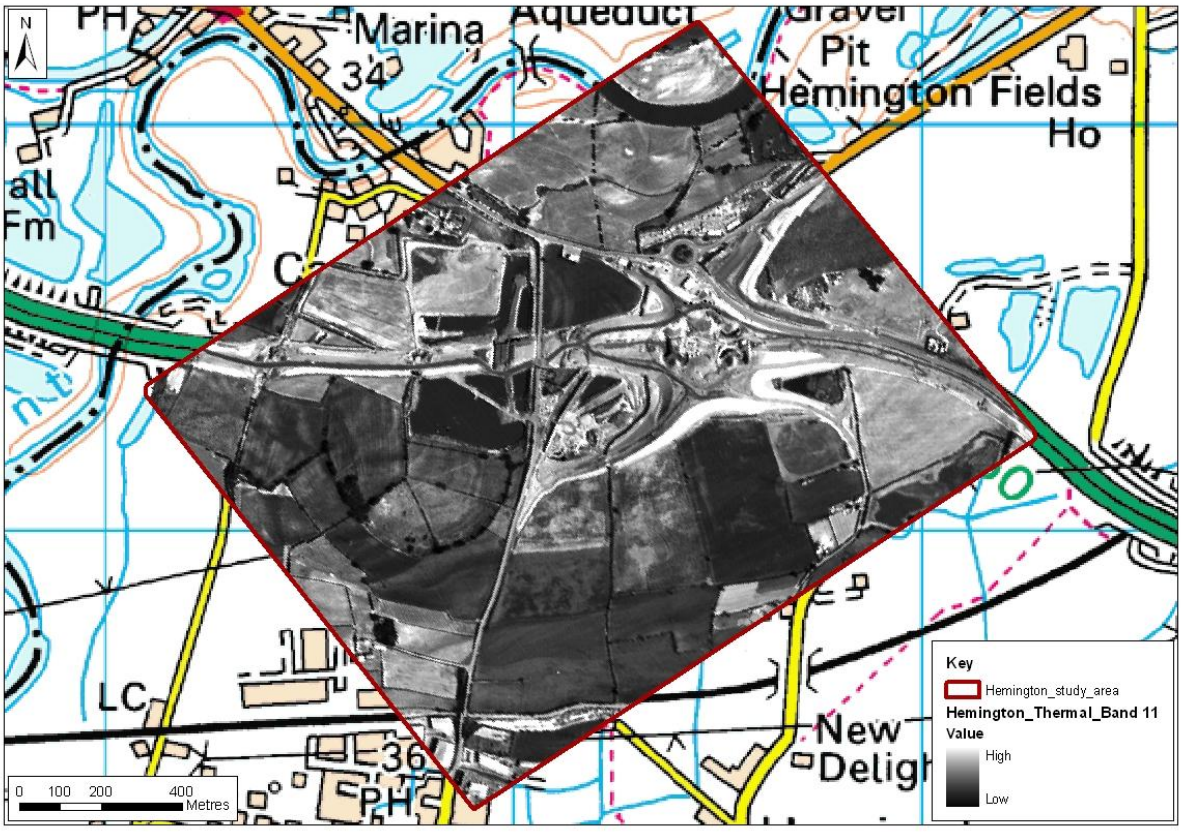

Figure **35**. Hemington, Leicestershire. ATM thermal data (band 11).

4.5 BARTON-IN-FABIS, NOTTINGHAMSHIRE

The Barton-in-Fabis study area has already been reviewed in section 3.2. It comprises a substantial meander of the Trent adjacent to the Roman Villa site at Glebe Farm. The clarity of detail revealed in the meander core in the Thermal (Fig. 36) and vegetation indices data (Fig. 62; appendix 1) is exceptional. The data

indicate a far more complex geomorphological development than might be anticipated from the present channel form. Briefly, the area comprises a channel draining the Mercia Mudstone ridge and terrace deposits to the south-east, on which the villa beneath modern Glebe Farm is sited, forming a complex confluence with palaeocourses of the Trent. There are clearly indicated terrace fragments within the meander core and perhaps some indication of anthropogenic features at the heart of the meander. Little of this complexity is apparent in the visible spectrum (TCC, Fig. 62) emphasising the role that multispectral remote sensing might play in the examination of such landscapes.

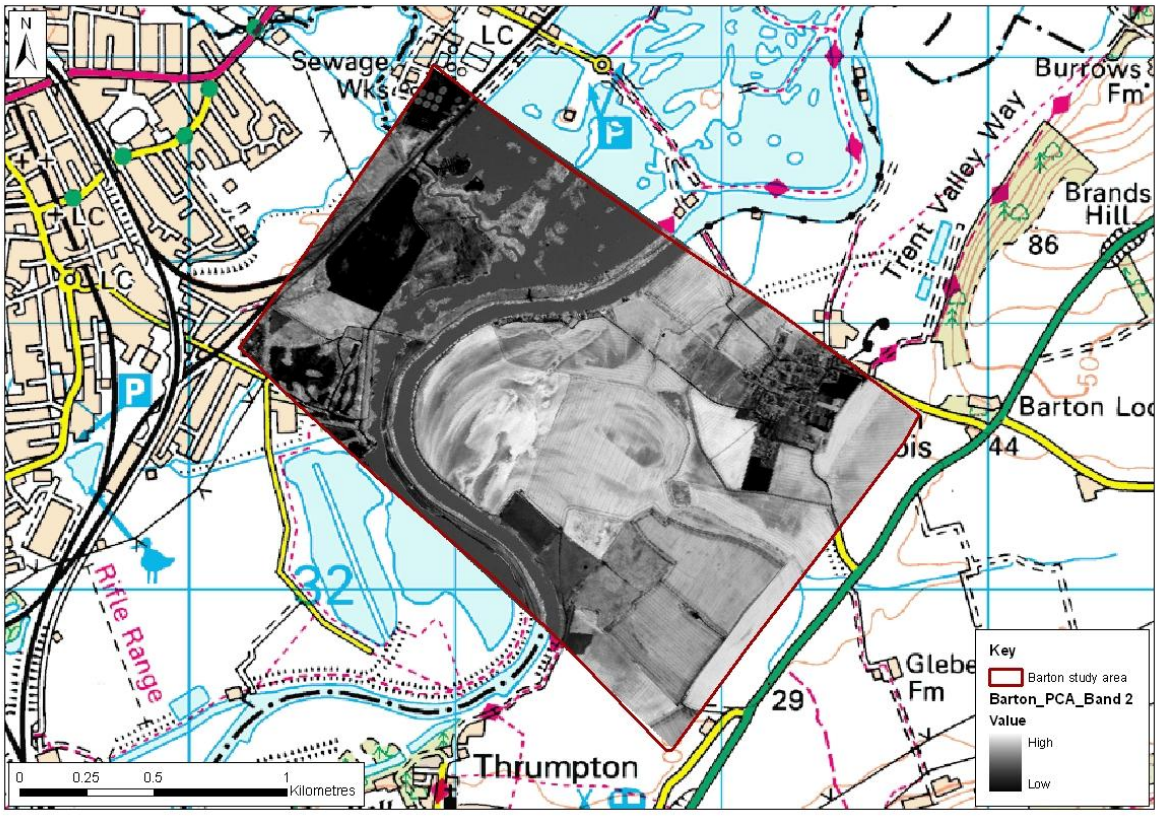

Figure 36. Barton, Nottinghamshire. ATM thermal data (band 11).

4.6 CLIFTON, NOTTINGHAMSHIRE

The Clifton study area comprises an approximately 2km2 area to the south-east of the River Trent on the southern outskirts of Nottingham. In contrast to the other areas examined the geology of this study segment is wholly Mercia Mudstone. The area is included as it forms the general setting for a "lost" monument, potentially of some regional importance, that is the possible hillfort of Brand's Hill, described by John Aubrey in his unpublished *Monumenta Brittanica* in the early 17th century, but subsequently entirely eradicated by ploughing. Conventional aerial photography has provided no indication of the site of the monument; multispectral remote sensing provides another approach to rediscovering the monument.

Unfortunately the ATM imagery provides no further evidence of the location of the monument described by Aubrey. Soil and vegetation contrast is most clearly evident in the thermal band (band 11; Fig 37). An extensive area of earthwork ridge and

furrow are clearly shown in the north-east of the image; however, no trace of anthropogenic features is evident in the arable fields that cover most of the remainder of Brands Hill. A sequence parallel of curvilinear cropmarks are apparent on the south-east side of Brands Hill, approximately following the 60m contour line. However, these cropmarks are not of archaeological origin, but rather are caused by skerry bands in the Mercia Mudstone and are common hereabouts. The location of Aubrey's monuments remains unknown.

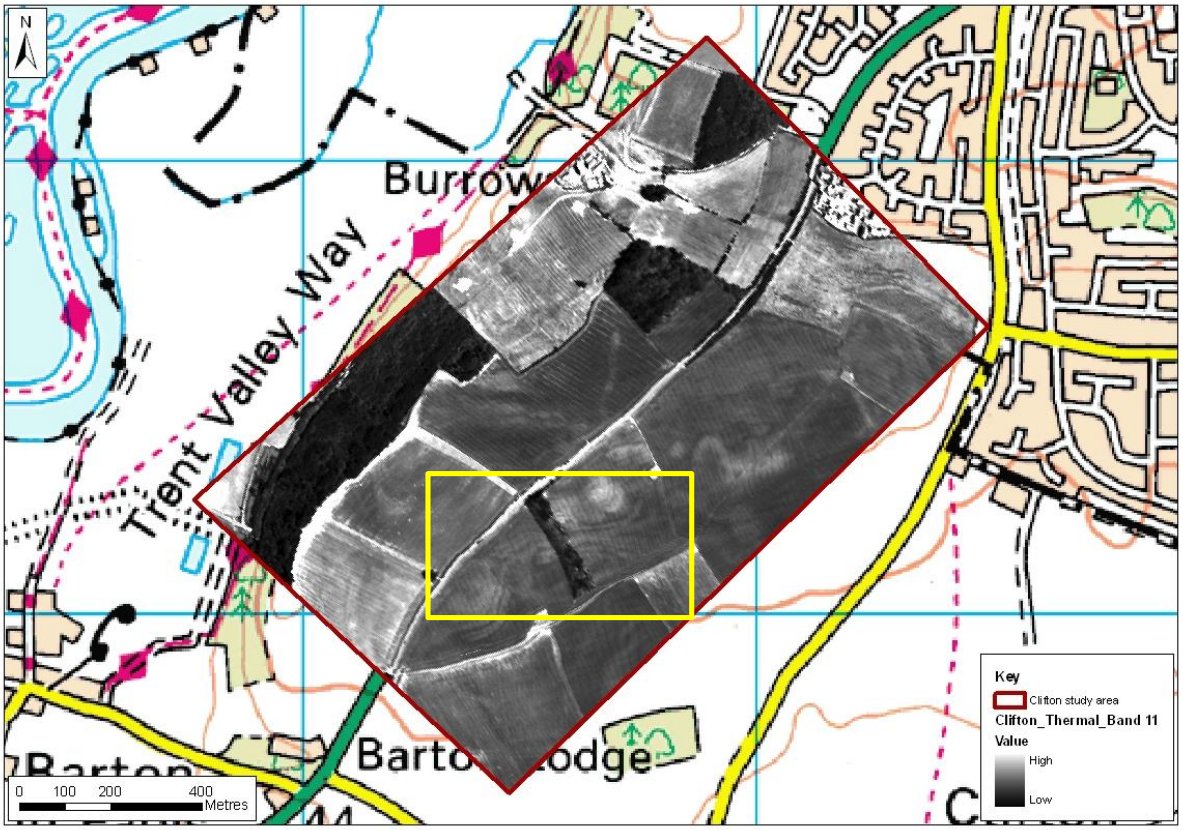

Figure 37. Clifton, Nottinghamshire. ATM thermal data (band 11). The distinctive cropmarks of skerry banding in the bedrock are indicated by the yellow box.

4.7 CARLTON, NOTTINGHAMSHIRE

This study area comprises approximately 2km2 of river terrace and floodplain to either side of the Trent between Radcliffe and Carlton selected because of the presence of anthropogenic cropmarks on the Holme Pierrepont terrace east of Carlton which were previously mapped by the English Heritage National Mapping Programme (NMP). Unfortunately none of the mapped cropmarks are apparent in the ATM data. Both the thermal band (11, Fig. 38) which provides the best overall definition of terrace deposits and the vegetation indices which rely on red/near infrared contrast (NDVI and TC Green; Fig. 64, appendix 1) clearly show geoarchaeological cropmarks of terrace and adjacent alluviated areas. Since these geological variations are well-evident, which suggests sufficient soil moisture deficit

to cause moisture stress in crops, it may be that the finer cropmarks of anthropogenic features were not resolved by the relatively coarse c 2m spatial resolution of the ATM data.

Figure 38. Carlton, Nottinghamshire. ATM thermal data (band 11).

4.8 STOKE BARDOLPH, NOTTINGHAMSHIRE

The Stoke Bardolph study area comprises approximately 6km2 of terrace and floodplain on the north and south banks of the Trent. The area south of the Trent has already been discussed in section 3.2 and CASI data for this same area is reviewed later in section 5.4. Fig.39 shows PCA2 and thermal band data for part of the study area north of the Trent selected for the presence of extensive anthropogenic cropmarks, including those of field systems, enclosures and ring-ditches, again previously mapped by the NMP. The fields containing cropmarks appear to have been bare earth at the time of the survey flight and no aspect of the cropmark landscape is evident here as soilmarks, although considerable soil variation is apparent, but perhaps represents largely the vestiges of post-medieval field boundaries removed to create one large field for more convenient cultivation.

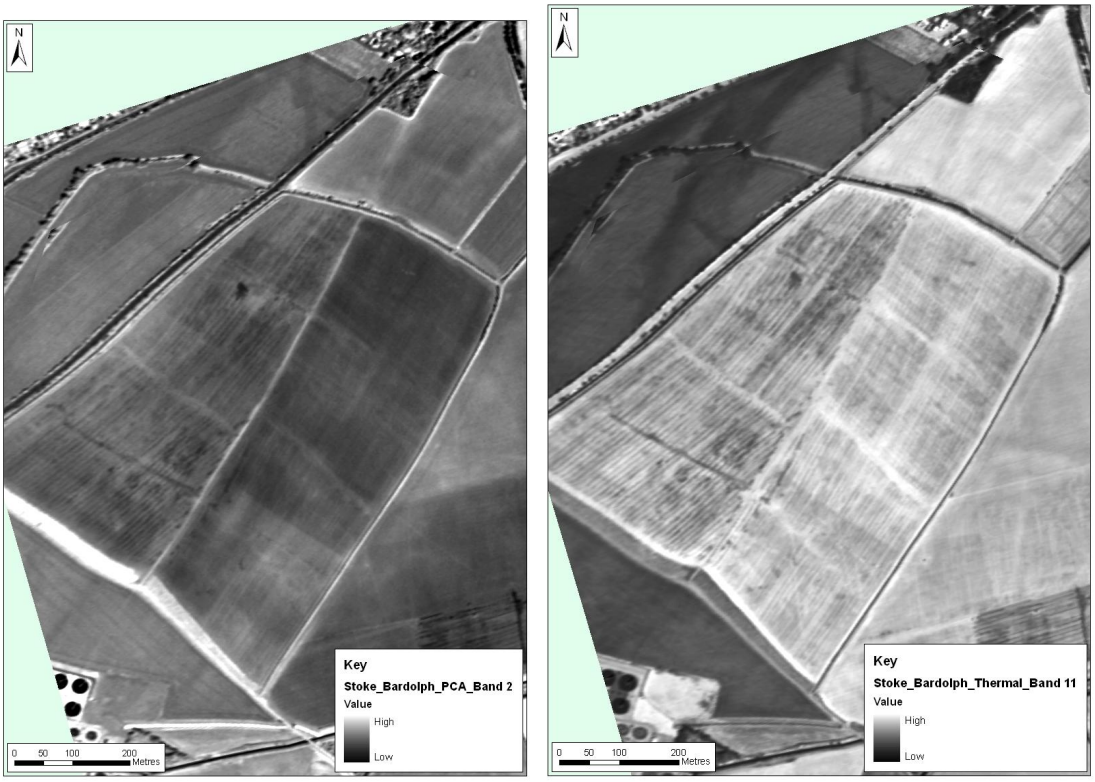

Figure 39. Stoke Bardolph, Nottinghamshire. Left, ATM thermal band 11; right ATM PCA 2.

This study area clearly highlights the natural limitations of ATM, and other multi and hyperspectral techniques; there must be a physical phenomenon to detect for these techniques to be of use. In the Stoke Bardolph data north of the Trent (section 3.2, Figs. 16-20) nascent cropmarks were revealed in the infrared part of the data as here slight contrast between parched and green crops were enhanced even though no cropmarks were evident in the visible spectrum. In the study area above the absence of crop, and the apparent lack of soilmarks for features documented as cropmarks (which incidentally probably indicates that the buried archaeology hereabouts is reasonably well preserved, or was in 1996) mean that there is no physical phenomenon indicating archaeology for the ATM sensor to detect, no matter what image enhancement techniques are employed.

4.9 BURTON MEADOWS, NOTTINGHAMSHIRE

This study area comprises a segment of Holme Pierrepont terrace and floodplain immediately south of the present course of the Trent between Burton Meadows and Shelford. ATM data for the substantial meander core of Burton Meadows has already been reviewed in section 3.2. Here we focus on a small section of terrace at Shelford, chosen because of the presence of extensive anthropogenic cropmarks mapped by the NMP. The terrace here is bisected by a sequence of parallel north-east to south-west aligned palaeochannels, probably relict braid channels and ATM data successfully indicate a number of cropmark features within one of the islands of terrace between the channels (Fig. 40). Both the cropmarks and terrace/channel variation are evident in the visible spectrum (TCC, Fig. 66, appendix 1) as well as through a variety of enhancement techniques. Vegetation indices are again particularly effective at enhancing the crop variations, while thermal data (Fig. 66, appendix 1) emphasises slight earthworks, including relict ridge and furrow.

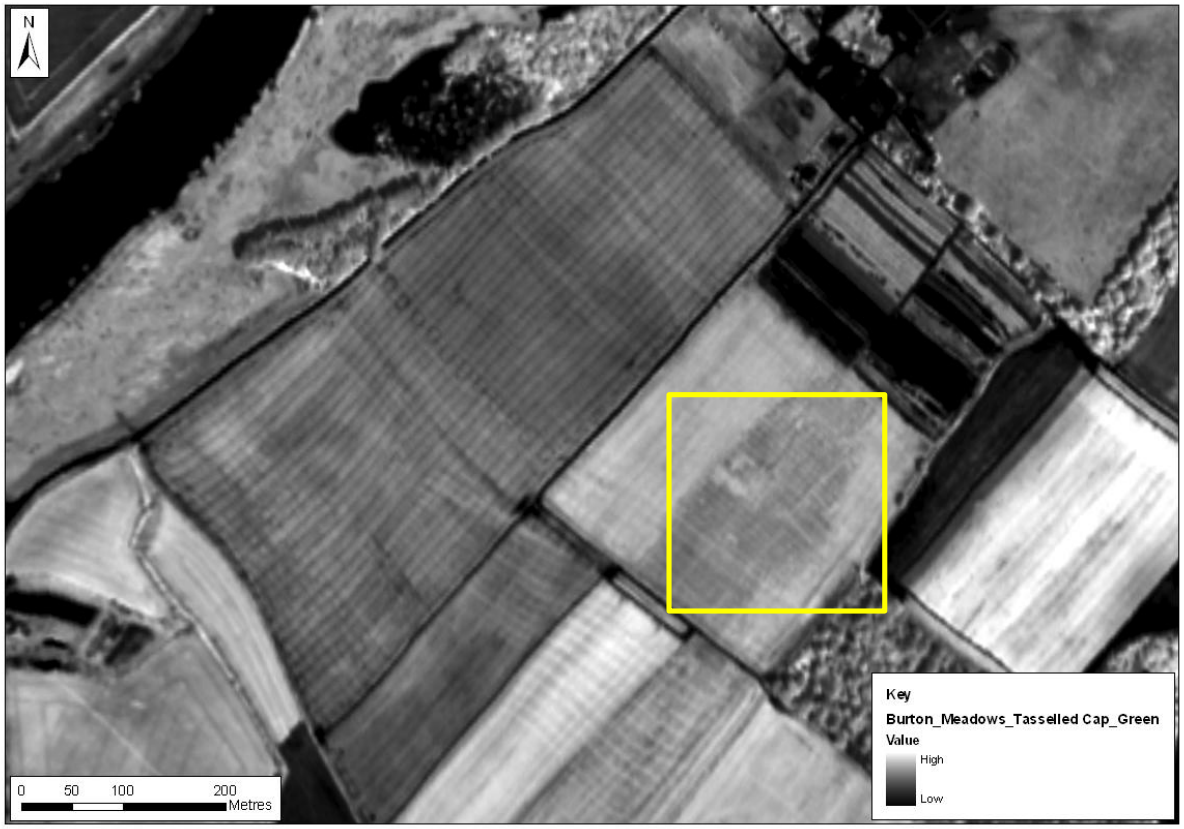

Figure 40. Burton Meadows, Nottinghamshire. ATM TC Green, cropmarks indicated in yellow.

However, many of the cropmarks mapped by the NMP reveal no trace in the ATM data; again this observation highlights the limits of these data as if no physical crop variations are evident, even when cropmark forming features are known to be present, the ATM sensor will not be able to detect or identify features. It is worth repeating that neither ATM, CASI or other similar techniques are “magic bullets” all rely on the presence of real physical phenomena, as does conventional aerial photography, and when these phenomena are absent the techniques will fail.

4.10 BLEASBY, NOTTINGHAMSHIRE

The Bleasby study area comprises approximately 1km2 of terrace and floodplain on the north side of the present channel of the Trent between the village of Bleasby and the river, selected largely because of the presence anthropogenic cropmarks, previously mapped by the NMP, in fields at the extreme north of the study area (outlined in yellow on Fig. 41).

Figure 41. Bleasby, Nottinghamshire. ATM thermal data (band 11).

ATM data successfully reveal subtle geomorphological detail in the lower terrace and floodplain, in common with most other study areas these are best realised in the thermal band (Fig. 41) or in vegetation indices, in particular TC green and wet (Fig. 67, appendix 1). However, the anthropogenic cropmarks, which include linear features and enclosures, are not at all well represented. Areas of crop variation in the general area of the cropmarks are apparent, particularly in the TC green and wet indices, but individual cropmarks cannot be resolved.

It seems likely in this instance that the failure to resolve cropmarks is a result of the limited spatial resolution of the ATM data, higher resolution imagery may well have succeeded in resolving cropmarks in this area.

4.11 FISKERTON NOTTINGHAMSHIRE

The Fiskerton study area comprises approximately 4km2 of floodplain and terrace focused on a substantial meander of the River Trent between the villages of East Stoke, to the south, and Fiskerton, to the north. Aspects of this study area have already been reviewed in section 3.2. A combination of thermal band and vegetation indices, particularly TC green, reveal the majority of the geomorphological detail.

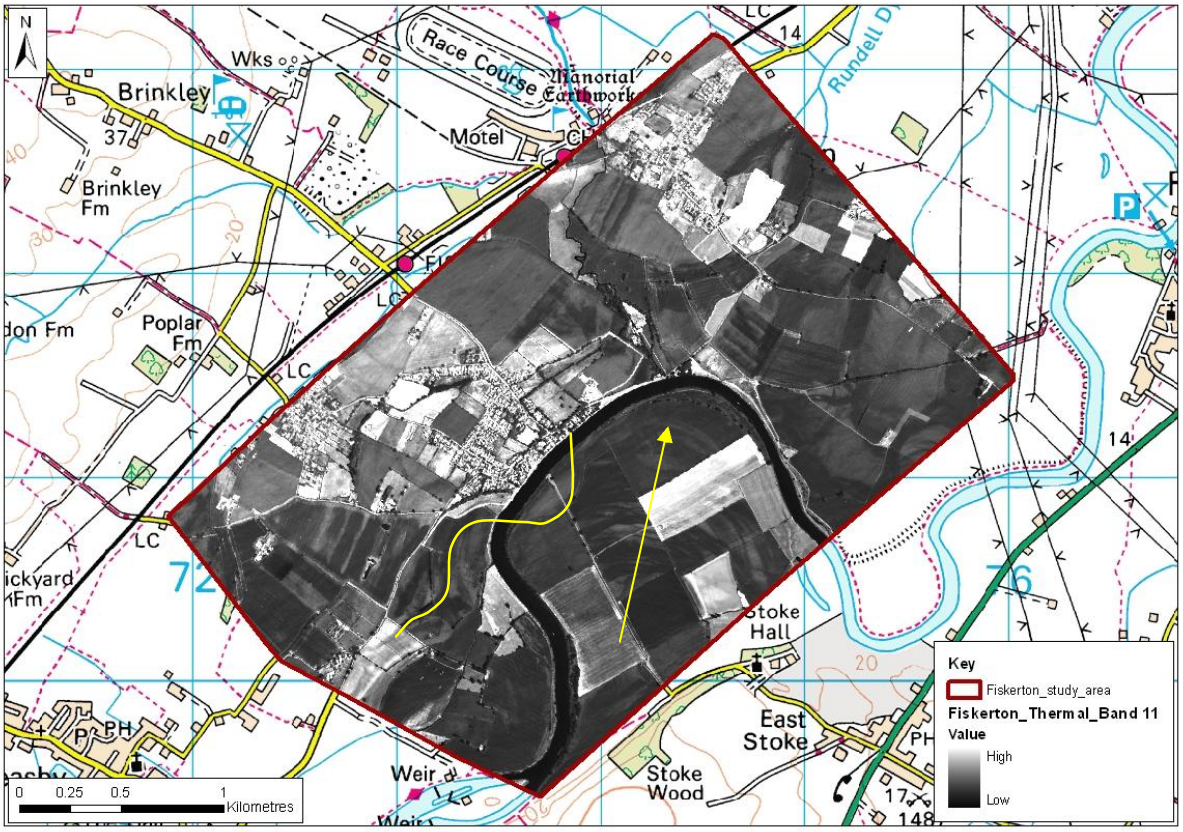

Figure 42. Fiskerton, Nottinghamshire. ATM thermal data (band 11).

Internal detail of the meander core is dramatically revealed in the ATM data, and includes clear evidence of ridge and swale, indicating progressive meander migration to the north (arrow on Fig. 42). Substantial areas of dryer gravel bar might provide a location for past river side activities and demonstrates how the use of ATM imagery can refine understanding of a seemingly homogenous geomorphological zone, indicating for example areas in which field investigation might be most profitably targeted.

In addition the imagery reveals a sinuous palaeochannels of the Trent cut by the present meandering channel and describing an earlier river line (yellow line on Fig. 42).

5 RESULTS: COMPACT AIRBORNE SPECTROGRAPHIC IMAGER (CASI)

5.1 INTRODUCTION

The following section considers the results obtained from analysis of Compact Airborne Spectrographic Imager (CASI) data covering four test areas in the Middle Trent Valley (Fig. 1). In each instance an identical suite on analytical techniques was employed and is discussed in summary. Techniques comprised production of:

- True Colour Composite (Bands 4-3-2)
- False Colour Composite (Bands 12-10-3)
- NDVI
- Principal Component Analysis

Test sites and the efficacy of the imagery and the analytical techniques employed are discussed in turn below and where relevant results are compared and contrasted with those obtained from ATM survey of the same area. Figures showing the results of all analytical techniques are shown in appendix 1; high resolution digital versions of the illustrative figures are provided on the DVD-ROM that accompanies this report.

5.2 BARTON-IN-FABIS, NOTTINGHAMSHIRE

The Barton in Fabis study area comprises the core of a substantial meander of the Trent adjacent to the site of a Roman villa at Glebe Farm. CASI data for the study area is significantly affected by spatial distortion introduced by poor attitude control and correction during flying, not all of which could be removed by geocorrection (Fig. 44).

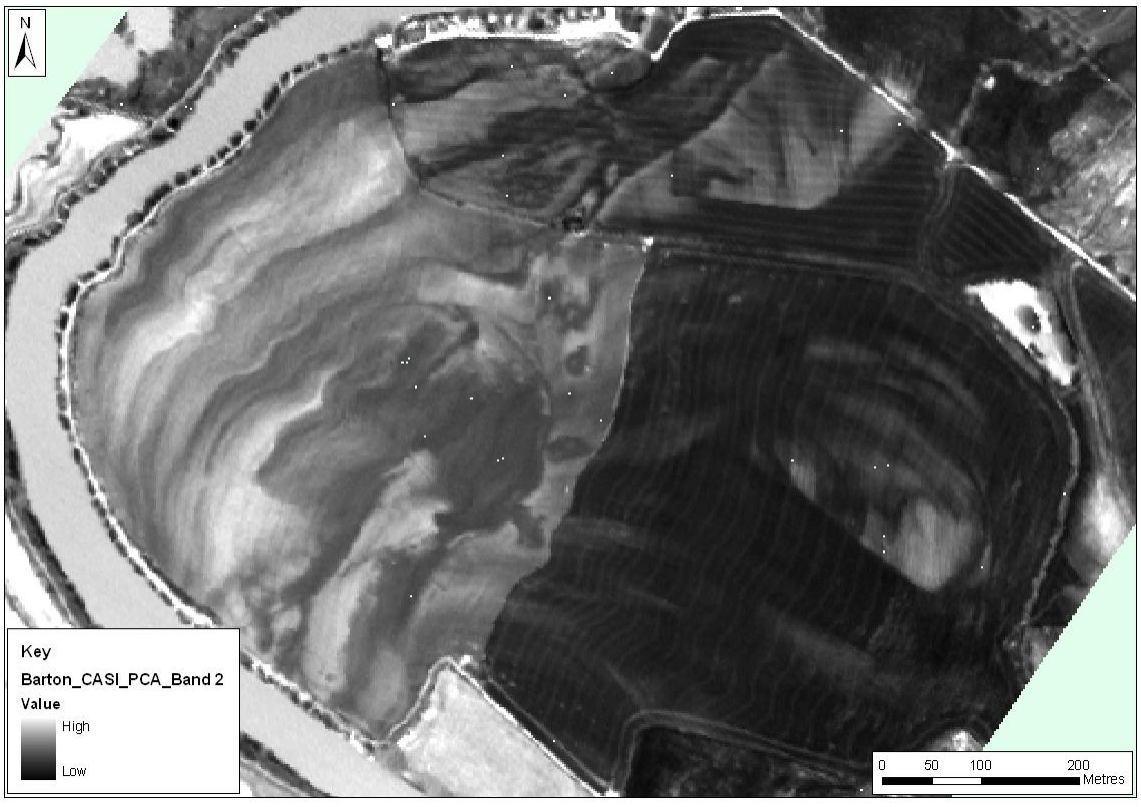

Figure 43. Barton in Fabis. CASI PCA2

None the less the data do dramatically reveal aspects of the internal geometry of the meander, little of which is evident in the visible spectrum (TCC, Fig. 69, appendix 1) but which is particularly evident in the infrared parts of the spectrum. Visual examination of principal component data has proven the most effective means of enhancing these data for display and interpretation; Fig. 43 shows the second principal component, which effectively summarises most of the image data contained in the red and infrared parts of the spectrum.

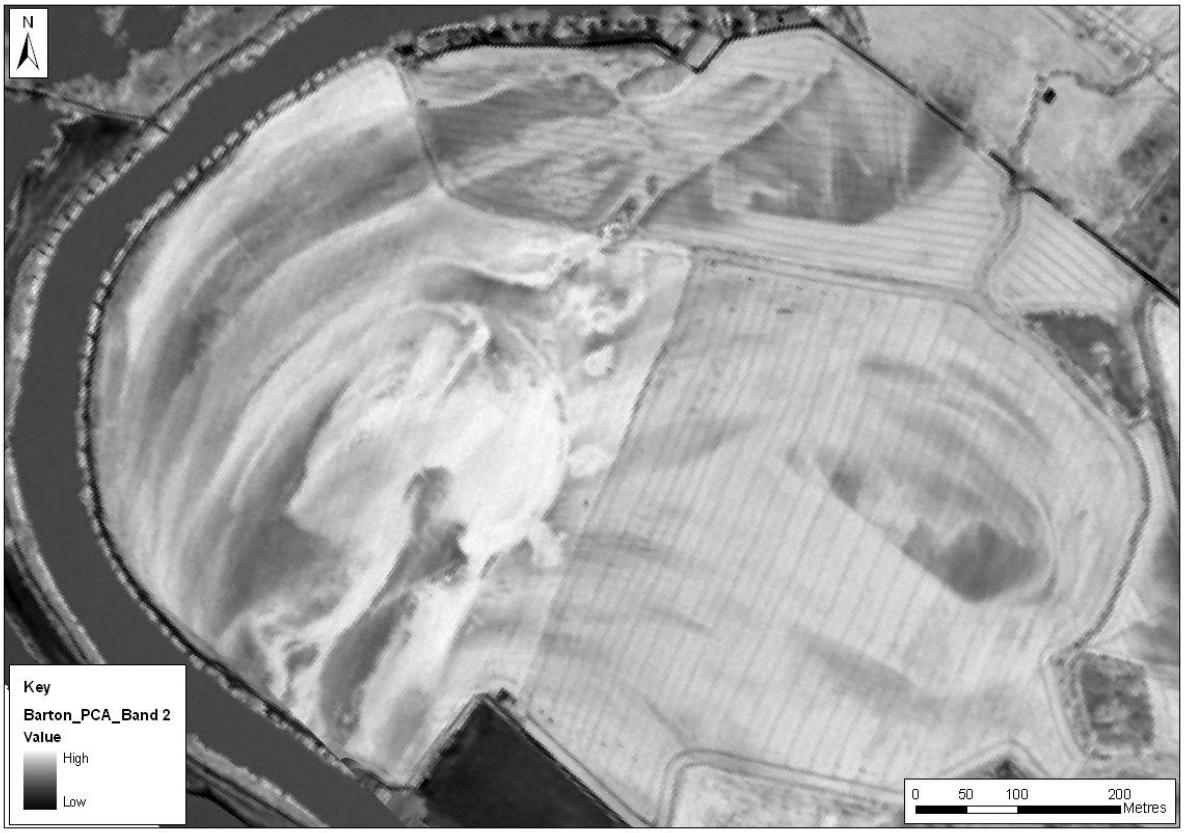

Figure 44. Barton in Fabis. ATM PCA2

Comparison of the CASI data with contemporary ATM imagery for the same area (Fig. 44) suggests that in this instance there is little revealed by CASI that is not also evident in the ATM imagery. In this instance the broader spectral coverage of the ATM data, including middle and thermal IR bands, and the fact that ATM lends itself to forms of enhancement not feasible with CASI (such as the tasselled cap transform) coupled with the lower spatial distortion, suggests that the CASI sensor offers little improvement on the ATM, which is probably to be preferred for geoarchaeological applications.

5.3 BURTON MEADOWS, NOTTINGHAMSHIRE

The Burton Meadows study area comprises a small section of terrace at Shelford, chosen because of the presence of extensive anthropogenic cropmarks mapped by the NMP the ATM data for which was examined in section 4.9. CASI imagery for this area is less affected by spatial distortion than that for Barton, although some is still evident.

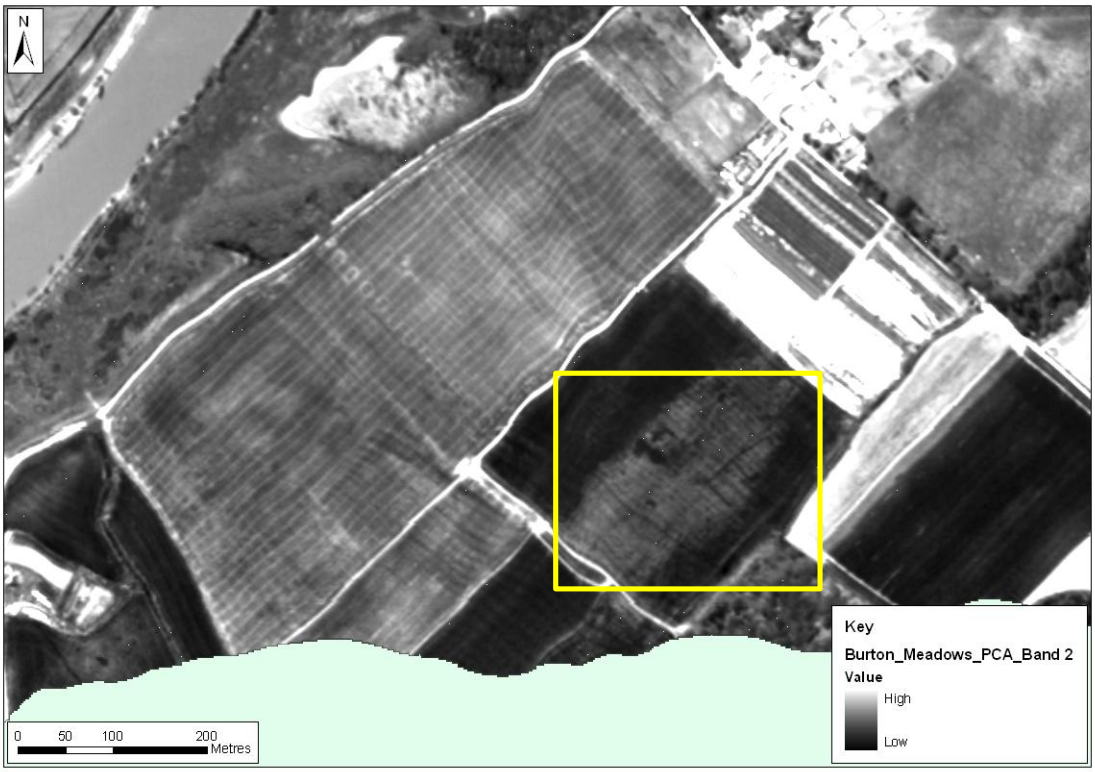

Figure 45. Burton Meadows. CASI PCA2

Once again, principal component analysis provided the most effective means of enhancing the CASI data (Fig. 45). Again similar features and levels of detail are evident in the CASI data when compared to contemporary ATM data for the same area (Fig. 46)

Figure 46. Burton Meadows. ATM PCA2

In particular there is no improvement in the resolution of cropmarks features visible in the ATM data (Fig. 46).

5.4 STOKE BARDOLPH, NOTTINGHAMSHIRE

The Stoke Bardolph study area comprises an area of gravel terrace with extensive cropmarks previously mapped by the NMP that proved hard to spot in the visible spectrum bands of ATM data (section 3.2) but which were dramatically revealed by enhancement techniques exploiting red / infrared contrasts. In this area, CASI data does appear to provide an improvement in ability to resolve anthropogenic cropmarks (compare CASI in Fig.47 with ATM in Fig. 48). This improvement is probably as result of CASI's finer spectral resolution in the crucial middle infrared part of the spectrum where difference between dry and green vegetation is enhanced.

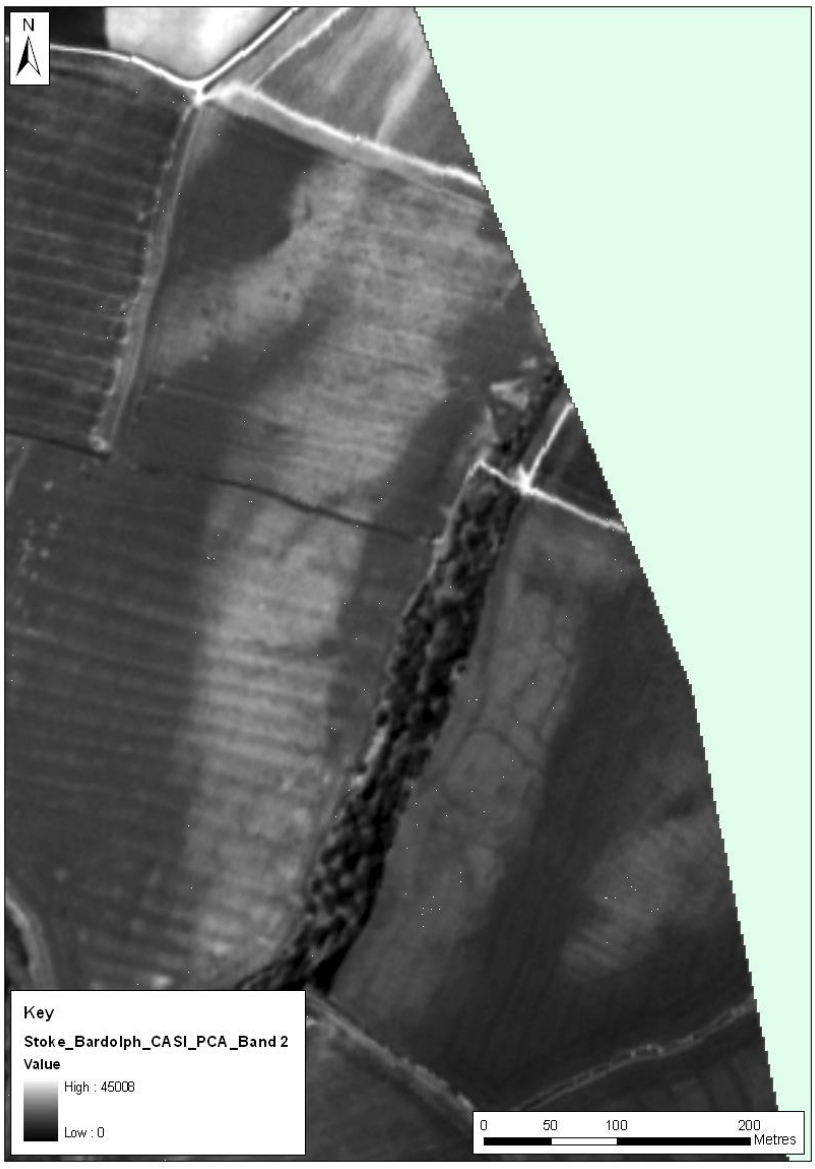

Figure 47. Stoke Bardolph, CASI PCA2

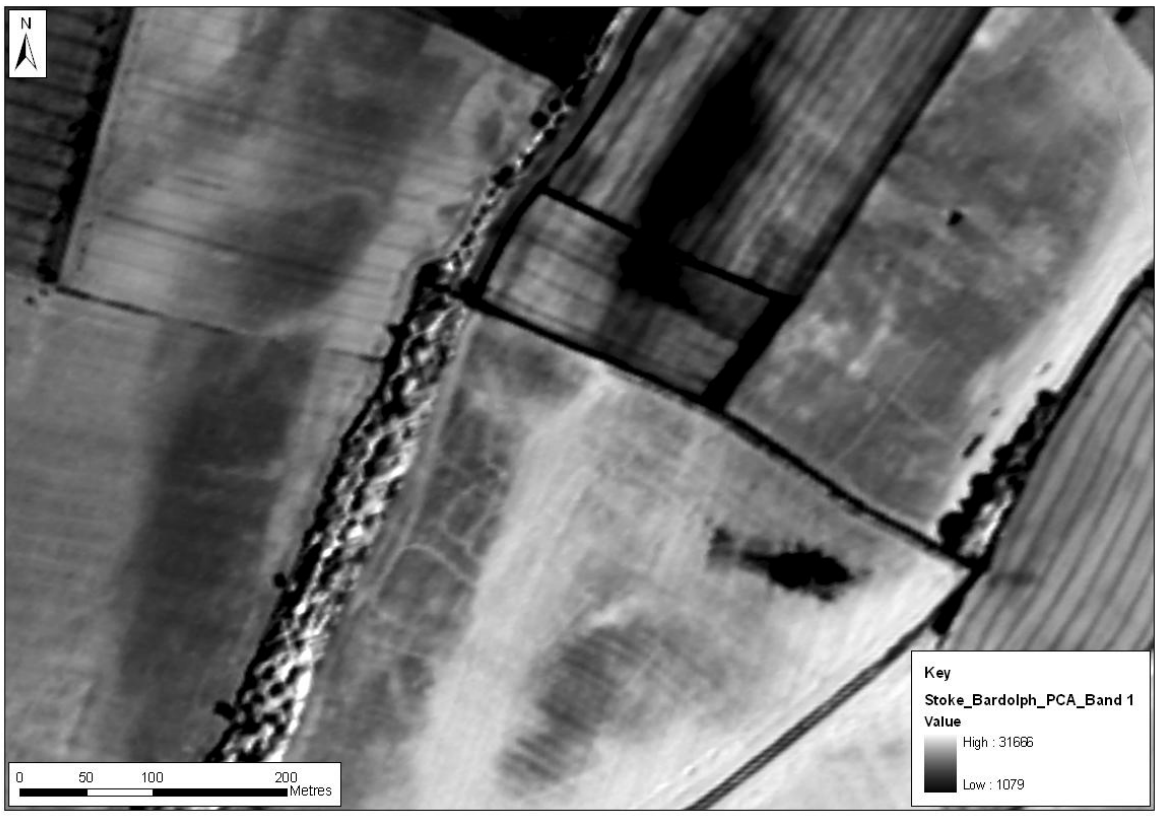

Figure 48. Stoke Bardolph, ATM PCA2

Examination of a range of enhancement techniques for CASI data (Fig. 49) suggest that, in common with ATM, vegetation indices such as NDVI that rely on red/ near infrared contrasts produce the most effective enhancement of anthropogenic cropmarks.

Data for the Stoke Bardolph study area suggest that in situations where cropmark visibility is limited in the visible spectrum, but crop differences are evident in the infrared, CASI results will be at least as good, and possibly exceed those obtainable from the ATM sensor.

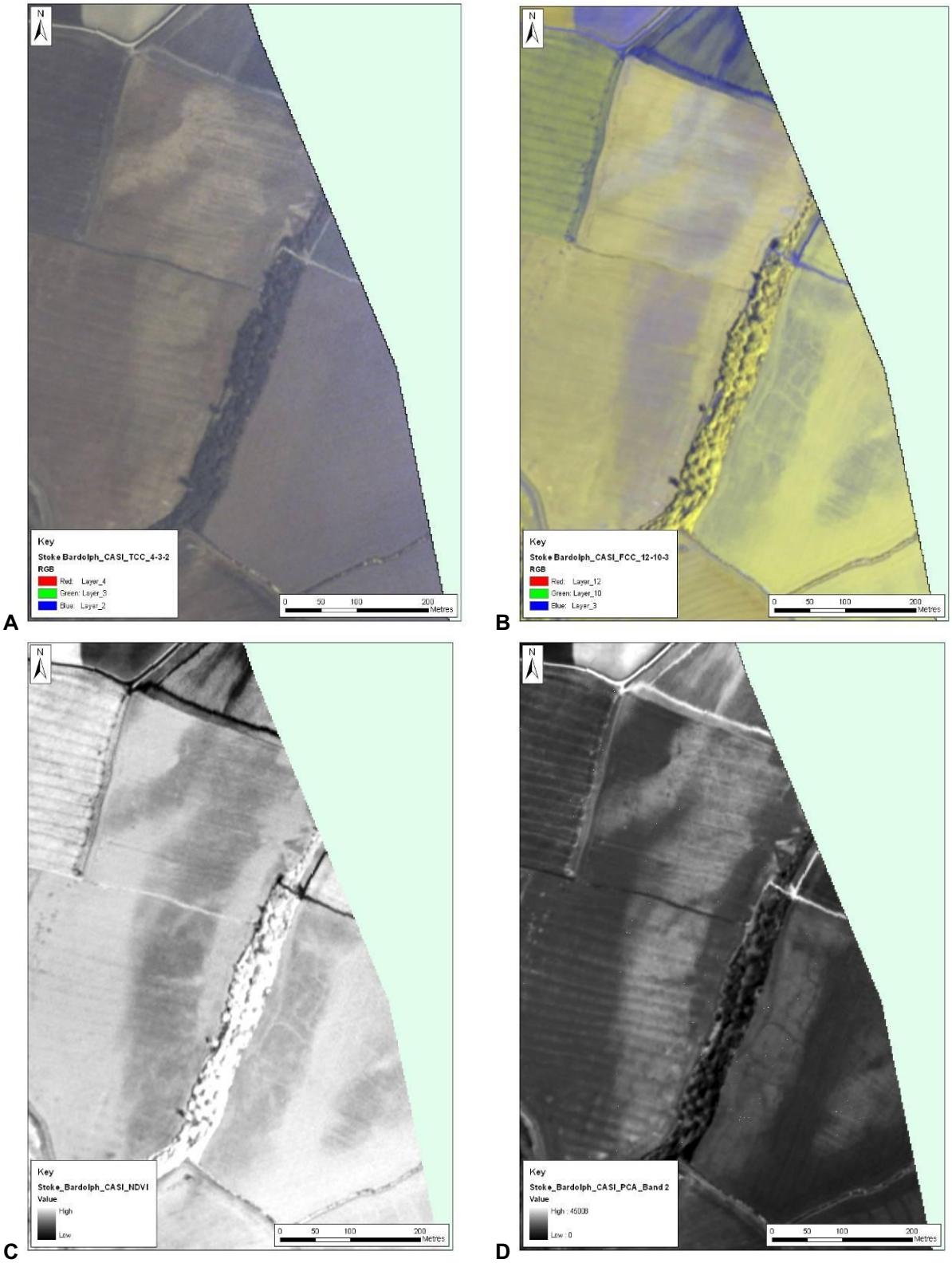

Figure 49. Stoke Bardolph, CASI A, True Colour Composite (4-3-2), B False Colour Composite (12-10-3), C NDVI, D Principal Component 2.

5.5 FISKERTON, NOTTINGHAMSHIRE

The Fiskerton study area comprises the same substantial meander of the Trent for which ATM data as examined on section 4.11.

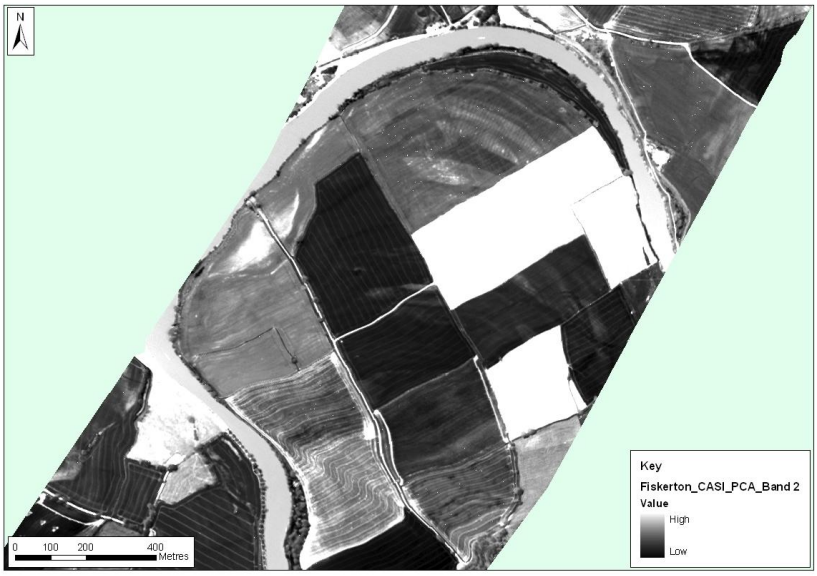

Figure 50. Fiskerton, CASI PCA2

CASI data for this area is again quite badly affected by spatial distortion, not all of which could be removed by geocorrection. Resolution of geomorphological details in the meander core is good, and certainly on par with that attained through use of the ATM sensor, (compare Figs. 50 and 51) and there appears to be some slight improvement in the clarity of some geoarchaeological cropmarks. However, access to thermal data, and the wider range of vegetation-based enhancement techniques available when using ATM data, again suggest that ATM is a preferable platform for geoarchaeological remote sensing.

Figure 51. Fiskerton, ATM PCA2

6 RESULTS: AISA EAGLE

6.1 STURTON-LE-STEEPLE, NOTTINGHAMSHIRE

AISA Eagle 34 band hyperspectral data for the study are were collected by Infoterra on 18th October 2007. At the point of hyperspectral survey much of the study area was bare earth, having been harvested and ploughed. To some extent this has limited the effectiveness of the hyperspectral survey as in general vegetation is far more likely to betray underlying geomorphological features through resulting variations in crop growth and character evidenced across the visible spectrum and particularly in the NIR. Nevertheless a suit of standard analytical processes were applied to the Eagle data in an attempt to identify aspects of terrace and floodplain geomorphology (Figs. 52-58).

A true colour composite image (Fig.52) shows approximately the equivalent of a colour aerial photograph of the study; general land use, I particular the brown tones of the bare earth fields is readily apparent. Features evident from the lidar flight can be identified on this image, largely as variations in soil colour and include a channel features crossing the terrace at A, rodden-like features on the floodplain at B and the summits of the gravel islands in the floodplain, evident as distinctly lighter soil colour at C. Similar areas of lighter soil are evident on the terrace edge at D, perhaps suggesting that both C and D represent areas of active erosion of terrace deposits by ploughing introducing sand and gravel from the underlying terrace into the ploughsoil. Beyond the southern edge of the study area the terrace edge in the vicinity of Littleborough is very clearly marked by variations in soil colour.

In general these same features are evident in the false colour composite image (Figure 53) which makes use of NIR bands to emphasis soil variation. Variations in soil character evident in this image, particularly to the south of the study area, might indicate varying aggregate character.

In general vegetation based analysis and indices are not particularly revealing using the available imagery. Eagle band 23, (Fig.54) which approximates to the point of maximum vegetation reflectance in the NIR, centred at 795nm, should indicate maximum difference between vigorous and senescent vegetation. Little is apparent in the bare earth areas, although variations in vegetation character reflecting the rodden-like features at B. Similarly the Normalised Difference Vegetation Index (NDVI; Fig. 55) which highlights the difference in red and NIR reflectance of vegetation, shows little of great significance beyond highlighting fields with growing crop (pale tones). The rodden-like features at A are again apparent. Eagle band 27 (Fig.56) equates to the NIR plateau at c 870nm, soil variations are slightly emphasised in this spectral region; the paler tones of features at B,C and D may indicate areas where terrace material of different spectral reflectance to the surrounding ploughsoil has been brought to the surface by deep ploughing.

Finally, Principal Component Analysis (PCA) was applied to the Eagle data. PCA removes redundancy in adjacent bands of a hyperspectral image brought about by correlation between bands by statistically generating a lesser number of bands that are uncorrelated and contain the majority of the variation in the original image. In this instance 5 principal components were generated to account for 99% of the variation in the original data. Component 2 (Fig. 57) provides a good visual summary of the soil and vegetation changes discussed, in particular rodden-like

features at A, possible areas of deep ploughing erosion at B and C and the clearly marked terrace adjacent to Littleborough at D. A pseudo three-dimensional view of PC2 draped over lidar terrain data in Fig. 58 clearly highlights the relationship between topography and soil and sediment character.

Figure 52. Eagle true colour composite (Band 13-9-3)

Figure 53. Eagle false colour composite (Band 34-21-13) highlighting soil and vegetation variations apparent in the NIR.

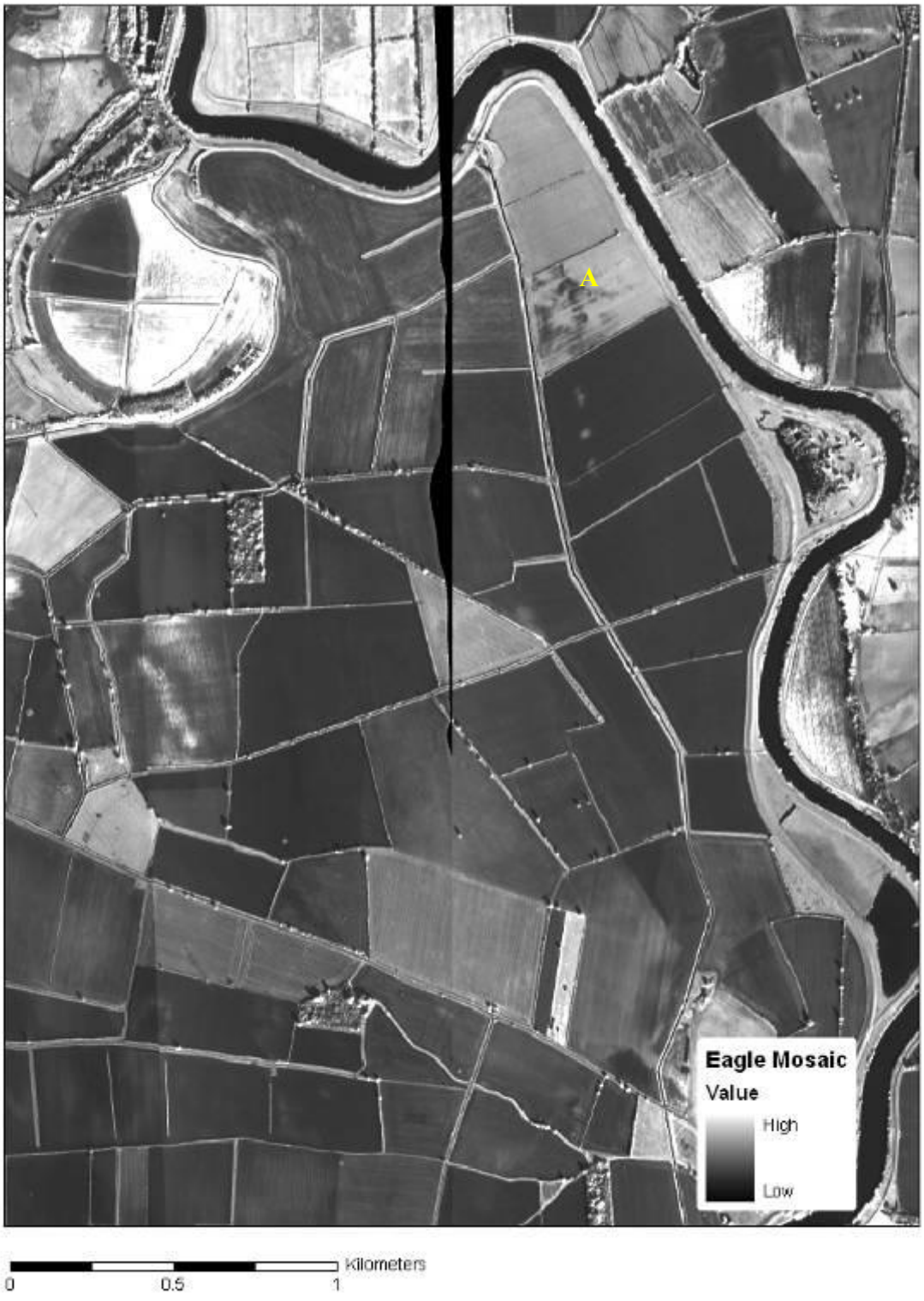

Figure 54. Eagle band 23 (maximum NIR reflectance of green vegetation). There is little variation across the study area which is largely bare earth.

Figure 55. Eagle NDVI. The lack of vegetation across most of the study area renders this index of limited use in identifying anthropogenic and geoarchaeological features of the landscape.

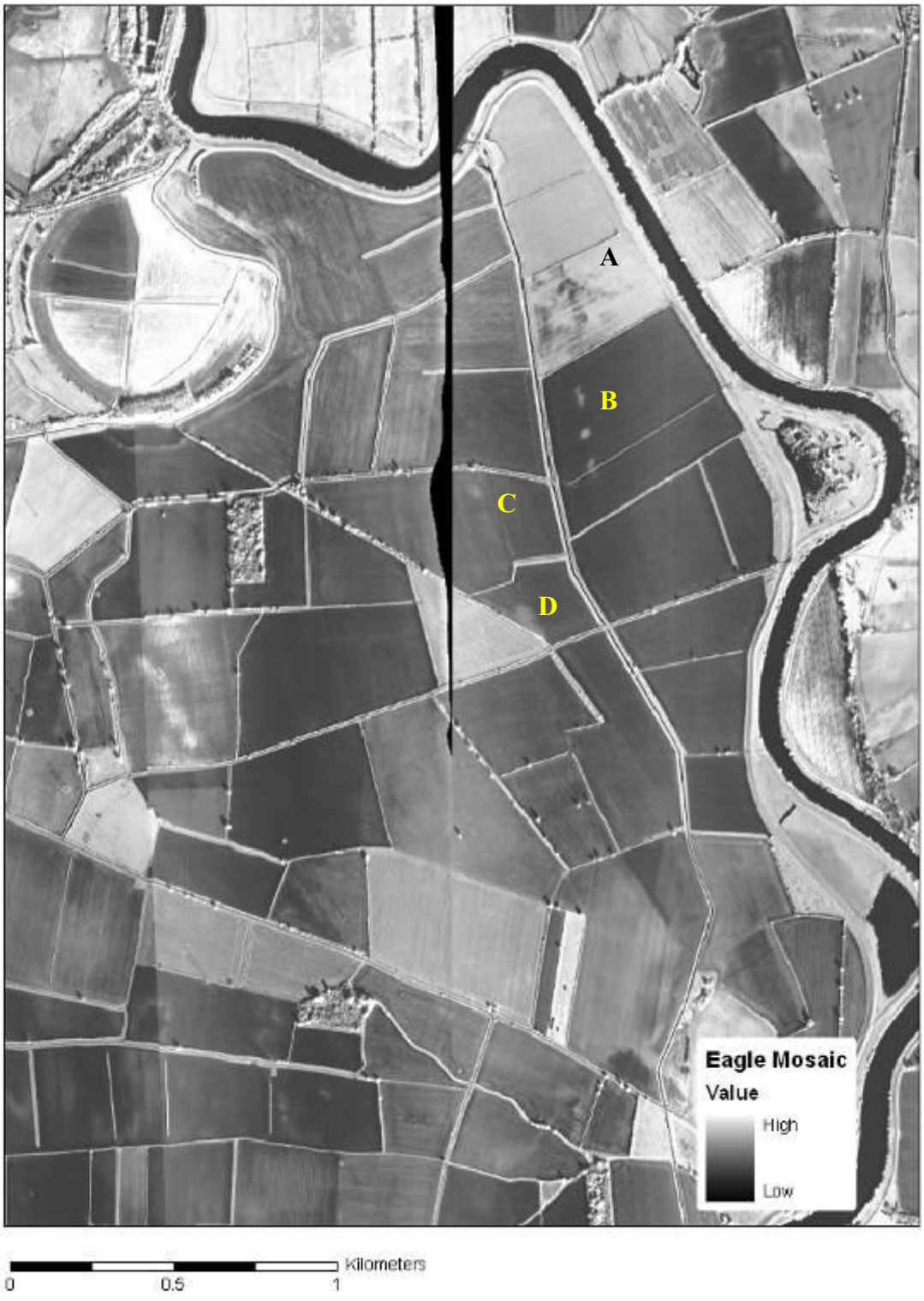

Figure 56. Eagle band 27, the NIR Plateau. Soil variations are most apparent at this part of the spectrum.

Figure 57. Eagle principal component 2. This band most effectively highlights the soil and vegetation variations across the study area.

Figure 58. Eagle Principal Component 2 draped over the lidar DSM. In combination these data effectively highlight the terrace edge.

7 CONCLUSIONS AND RECOMMENDATIONS

7.1 IMAGERY SOURCES

The study compared Daedalus 1268 Airborne Thematic Mapper, Compact Spectrographic Imager and AISA Eagle sensor data. In general each sensor performed well. It was possible to directly compare CASI and ATM and contemporary data were available for the study area. Analysis of the effectiveness of Eagle data was limited by the fact that no other contemporary data exist for comparison, and the data was acquitted outside of the cropmark season. The following conclusions are offered:

- The **ATM** sensor performed well in all conditions. Its wide spectral resolution and the presence of a thermal band were particularly advantageous for geoarchaeological mapping and in areas of permanent pasture for earthwork detection. In general it is suggested that the ATM sensor is the preferred choice for geoarchaeological application.

- The **CASI** sensor performed well, but was hampered by a high degree of spatial distortion in the data, a problem associated with this sensor platform. In no area did CASI significantly outperform ATM, but there were some indications that it may prove more effective at resolving anthropogenic cropmarks. CASI data examined in the present study were at the same spatial resolution as the ATM data (c. 2m). It is theoretically possible to acquire CASI at a higher spatial resolution (up to c. 1m); a higher spatial resolution coupled with the fine spectral resolution of CASI suggest it has the potential to be a highly effective tool for cropmark detection and mapping, although that potential is unrealised with the presently available data.

- Assessment of the **Eagle** sensor was hampered by the lack of direct comparable data and the season. However, the limited data examined proved highly effective at detecting geoarchaeological detail; this coupled with the combination of high spectral and spatial resolution suggest the Eagle platform offers great potential for both archaeological and geoarchaeological mapping.

- In general, and until the archaeological potential of Eagle data is fully explored, it is suggested that **the Daedalus ATM sensor provides the best combination of spatial an spectral resolution for archaeological prospection in alluvial environments**

7.2 IMAGE PROCESSING TECHNIQUES

A range of image processing techniques were investigated, in general it is concluded that:

- For all sensor platforms, **true colour composite** images provide a poor indication of the overall information contained in the image; this is largely due to the fact that crop and soil variations indicating archaeology are most strongly evident beyond the visible spectrum.

- **False colour composite** images which make use of near infrared bands increase the visibility of cropmarks, but may be difficult to visually interpret due to their garish colouring

- The use of **ATM thermal data** was the single biggest contributor to the identification of geoarchaeological cropmarks, and earthwork features in areas of pasture.

- **Vegetation indices** which rely on ratios of red to near infrared reflection (NDVI, TC wet and green) significantly enhance the visibility of both geoarchaeological and anthropogenic cropmarks.

- The **TC green and wet** transforms performed well on ATM data and offer a useful new way of enhancing these data for archaeological analysis as they provide indicators of aspects of the ground surface of direct interest to archaeologists. TC wet in particular may offer a remote way of determining the relative wetness of deposits in alluvial environments.

- **Principal component analysis** provided a rapid and robust means of summarising the content of complex multi-band data. In general single component viewed as greyscale images were easier to interpret than false colour composites made by combining three components. It is suggested that use of PCA should form part of the routine suite of techniques for archaeological image analysis. Further work is required to determine the extent to which individual components reflect actual physical characteristics of vegetation and soils.

- Automatic **image classification** has little to offer archaeologists. In general there is insufficient spectral contrast between archaeologically induced crop and soil variations and background values for classification to function effectively. Effective archaeological image interpretation requires the intervention of a suitably experienced human.

7.3 CAVEATS AND CAUTIONS

Airborne multispectral (MS) and hyperspectral (HS) imagery provides a significant and highly productive tool for the aerial archaeologist toolkit, but the techniques has its limitations and is in no sense a replacement for conventional aerial photography. The research undertaken here has demonstrated the physical characteristics of crops and soils that reflect underlying archaeology. Where these physical characteristic are expressed, multi and hyperspectral imagery will usually be able to detect them, even if they are not apparent in the visible spectrum and so invisible to conventional photography. However, where there is no physical effect from archaeology on vegetation and soils these techniques will fail in the same way as will conventional photography.

The strength of MS and HS techniques lies in their combination of rapid broad area coverage combined with a data collection beyond the visible spectrum, but flights are expensive and there is no sense in which a single MS flight could substitute for a season of opportunistic flying using conventional photography. Rather it is

suggested that MS and HS data collection form part of a balanced approach to airborne data collection. In seasons when crop mark formation is good then a well-timed MS flying campaign, at the time when in general cropmark formation is at its height, might be expected to reveal as much, and probably significantly more, than a single conventional flight, and it is suggested that as a technique it is most appropriately used in this way to supplement conventional aerial archaeology.

7.4 FUTURE DIRECTIONS

It is suggested that airborne MS and HS techniques be adopted as part of the standard suite of techniques used for aerial archaeological survey.

There is much work yet to be done in investigating the potential of existing archive ATM and CASI data for river valleys beyond the Trent. The potential of Eagle data has yet to be fully explored, but data are available for the Trent Valley to facilitate further exploration of this platform.

More ambitiously, it is suggested that a campaign of ATM and Eagle flying be undertaken to investigate a well-documented river valley, such as the Trent, with flights timed to coincide with the time of maximum cropmark definition, and accompanied by conventional, vertical and oblique aerial photography in order to compare and contrast the effectiveness of these techniques. The use of the Eagle sensor could usefully be supplemented by its twin, the Hawk, which records data into the thermal parts of the spectrum. The opportunity should also be taken for comprehensive ground based data collection (soil moisture deficit, etc.) in order to calibrate the physical characteristics that influence these techniques.

8 REFERENCES

Allsop, J.M. 1992 'The British Geological Survey: Geoprospecting Techniques Applied to the Archaeological Landscape.' In Spoerry, P. (ed) *Geoprospection in the Archaeological Landscape. Oxbow Monograph* 18, Oxford, 121-140.

Baker, S. 2003. *The Trent Valley: Palaeochannel Mapping from Aerial Photographs*. Trent Valley Geoarchaeology Research Report. Nottingham: Trent & Peak Archaeological Unit.

Ben-Dor et al., 2001 E. Ben-Dor, M. Kochavi, L. Vinizki, M. Shionim and J. Portugali, Detection of buried ancient walls using airborne thermal video radiometry, *International Journal of Remote Sensing* **22** (2001) (18), pp. 3689–3702.

Ben-Dor et al., 2002 E. Ben-Dor, K. Patkin, A. Banin and A. Karnieli, Mapping of several soil properties using DAIS-7915 hyperspectral scanner data—a case study over clayey soils in Israel, *International Journal of Remote Sensing* **23**. 1043–1062

Benz et al., 2004 U.C. Benz, P. Hofmann, G. Willhauck, I. Lingenfelder and M. Heynen, Multi-resolution, object-oriented fuzzy analysis of remote sensing data for GIS-ready information, *ISPRS Journal of Photogrammetry and Remote Sensing* **58**. 239–258

Carey, C. Brown, T., Challis, K. Howard, A.J. and Cooper, L. 2006. Predictive modelling of multi-period geoarchaeological resources at a river confluence: a case study from the Trent-Soar, UK. A*rchaeological Prospection.* Vol 13, No4

Challis, K. and Howard, A.J. 2006. A review of Remote Sensing in Alluvial Environments. A*rchaeological Prospection.* Vol 13, No4: 231-240

Challis, K. 2006. Airborne laser altimetry in alluviated landscapes. A*rchaeological Prospection.* Vol 13, No2: 103-127

Challis, K. 2005. Airborne LiDAR: A Tool for Geoarchaeological Prospection in Riverine Landscapes. in Stoepker, H. (ed) *Archaeological Heritage Management in Riverine Landscapes.* Rapporten Archeologische Monumentenzorg, 126: 11-24

Crist, E.P ad Cicone, R.C. 1984. A physically-based transformation of thematic mapper data – the TM Tasseled Cap. *IEEE Transactions on Geoscience and Remote Sensin.* GE-22: 256-263.

Davidson, D.A. & Watson, A.L. 1995. Spatial variability in soil moisture as predicted from airborne thematic mapper (ATM) data. *Earth Surface Processes and Landforms* 20, no 3: 219-230.

De Laet, V., Paulissen, E. and Waelkens, M. 2007. Methods for the extraction of archaeological features from very high resolution Ikonos-2 remote sensing imagery, Hisar (southwest Turkey). *Journal of Archaeological Science* 34: 830-841.

Harris, A. Bryant, R.G. & Baird, A.J. in press. Detecting near-surface moisture stress in *Sphagnum* spp. *Remote Sensing of Environment.*

Garton, D. & Malone, S. 1998. Geomorphology from aerial photographs in the Trent Valley. In Challis, K. (ed) Fieldwork by Trent & Peak Archaeological Trust in Nottinghamshire, 1996-7. *Transactions of the Thoroton Society of Nottinghamshire* 102: 139-141.

Kvamme K. 2006. Integrating multi-dimensional geophysical data. *Archaeological Prospection* 13: 57–72.

Knight, D. and Howard, A.J. 2004. *Trent Valley Landscapes.*

Lasaponara, R. and Masini, N. 2007. Detection of archaeological cropmarks by using satellite Quickbird multispectral imagery. *Journal of Archaeological Science* 33: 214-221.

W.D. Liu, F. Baret, X.F. Gu, B. Zhang, Q.X. Tong and L.F. Zheng, 2003. Evaluation of methods for soil surface moisture estimation from reflectance data, *International Journal of Remote Sensing* **24**. 2069–2083

Mather, P.M. 2004. *Computer Processing of Remotely-Sensed Images*. Chichester, Wiley.

Powlesland, D., Lyall, J., Hopkinson, G,. Donoghue, D., Beck, M., Harte, A., and Stott, D. 2006. Beneath the sand - remote sensing, archaeology, aggregates and sustainability: a case study from Heslerton, the Vale of Pickering, North Yorkshire, UK**.** A*rchaeological Prospection.* Vol 13, No4: 291-299

Powesland D, Lyall J, Donoghue D. 1997. Enhancing the record through remote sensing: the application and integration of multi-sensor, non-invasive remote sensing techniques for the enhancement of the Sites and Monuments Record. Heslerton Parish Project, N Yorkshire, England. *Internet Archaeology* 2.

Rainey, M.P., Tyler, A.N., Gilvear, D.J., Bryant, R.G. & McDonald, P. 2003. Mapping intertidal estuarine sediment grain size distributions through airborne remote sensing. *Remote Sensing of Environment* 86: 480-490.

Rowlands, A. and Sarris, A. 2007. Detection of exposed and subsurface archaeological remains using multi-sensor remote sensing. *Journal of Archaeological Science* 34: 795-803.

Todd, S.W., Hoffer, R.M. and Milchunas, D.G. 1998. Biomass estimation on grazed and ungrazed rangelands using spectral indices. *International Journal of Remote Sensing* 19,3: 427-438.

Vining, B.R. and Wiseman, J. 2007. Multispectral synthetic aperture radar remote-sensing-based models for Holocene coastline development in the Ambracian Gulf, Epirus, Greece. *Archaeological Prospection* 13

Winterbottom SJ. Dawson T. 2005. Airborne multi-spectral prospection for buried archaeology in mobile sand dominated systems. *Archaeological Prospection*. 12: 205-219.

Yang, X. 2007. Integrated use of remote sensing and geographic information systems in riparian vegetation delineation and mapping. *International Journal of Remote Sensing* 28,2: 353-370.

APPENDIX 1: ATM AND CASI IMAGES OF TEST SITES

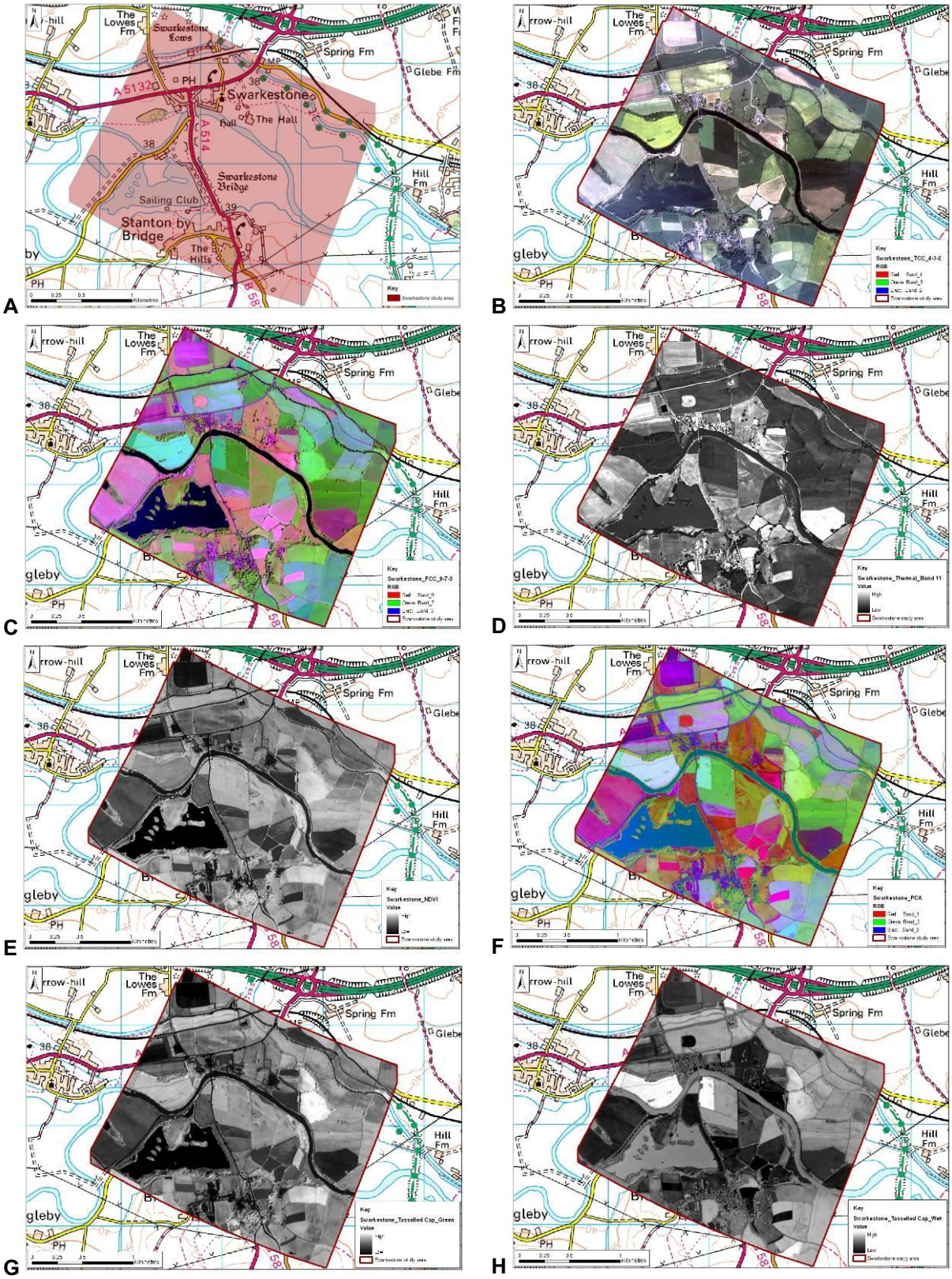

Figure 59. Swarkestone ATM: A Study area, B True Colour Composite (4-3-2), C False Colour Composite (9-7-3), D Thermal (12), E NDVI, F Principal Components 1-3, G Tasselled Cap Green, H Tasselled Cap Wet.

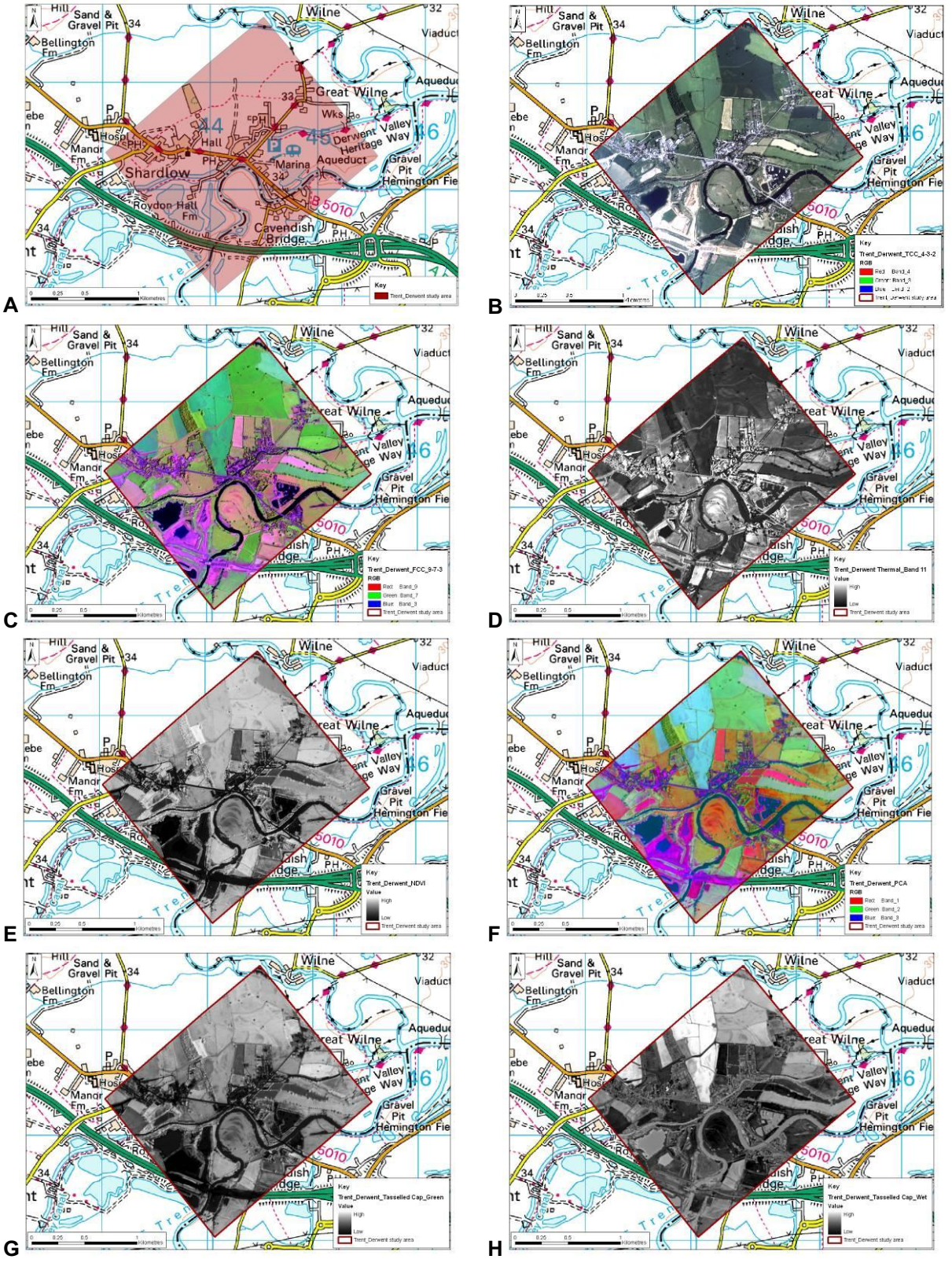

Figure 60. Trent-Derwent Confluence ATM: A Study area, B True Colour Composite (4-3-2), C False Colour Composite (9-7-3), D Thermal (12), E NDVI, F Principal Components 1-3, G Tasselled Cap Green, H Tasselled Cap Wet

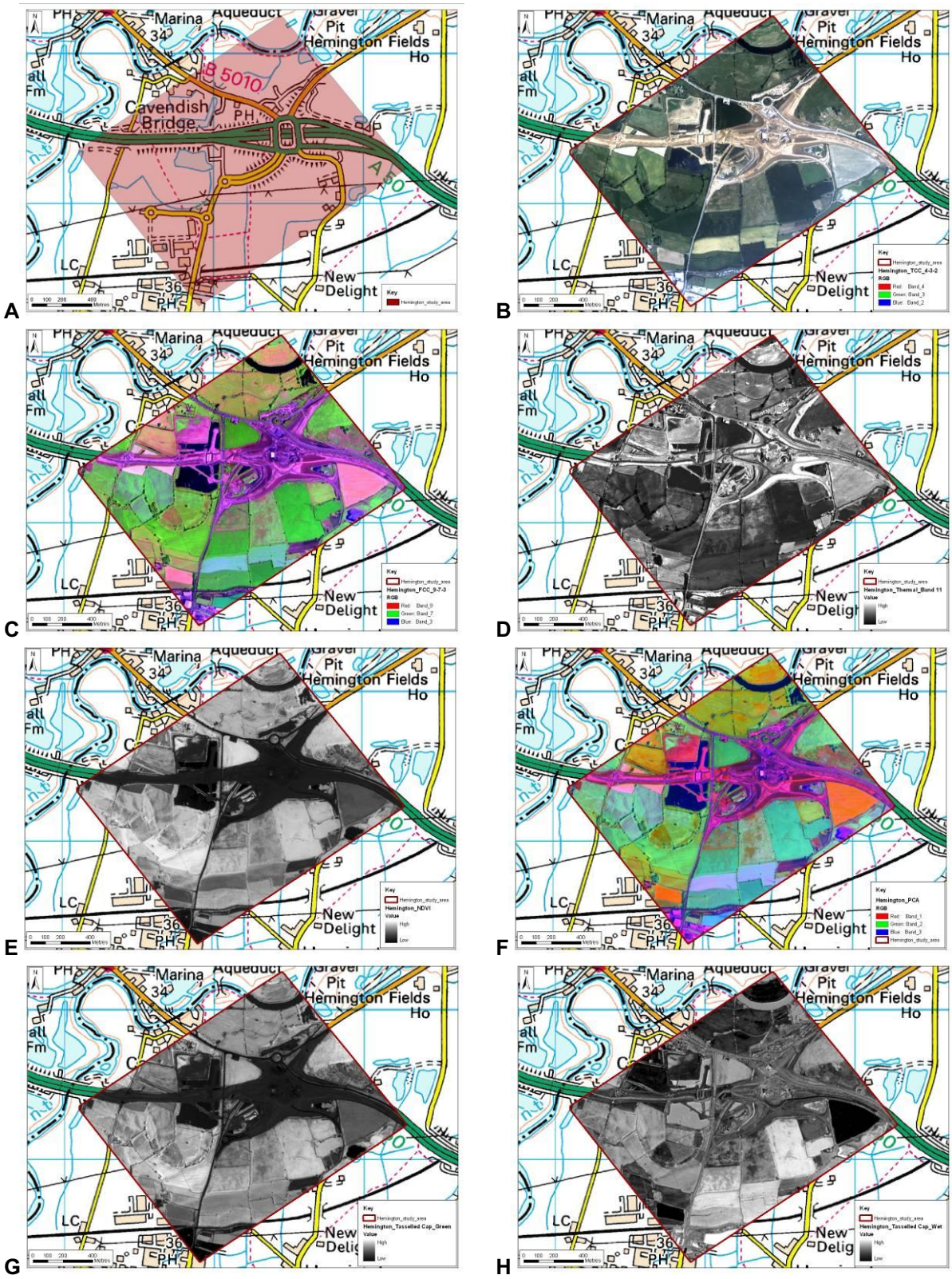

Figure 61. Hemington ATM: A Study area, B True Colour Composite (4-3-2), C False Colour Composite (9-7-3), D Thermal (12), E NDVI, F Principal Components 1-3, G Tasselled Cap Green, H Tasselled Cap Wet

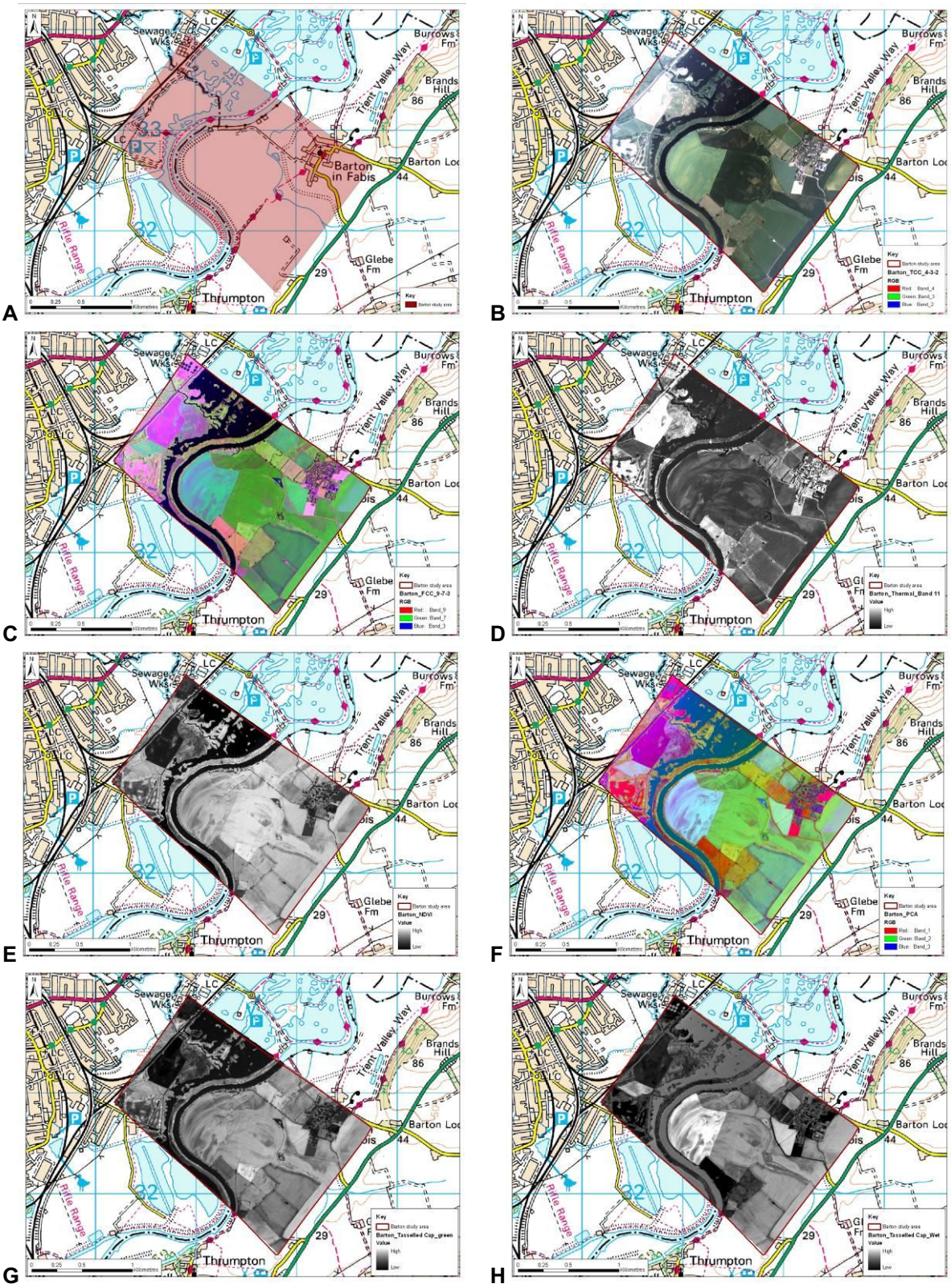

Figure 62. Barton ATM: A Study area, B True Colour Composite (4-3-2), C False Colour Composite (9-7-3), D Thermal (12), E NDVI, F Principal Components 1-3, G Tasselled Cap Green, H Tasselled Cap Wet

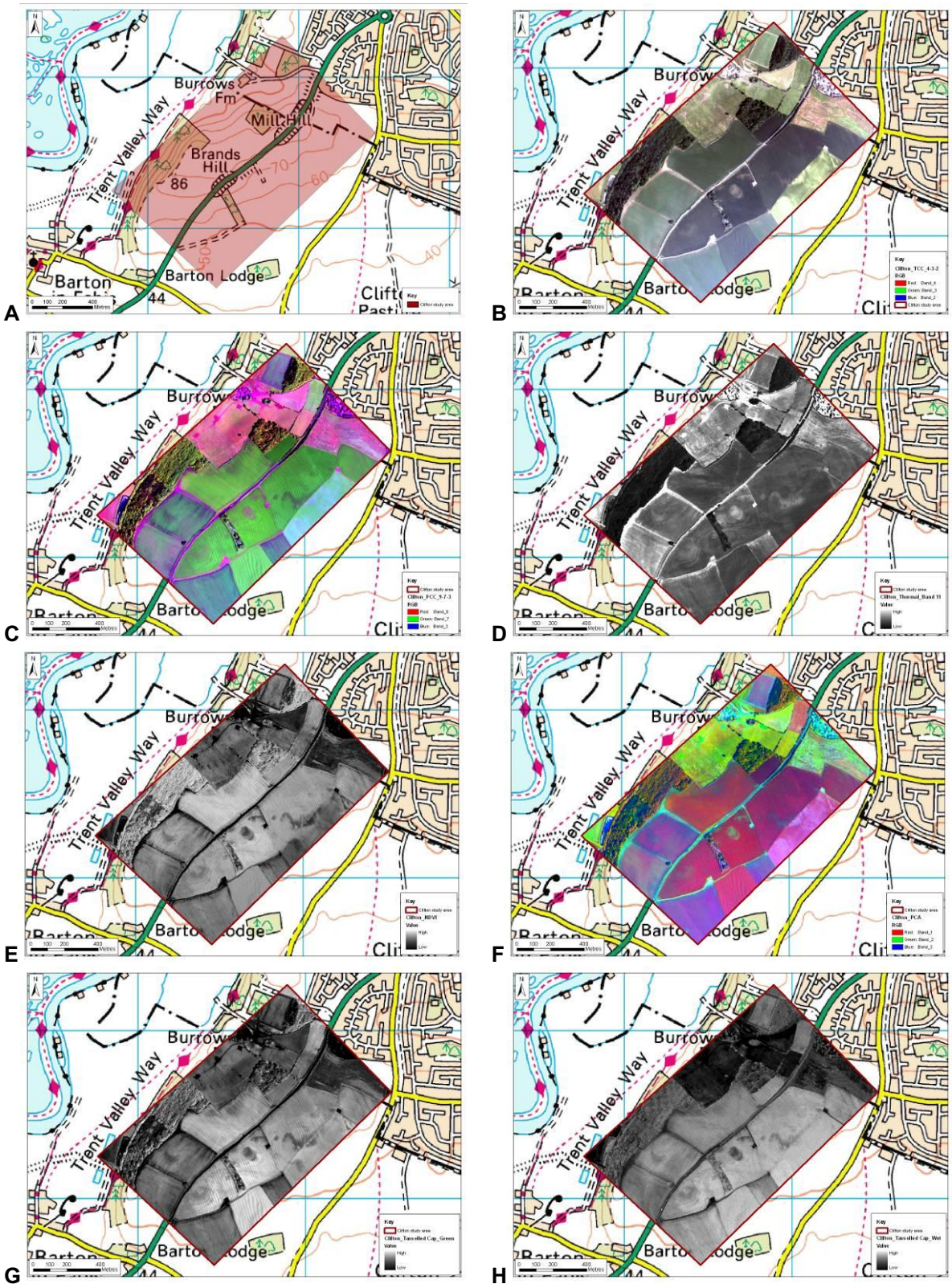

Figure 63. Clifton ATM: A Study area, B True Colour Composite (4-3-2), C False Colour Composite (9-7-3), D Thermal (12), E NDVI, F Principal Components 1-3, G Tasselled Cap Green, H Tasselled Cap Wet

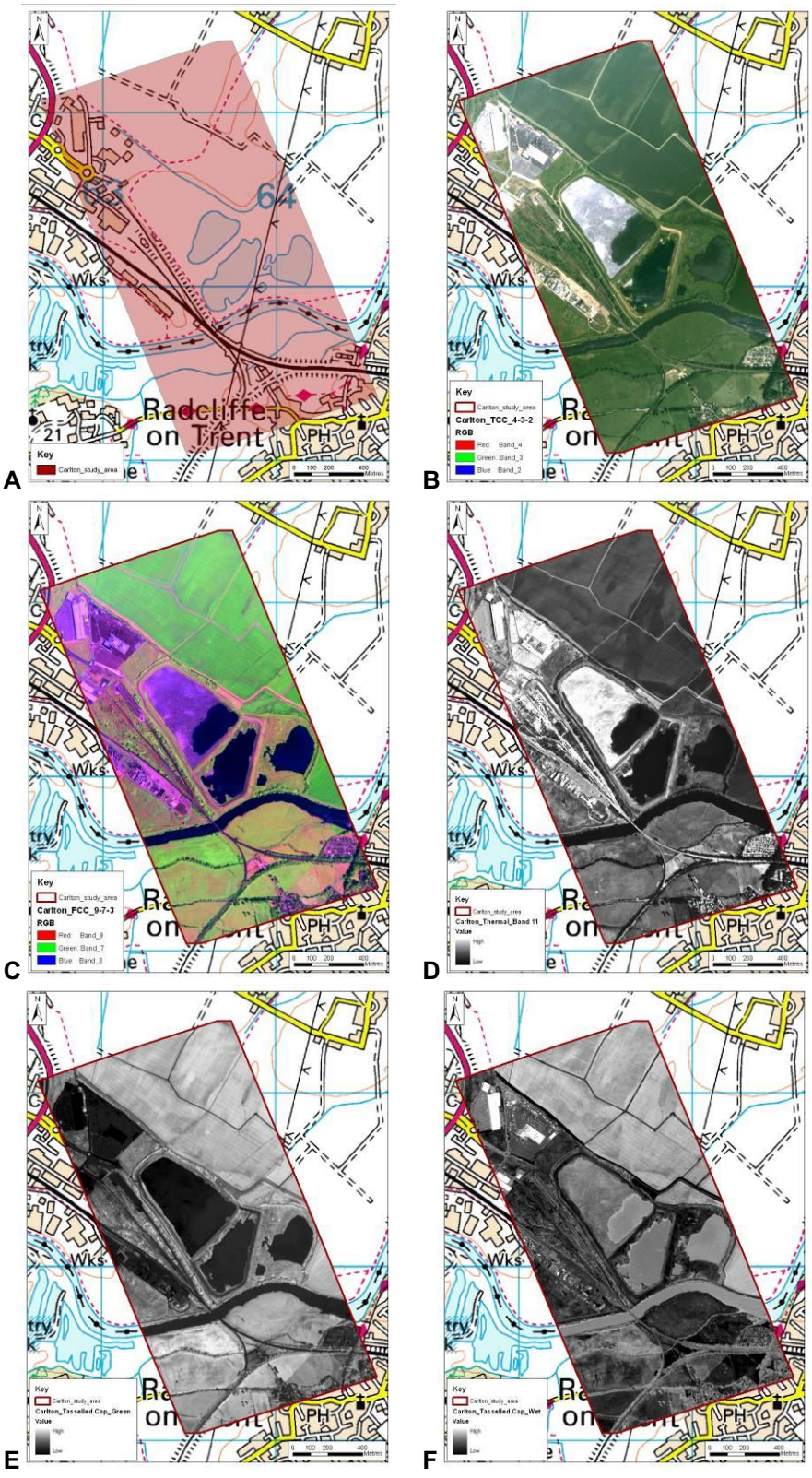

Figure 64. Carlton ATM: A Study area, B True Colour Composite (4-3-2), C False Colour Composite (9-7-3), D Thermal (12), E Tasselled Cap Green, F Tasselled Cap Wet

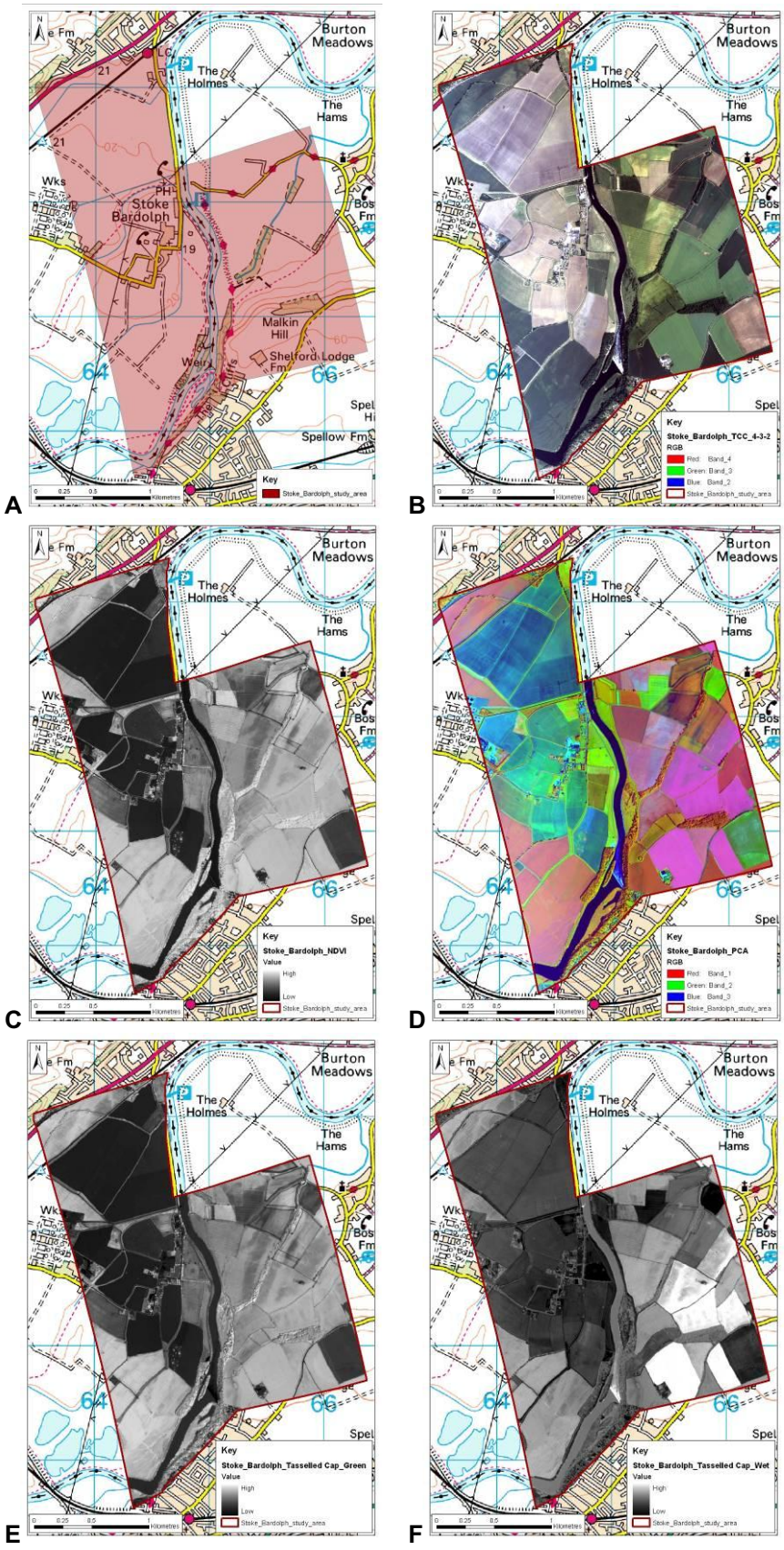

Figure 65. Stoke Bardolph ATM: A Study area, B True Colour Composite (4-3-2), C NDVI, D Principal Components 1-3, E Tasselled Cap Green, F Tasselled Cap Wet

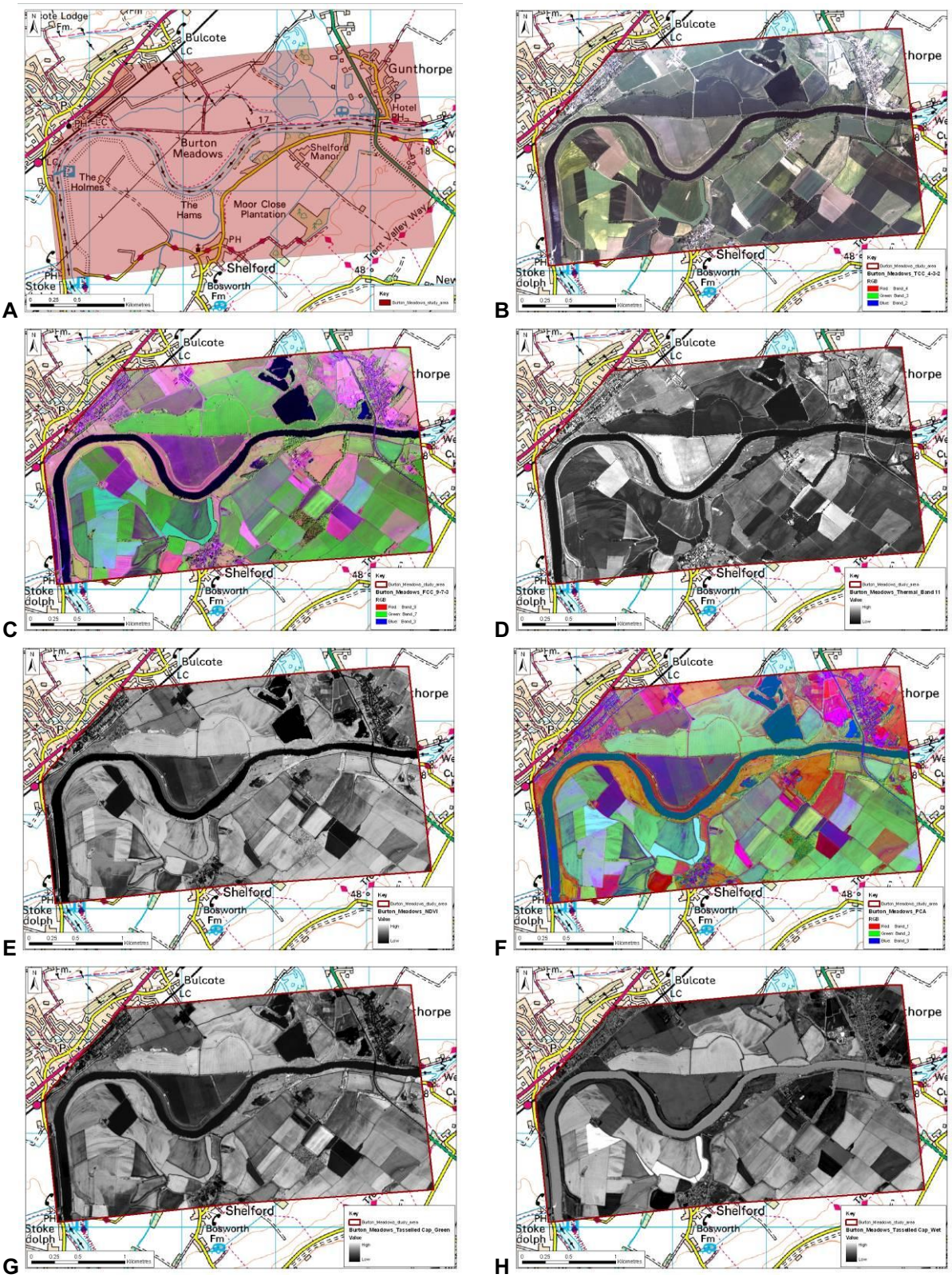

Figure 66. Burton Meadows ATM: A Study area, B True Colour Composite (4-3-2), C False Colour Composite (9-7-3), D Thermal (12), E NDVI, F Principal Components 1-3, G Tasselled Cap Green, H Tasselled Cap Wet

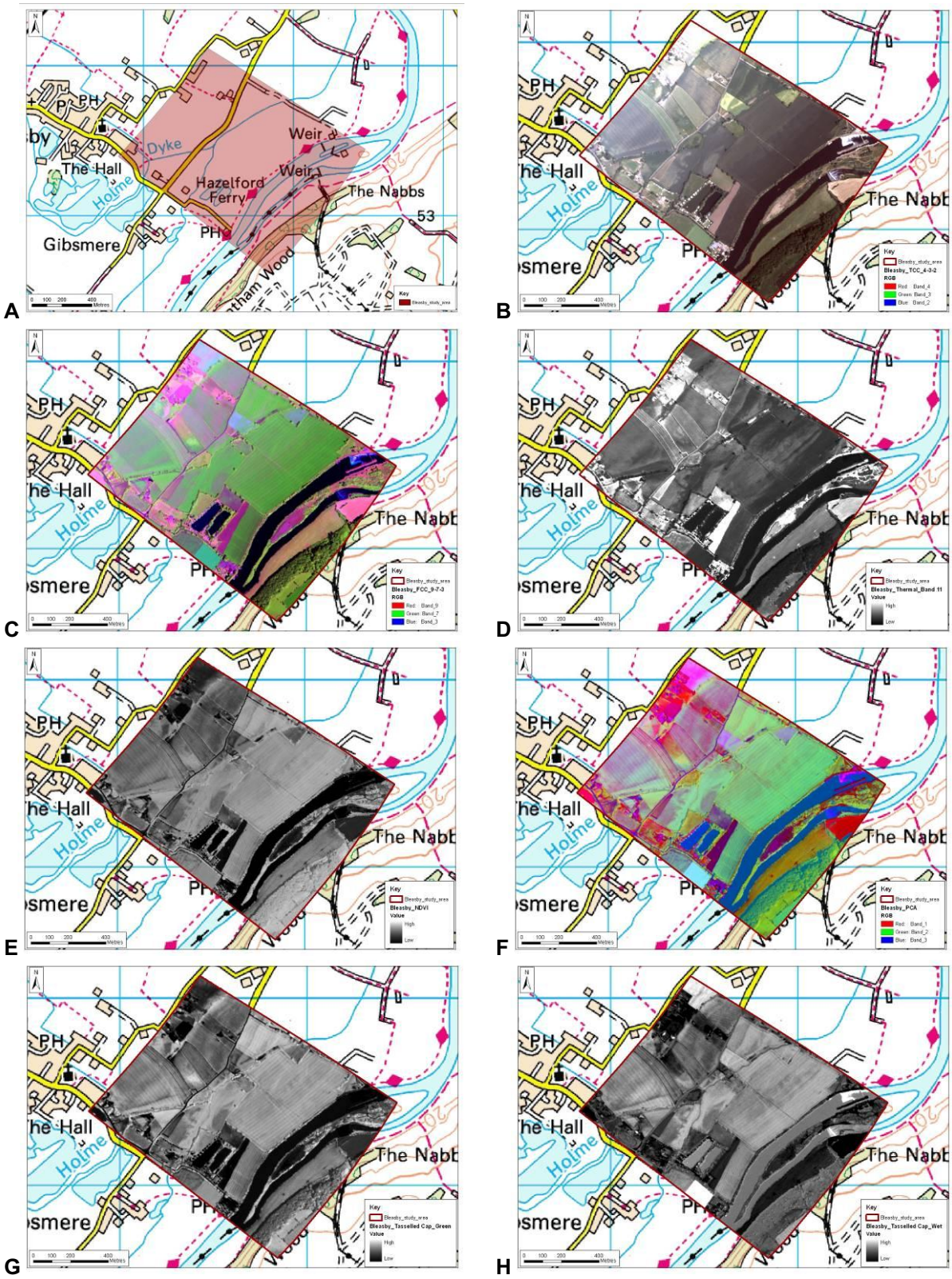

Figure 67. Bleasby ATM: A Study area, B True Colour Composite (4-3-2), C False Colour Composite (9-7-3), D Thermal (12), E NDVI, F Principal Components 1-3, G Tasselled Cap Green, H Tasselled Cap Wet

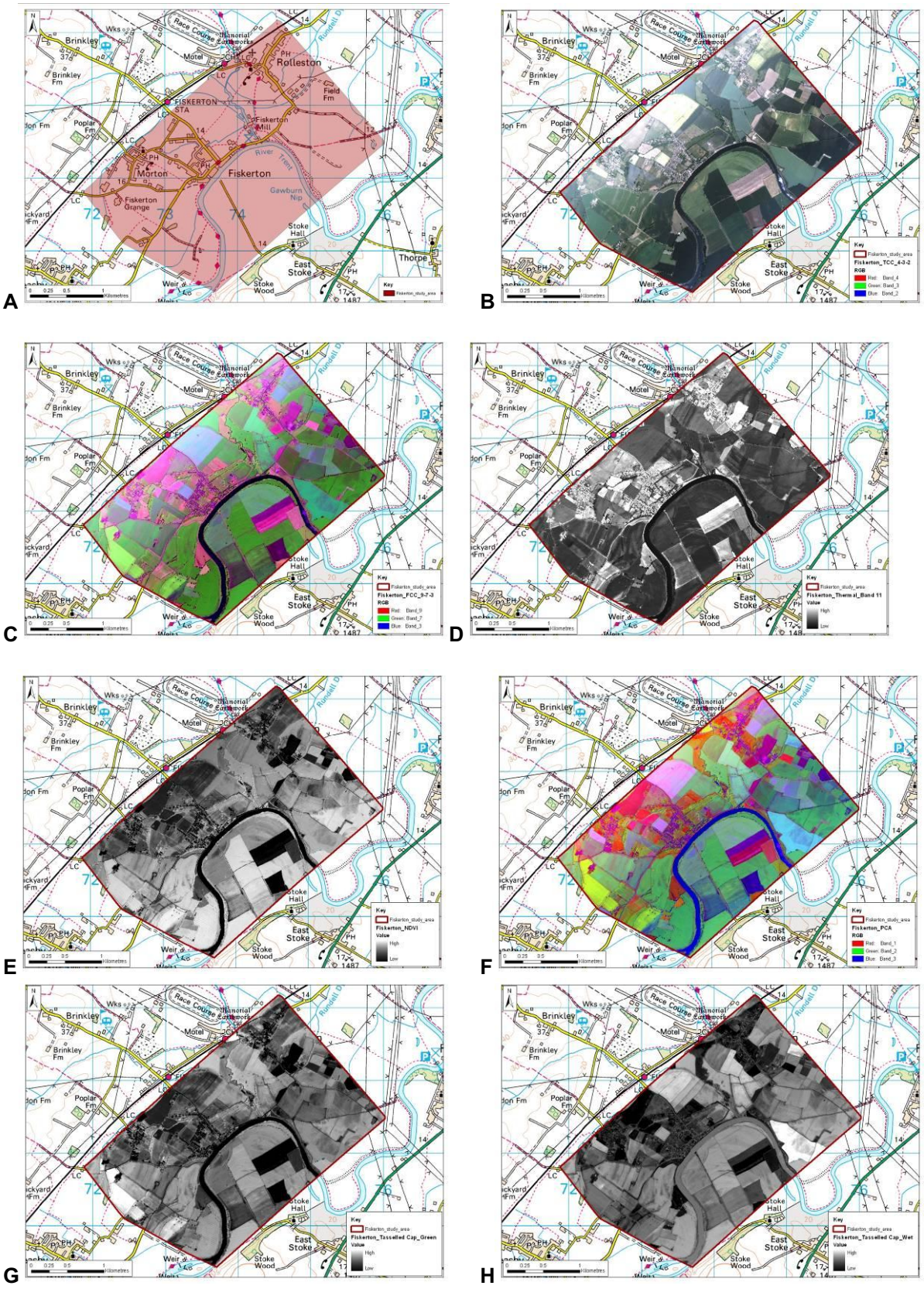

Figure 68. Fiskerton ATM: A Study area, B True Colour Composite (4-3-2), C False Colour Composite (9-7-3), D Thermal (12), E NDVI, F Principal Components 1-3, G Tasselled Cap Green, H Tasselled Cap Wet

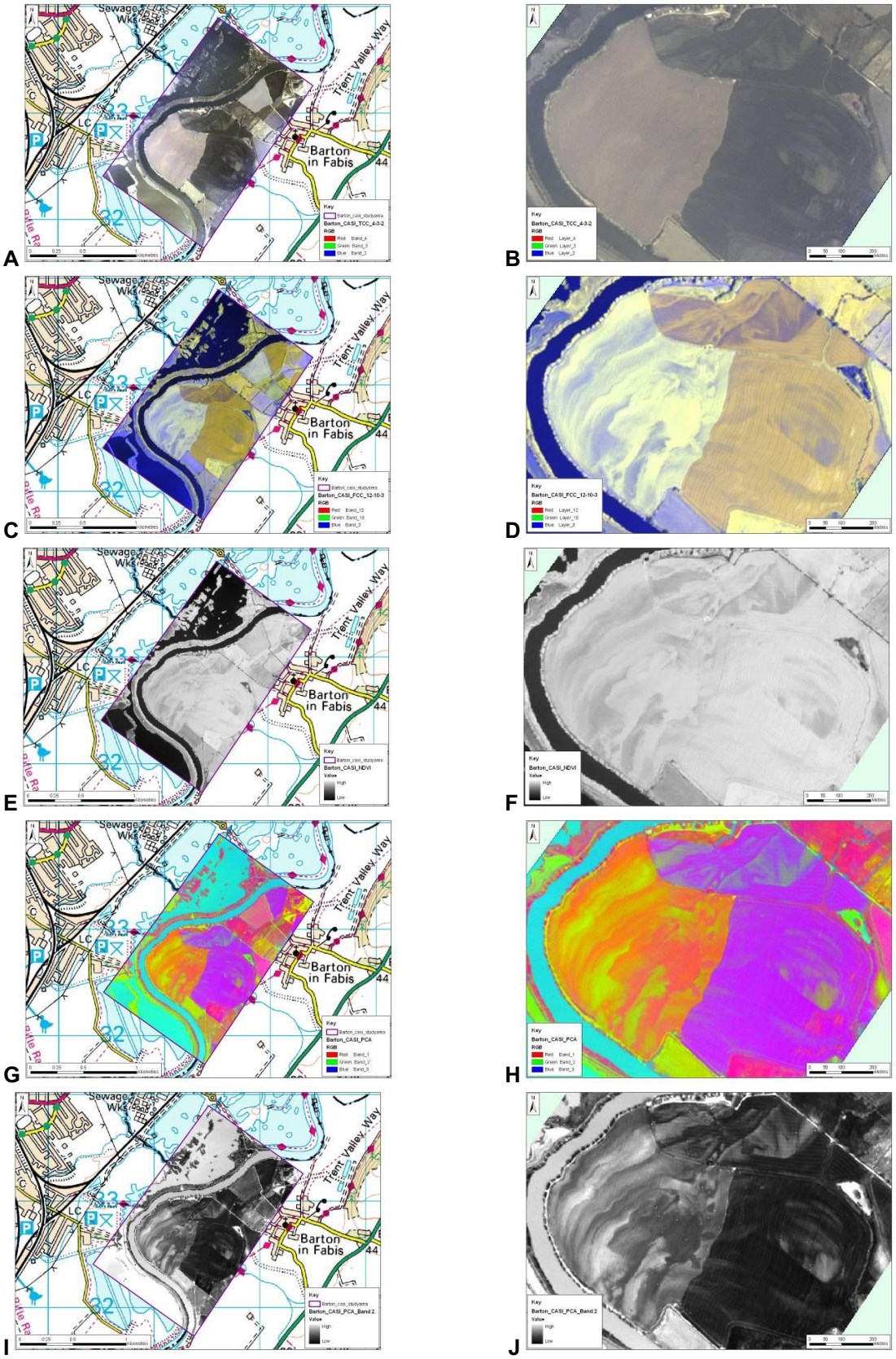

Figure 69. Barton CASI: A-B True Colour Composite (4-3-2), C-D False Colour Composite (12-10-3), E –F NDVI, G-H Principal Components 1-3, I-J Principal Component 2

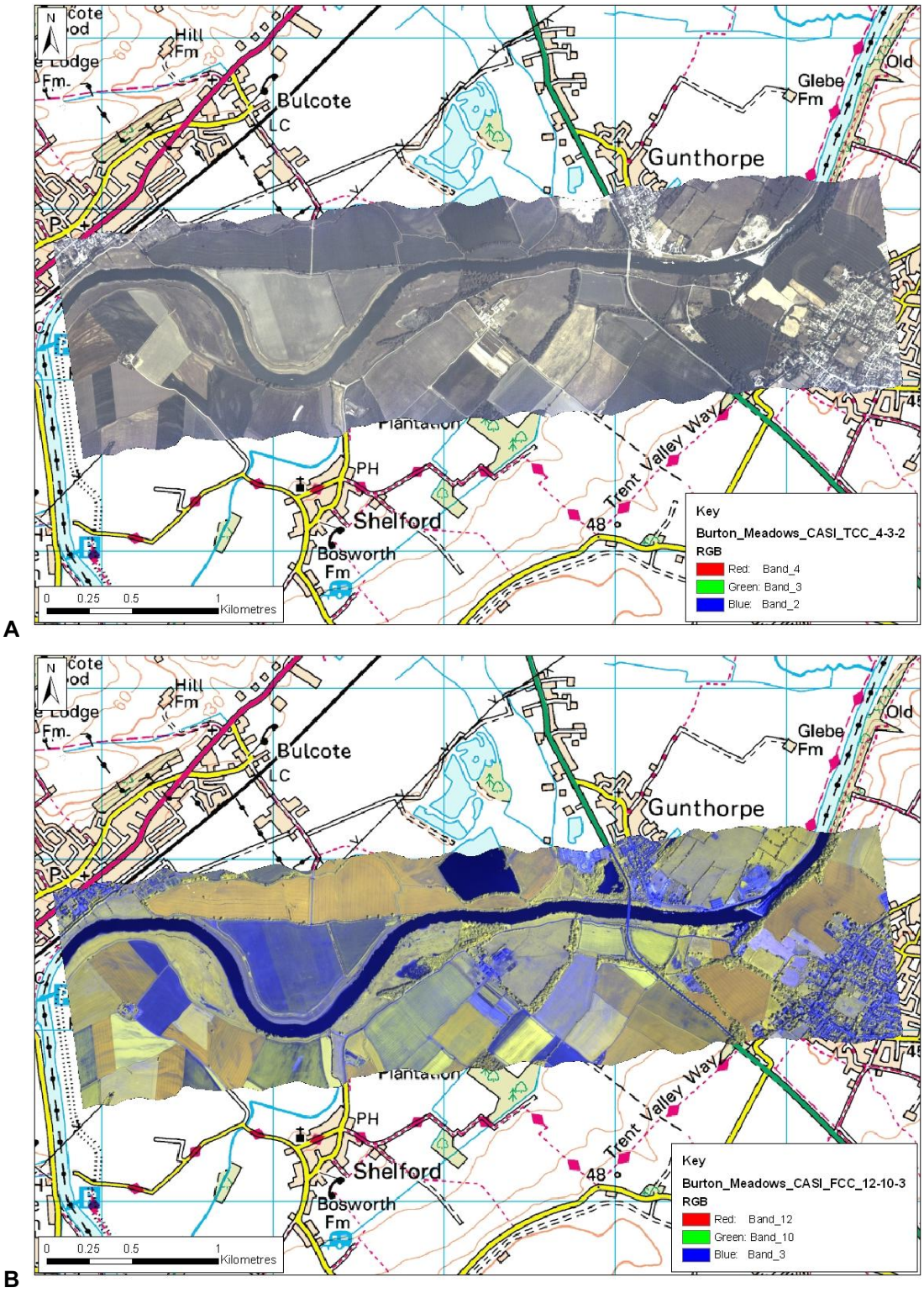

Figure 70. Burton Meadows CASI, A True Colour Composite (4-3-2), B False Colour Composite (12-10-3)

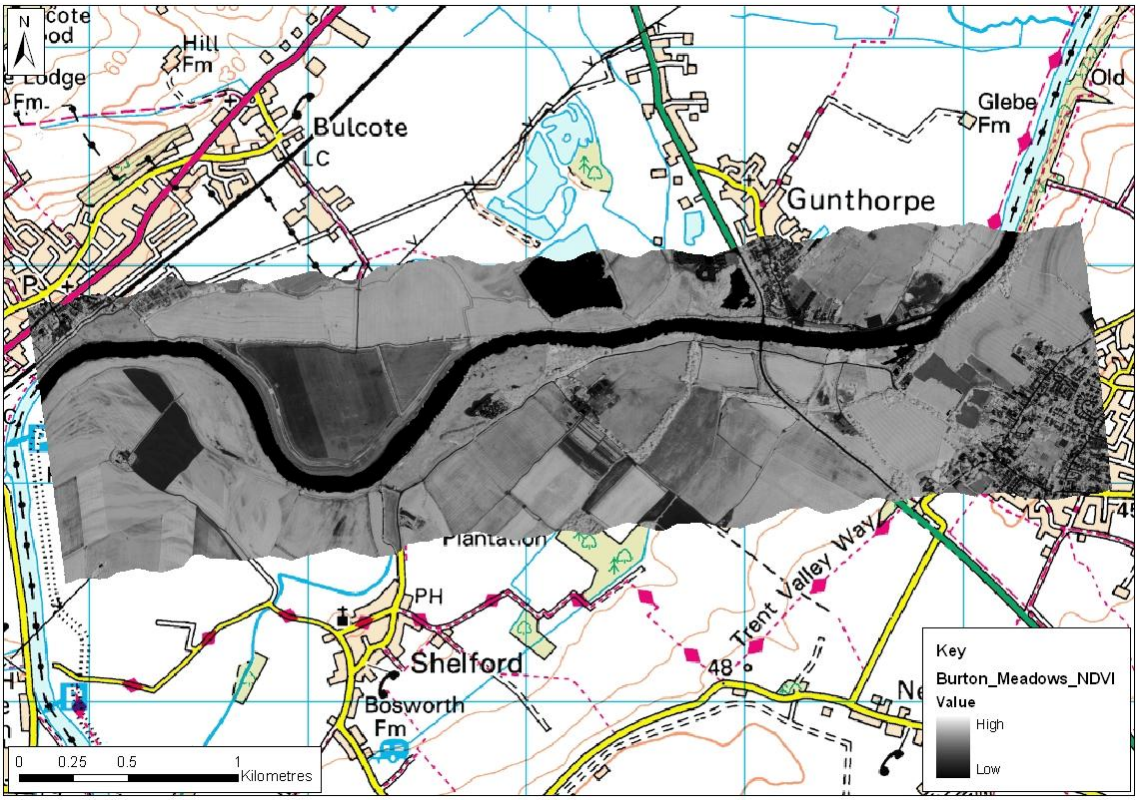

C

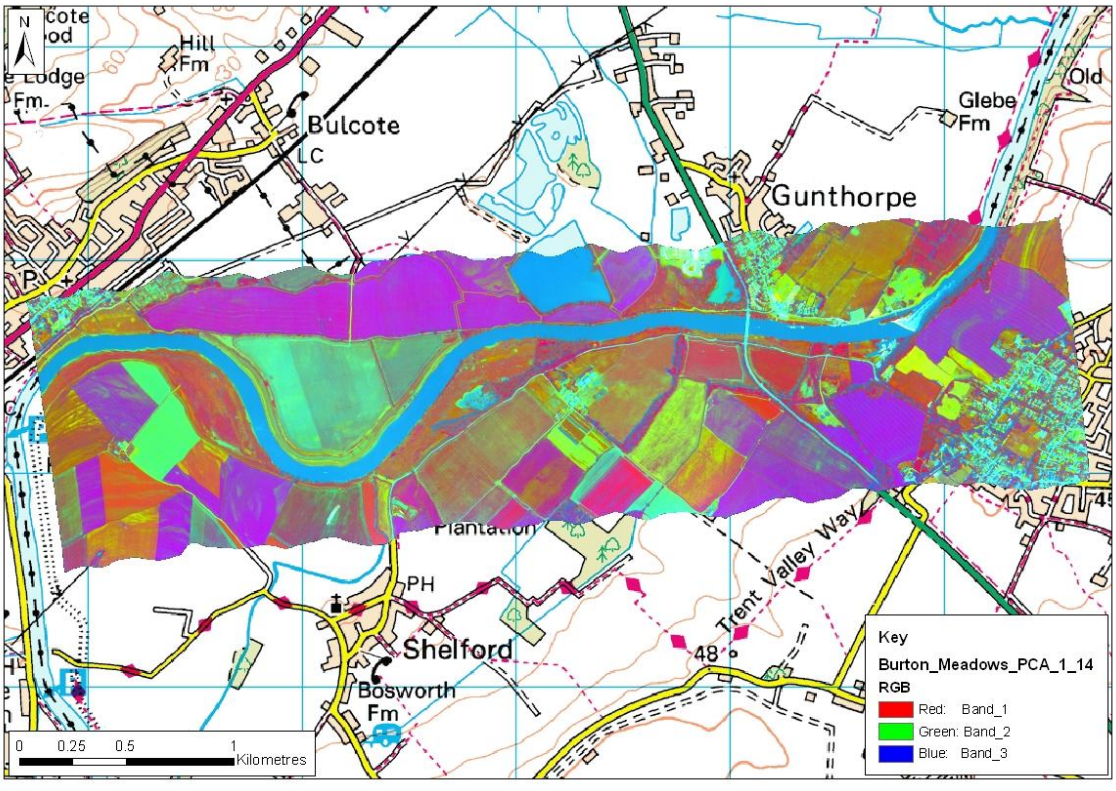

D

Figure 71. Burton Meadows CASI, C NDVI, D Principal Components 1-3

E

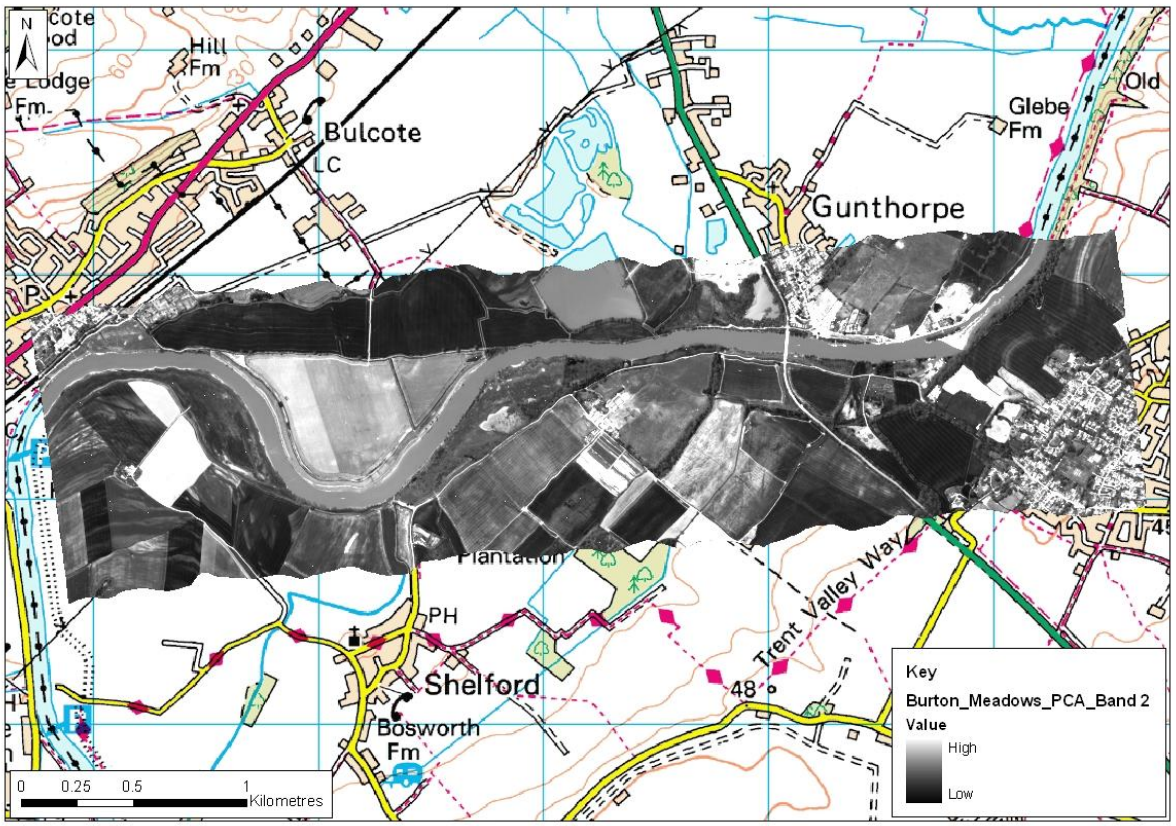

Figure 72. Burton Meadows CASI, E Principal Component 2

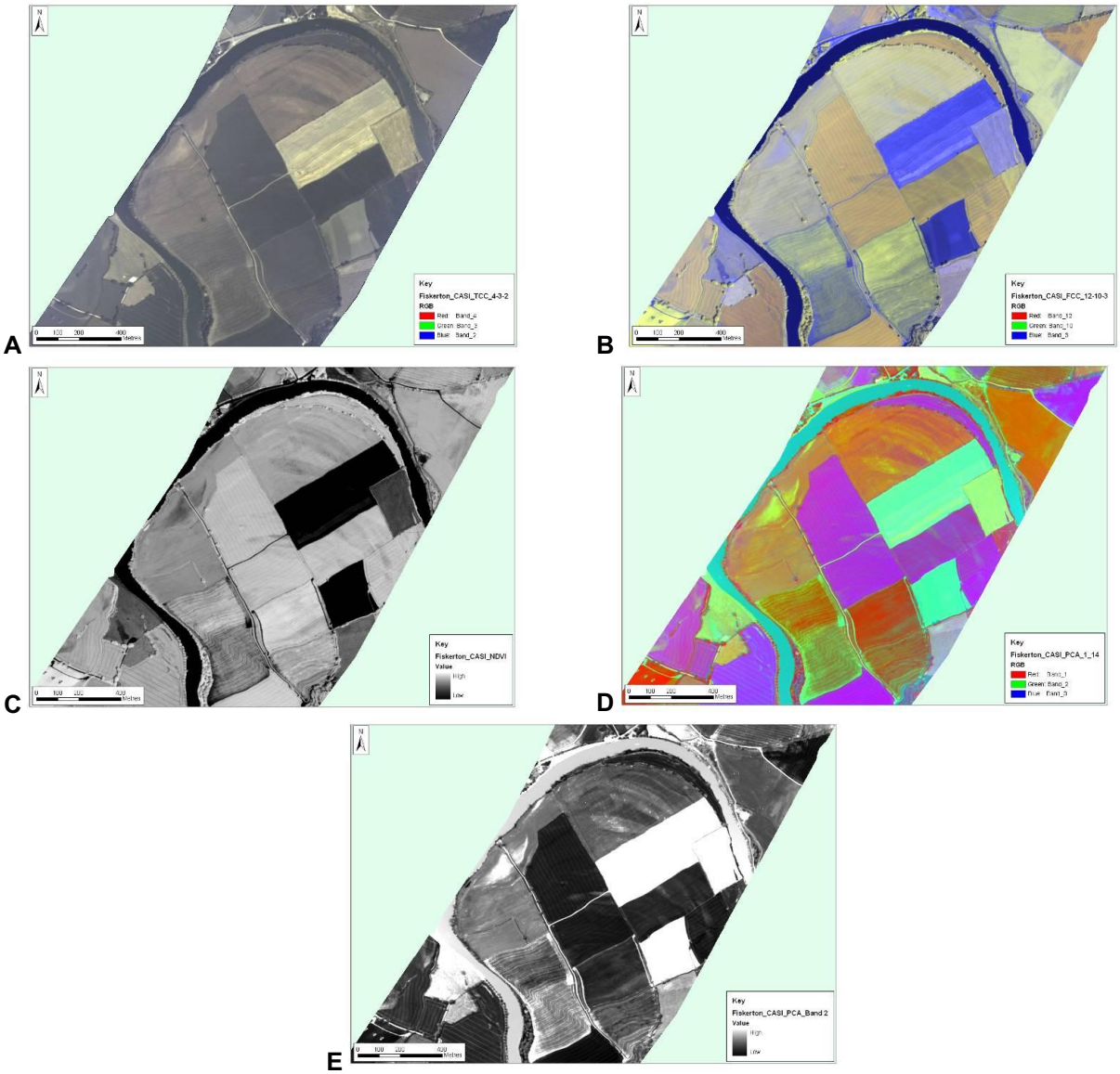

Figure 73. Fiskerton CASI: A True Colour Composite (4-3-2), B False Colour Composite (12-10-3), C NDVI, D Principal Components 1-3, E Principal Component 2


birmingham
archaeology